NASA Contractor Report 172279

NASA-CR-172279
19840007200

NONLINEAR VISCOELASTIC CHARACTERIZATION OF STRUCTURAL ADHESIVES

M. A. Rochefort and Hal F. Brinson

VIRGINIA POLYTECHNIC INSTITUTE AND STATE UNIVERSITY
Blacksburg, Virginia 24061

Grant NAG1-227
December 1983

NASA
National Aeronautics and
Space Administration

Langley Research Center
Hampton, Virginia 23665

NONLINEAR VISCOELASTIC CHARACTERIZATION OF STRUCTURAL ADHESIVES

M. A. Rochefort*, Research Assistant
and
Hal F. Brinson, Professor

A Joint Project in: The Center for Adhesion Science
and
The Department of Engineering Science and Mechanics
Virginia Polytechnic Institute and State University
Blacksburg, VA 24061

Grant NAG-1-227
National Aeronautics and Space Administration
Langley Research Center
Hampton, VA 23665

*Now associated with Applied Research Associates, Inc., Alexandria, VA. (This report is essentially the M.S. Thesis of M. A. Rochefort.)

TABLE OF CONTENTS

LIST OF FIGURES

Pages missing from the original document

Pages missing from the original document

LIST OF TABLES

LIST OF SYMBOLS

ε_{ij}	strain tensor
σ_{ij}	stress tensor
S_{ijkl}	compliances
σ°_{kl}, σ_o	time independent stress
$H(t)$	Heaviside step function
$D(t)$	creep compliance
D_o	initial creep compliance
$\Delta D(t)$	transient creep compliance
b_σ	TSSP vertical shift factor
ξ	TSSP reduced time parameter
a_σ	horizontal shift factor due to stress
g_o, g_1, g_2	stress dependent parameters
ψ, ψ'	Schapery reduced time parameters
$\varepsilon_c(t)$	uniaxial creep strain
$\varepsilon_r(t)$	uniaxial recovery strain
C	linear creep parameter
n	exponent
λ	nondimensional time
$\Delta\varepsilon_1/g_1$	vertical shift factor
$\Delta\varepsilon_1$	transient creep at time t_1
$\bar{\varepsilon}_r$	shifted recovery strain
ε_o	instantaneous creep strain
C'	creep coefficient
m	Findley creep coefficient

Chapter 1

INTRODUCTION

Background Information

The connection or the joining of components is an integral part of engineering structural design. This is especially true of the aerospace industry, where many thousands of structural components must be joined to form a single aircraft. Any decrease in the overall structural weight of an aircraft results in a corresponding increase in its allowable payload, thereby making the aircraft more cost efficient. This economic incentive has been a major factor behind the increased usage of lightweight metallic and composite materials in structural aircraft components in recent years. For the (high strength/low weight) "advanced" composite materials, conventional fasteners such as rivets are inefficient, as they sever the strong reinforcing fibers. In the case where metallic components are to be fastened, riveting causes high stress concentrations around the rivet holes, reducing the fatigue resistance of the particular components. An additional drawback of riveting is that rivets are sometimes made of steel and therefore may add significantly to the total weight of the structure. One way to avoid the use of rivets and their attendant problems is the use of adhesive bonding to fasten structural components.

The desire to minimize weight as well as the economy and efficiency of construction in a variety of industries has created the recent interest in high strength structural adhesives. Structural

components are often subjected to extreme variations in temperature and humidity, as well as stress. Obviously, any relatively new procedure such as adhesive bonding must first go through an exhaustive testing and analysis program before actual implementation is allowed. One of the largest in depth research efforts conducted to better understand adhesive bonding was the "Primary Adhesively Bonded Structures Technology" (PABST) program [1-6] conducted by McDonnell Douglas for the USAF Flight Dynamics Laboratory. The PABST program spanned a period of five years (1975-1980) and has been described as, "one of the most successful technology development programs ever undertaken" [3].

Some of the advantages of adhesive bonding over riveting (summarized from references [1-23]) are as follows:

* Force distribution over a comparatively large area resulting in relatively low stresses
* Reduction in total weight of the structure
* Possibility of eliminating high stress concentrations at rivet holes
* Favorable vibration damping
* Joint resistance to corrosion (with proper surface preparation)
* Reduced initial and maintenance costs

Although the future of adhesive bonding looks quite promising, there are a few problems associated with the analysis and design of bonded joints which must be solved before adhesive bonding can be utilized to its fullest capabilities. The most important of these problems is the continued use of the single-lap bonded test coupon as

the basic standard for determining the thin film shear properties of adhesively bonded joints. The single-lap test forms the basis of most military adhesive specifications as well as being a current ASTM standard (ASTM D 1002). The results obtained via this standard test have been shown to vary with the thickness of the adhesive layer as well as with the type of adherend material used. An additional peculiarity of the single-lap test is that, "even though it is described as a shear test, the failure load is rarely if ever influenced by the shear strength of good structural adhesives" [4]. Clearly, a better standard test specimen is needed if thin film adhesive shear properties are to be determined accurately.

In recent years there has been an increasing trend toward using the thick-adherend short-overlap test coupon [20] as the basis for determining accurate thin film shear stress-strain adhesive response. With the development of the KGR-1 extensometer [20] by R. B. Krieger at American Cyanamid, accurate shear strain measurement for the thick-adherend test specimen is now possible. Although the thick-adherend short-overlap test is generally considered to be superior to the single-lap test for determining thin film adhesive shear properties [24], it is not an official ASTM standard at the present time.

An additional specimen geometry presently under investigation is the cracked-lap-shear (CLS) specimen [18,19]. The CLS specimen was developed by Lockheed to simulate Mode I/Mode II ratios typical of bonded aircraft structures [19]. The CLS test specimen is currently being subjected to round robin examination by several ASTM committees. At this point it appears as though the CLS specimen may turn out to be

a very useful test geometry for determining accurate in situ adhesive properties.

In general, most adhesives are polymers and recently epoxy based materials have become very popular [25-28]. The nature of polymers is such that they have viscoelastic or time dependent moduli and strength properties which are greatly influenced by environmental conditions, especially temperature and humidity. The time dependent nature of the adhesive causes the bonded joint to be time dependent as well. The time dependent response of adhesively bonded joints raises questions regarding their long term reliability under creep or other more complicated loading. A delayed failure (creep rupture) long after the initial design and fabrication process is possible. Thus, a method is needed by which long term (a few years) bonded joint response can be predicted from short term (a few days at most) testing.

Review of Literature

The eccentricity of the applied loads as well as the bending due to the nature of the joint, both serve to complicate the stress analysis of the single-lap test specimen. The first and probably most often quoted paper on the stress analysis of the single-lap joint was presented by Goland and Reissner [34] in 1944. Their solutions, based on the bending of cylindrical plates, are applicable to only two limiting cases: (1) when the adhesive flexibility can be neglected, and (2) when the adhesive is relatively flexible. The solutions are based on the principle of minimum potential energy and are restricted to linear isotropic materials and identical adherends. Thermal effects were

neglected in the solutions.

The stress analysis of bonded joints has received a great deal of attention since the early work of Goland and Reissner. Many researchers have attempted to predict the stresses in bonded joints using closed form analytical solutions. However, the resulting equations that must be solved are extremely complicated thus requiring that simplifying assumptions be made as in the Goland and Reissner solutions. Recently, the finite element method has been used extensively in the analysis of bonded joints [18,19,35-37]. The nonlinearity of the adhesive has been taken into account [18,19] as well as thermal effects [35]. The time dependent behavior of a linear viscoelastic adhesive has also been modeled via the finite element method [36,37].

The common denominator between all of the bonded joint analyses performed to date, whether closed form or finite element, is that they all require both Young's modulus and the shear modulus for the adhesive layer in order to calculate the stress distribution. Young's modulus is usually obtained from a tensile test of the bulk adhesive, while the shear modulus is determined via a single-lap shear test. As mentioned previously, due to inherent problems with the single-lap specimen, the shear modulus may be more accurate if obtained from a thick-adherend short-overlap shear specimen.

Efforts have been made to determine whether the mechanical properties of an adhesive in a joint can be related to the properties of the bulk adhesive [38-41]. Even though great care is taken to cure the adhesive identically for both situations, the thin film adhesive shear properties in general, cannot be related to the bulk tensile

properties. Although this is the case, a common practice in the past has been to use the bulk mechanical properties of adhesives for the analysis and design of bonded joints [9].

Accurate predictions of time dependent bonded joint response have been made based on the time dependent bulk tensile adhesive properties of a linear viscoelastic adhesive [36,37]. However, the accuracy of these predictions is a direct consequence of the linear conditions of small stresses and strains. Under conditions of large deformations, as when failure is approached, this technique would not yield satisfactory results. In the large strain situation both the bulk and the thin film material properties would be required for analysis.

Objective of Overall Research Program

The present investigation represents the first phase of a multi-year Virginia Tech-NASA Langley collaborative research program on "The Viscoelastic Characterization and Lifetime Predictions of Structural Adhesives." The overall objective of this research effort is the development of an accelerated characterization procedure which would allow the prediction of failures in adhesively bonded joints long after the initial design and fabrication process, based on short term testing.

The purpose of this first phase was to study the uniaxial tensile viscoelastic behavior of two commonly used structural adhesives, FM-73* and FM-300*, both in bulk form. A nonlinear viscoelastic characterization procedure was to be applied to the uniaxial tensile

*Manufactured by the American Cyanamid Company.

creep and creep recovery data for both materials. Initially, a procedure due to Schapery [29-32] was to be attempted in which he assumed a creep power law. However, as will be shown subsequently, the power law parameters could not be determined for each of our particular cases as he originally suggested.

The Schapery procedure has been utilized in the past at VPI for adhesive characterization. Cartner [25] successfully employed the method to characterize another epoxy structural adhesive, Metlbond 1113-2, in bulk form, under uniaxial tensile loading.

Recent research by Peretz and Weitsman [33] has verified the ability of the Schapery method to characterize the uniaxial tensile creep and creep recovery response of FM-73, in bulk form, at 30°C (86°F).

The goal of the current research effort was to learn how to predict the long term uniaxial tensile creep and creep recovery response at any arbitrary temperature and stress level from short term data through the use of a nonlinear viscoelastic mathematical model such as that of Schapery [29-32] or others.

The long term goal would be of course to utilize the time dependent uniaxial tensile bulk adhesive properties (determined in the present investigation) to predict time dependent bonded joint response under linear conditions. This could be done using a procedure similar to that employed in references [36,37].

A logical extension would be to use a nonlinear viscoelastic method to characterize bonded joint response. To the author's knowledge, a nonlinear viscoelastic characterization procedure has not previously

been utilized for the characterization of adhesively bonded joints. Upon such satisfactory characterization of a bonded joint the analysis could be combined with a time dependent failure model such as developed by Zhurkov [42] or Crochet [43] in order to predict long term failures. Such a procedure would give a methodology with which the time dependent response of adhesively bonded joints could be determined from the instant of initial loading until failure occurs, thus accomplishing the overall project goal.

Chapter 2

APPROACHES FOR VISCOELASTIC MODELING

Linear Viscoelasticity

The constitutive equation for linear elastic materials is given by,

$$\varepsilon_{ij} = S_{ijkl}\sigma_{kl} \tag{1}$$

where S_{ijkl} are the compliances. For linear viscoelastic materials under creep loading,

$$\varepsilon_{ij}(t) = S_{ijkl}(t)\sigma^0_{kl} \tag{2}$$

where σ^0_{kl} is the time independent stress level and S_{ijkl} are the creep compliances.

For more general loading states, one may express the strain response as,

$$\varepsilon_{ij}(t) = S_{ijkl}(t)\sigma^0_{kl}\, H(t) + S_{ijkl}(t - t_1)\sigma^1_{kl}\, H(t - t_1) + \ldots \tag{3}$$

which may be generalized by the following Convolution integral:

$$\varepsilon_{ij}(t) = \int_{-\infty}^{t} S_{ijkl}(t - \tau)\, \frac{d\sigma_{kl}(\tau)}{d\tau}\, d\tau \tag{4}$$

When the material is unaffected by events prior to t = 0, the lower limit of the integral may be changed to zero.

For uniaxial loading and no prior stress history, the stress-strain constitutive equation may be written as,

$$\varepsilon(t) = \int_{0}^{t} D(t - \tau)\, \frac{d\sigma(\tau)}{d\tau}\, d\tau \tag{5}$$

where $\varepsilon(t)$ is the time varying strain output for an arbitrary time varying stress input, $\sigma(t)$, and $D(t)$ is the creep compliance. Alternatively, equation (5) may be written as,

$$\varepsilon(t) = D_o\sigma(t) + \int_o^t \Delta D(t - \tau) \frac{d\sigma(\tau)}{d\tau} d\tau \qquad (6)$$

where the creep compliance has been separated into initial and transient components such that,

$$D(t) = D_o + \Delta D(t) \qquad (7)$$

The Convolution integral of equation (4), as well as the analogous equations (5) and (6), are all forms of the Duhamel or Boltzmann superposition integral.

Time Temperature Superposition Principle (TTSP)

The aim of any accelerated characterization scheme is that one can in some way use short term experimental data to predict long term material response. The Time Temperature Superposition Principle (TTSP) initially proposed by Leaderman [44] has been widely used for the accelerated characterization of polymers. The basic premise of the TTSP is that compliance curves at different temperatures are of the same basic shape, but only shifted in time. The implication of the TTSP is that compliance data at several different temperatures may be shifted horizontally in log time (vertical shifting may also be required) to produce a smooth "master curve" approximating the compliance over several decades of time. Although it has been successfully employed below the glass transition temperature, T_g, the TTSP is

rigorously justifiable only above the T_g. It should be noted that even though it is not a requirement of the theory, the TTSP is usually associated with linear viscoelasticity [45]. For a detailed discussion of the TTSP and of the various techniques utilized to determine the amount of horizontal and vertical shifting required to produce a smooth "master curve" the reader is directed to the work of Griffith [45].

The recent research of Kenner, Knauss, and Chai [46] employed the TTSP for the accelerated characterization of FM-73. Bulk shear creep compliance curves for several temperatures (above and below the T_g) were shifted both vertically and horizontally to form a "master curve" at 20.5°C, extending over sixteen decades of log time. The applied torsional stresses were sufficiently small that linear viscoelastic behavior was assumed.

Time Stress Superposition Principle (TSSP)

Analogous to the TTSP is the Time Stress Superposition Principle (TSSP) which may be given by the basic equation,

$$D(\sigma,T) = D_0(\sigma) + b_\sigma \Delta D(\xi) \tag{8}$$

where b_σ is the vertical shift factor, ξ is the reduced time given by $\xi = \frac{t}{a_\sigma}$ and a_σ is the horizontal shift factor due to the stress level. The implication of the TSSP is that isothermal compliance data at various stresses (for nonlinearly viscoelastic materials) may be shifted both horizontally and vertically to form a "master curve" predicting long term compliance based on short term testing.

Time Temperature Stress Superposition Principle (TTSSP)

The similarities between the TTSP and the TSSP are apparent. In the TTSP, temperature is the accelerating parameter whereas in the TSSP stress is the accelerating parameter. It would seem logical that an accelerated characterization technique which would simultaneously employ both stress and temperature as accelerating parameters would be possible. Indeed, elements of the TTSP and the TSSP have been utilized to form the Time Temperature Stress Superposition Principle (TTSSP). Again the reader is directed to the work of Griffith [45], which discussed the determination of the appropriate horizontal and vertical shift functions for the TTSSP.

The application of the TTSP as well as the TSSP and the TTSSP is graphical in nature requiring a large data base and thereby creating a tedious and time consuming approach.

Analytical Nonlinear Viscoelastic Approaches

Several techniques have been developed to account for nonlinear viscoelatic behavior [29-32,47-60]. The theories of Green and Rivlin [47], Green, Rivlin, and Spencer [48], and Green and Naghdi [49], are all triple integral representations which are very difficult to solve. Also difficult to solve are the coupled first order nonlinear differential equations of Walker [50], and Krempl [51-56]. Two relatively simple nonlinear theories are those of Schapery [29-32], and Findley [57-60]. Although essentially an empirical curve fitting procedure, the Findley technique is simple to utilize and has been successfully employed for long term creep predictions.

Because elements of both the Schapery and Findley methods will be used subsequently to analyze data, these two approaches will be briefly reviewed here.

Schapery Method

The first nonlinear viscoelastic characterization procedure employed in the current work was developed by R. A. Schapery [29,30] in the late 1960's. The derivation of the theory is too lengthy and detailed to discuss here, but is reviewed and discussed in detail by Hiel [61].

Schapery's nonlinear viscoelastic stress-strain equation for one dimensional loading may be written as [30],

$$\varepsilon(t) = g_0 D_0 \sigma(t) + g_1 \int_0^t \Delta D(\psi - \psi') \frac{d}{d\tau} [g_2 \sigma(\tau)] d\tau \tag{9}$$

where D_0 and $\Delta D(\psi)$ are the initial and transient components of the linear viscoelastic creep compliance. The reduced time parameters,

$$\psi = \psi(t) = \int_0^t \frac{dt'}{a_\sigma}$$
$$\psi' = \psi'(\tau) = \int_0^\tau \frac{dt'}{a_\sigma} \tag{10}$$

are a function of the stress dependent shift function, a_σ. The quantities, g_0, g_1 and g_2, are stress dependent properties that represent the nonlinear nature of a material and must be determined experimentally. When $g_0 = g_1 = a_\sigma = 1$, equation (9) reduces to the Modified Superposition Principle (MSP) proposed by Leaderman [44]. When all stress

dependent properties, g_0, g_1, g_2 and a_σ, are taken to be equal to one, equation (9) reduces to the Boltzmann superposition integral of equation (6). Though not specifically stated by Schapery, his approach represented by equation (9) is a mathematical statement of the Time Stress Superposition Principle (TSSP), which was discussed previously.

All of the material properties in equation (9) can be evaluated from the data obtained from a creep and creep recovery test [32]. In this test, a specimen is subjected to a constant stress, σ_0, which is maintained until time t_1, then removed (Figure 1). The stress input for a uniaxial creep and creep recovery test is given by,

$$\sigma(t) = \sigma_0 H(t) - \sigma_0 H(t - t_1) \tag{11}$$

where σ_0 is the time independent input stress level, and H(t) is the Heaviside step function defined as,

$$\begin{aligned} H(t) &= 0, \text{ when } t < 0 \\ H(t) &= 1, \text{ when } t > 0 \end{aligned} \tag{12}$$

Substitution of equation (11) into equation (9) can be shown to yield,

$$\varepsilon_c(t) = [g_0 D_0 + g_1 g_2 \Delta D(\frac{t}{a_\sigma})]\ \sigma_0 \tag{13}$$

and

$$\varepsilon_r(t) = [g_2 \Delta D(\frac{t_1}{a_\sigma} + t - t_1) - g_2 \Delta D(t - t_1)]\ \sigma_0 \tag{14}$$

for the creep and creep recovery strain, respectively.

If it is assumed that the compliance follows a power law in time, as do many polymers, the transient portion may be written as,

$$\Delta D(\psi) = C\psi^n \tag{15}$$

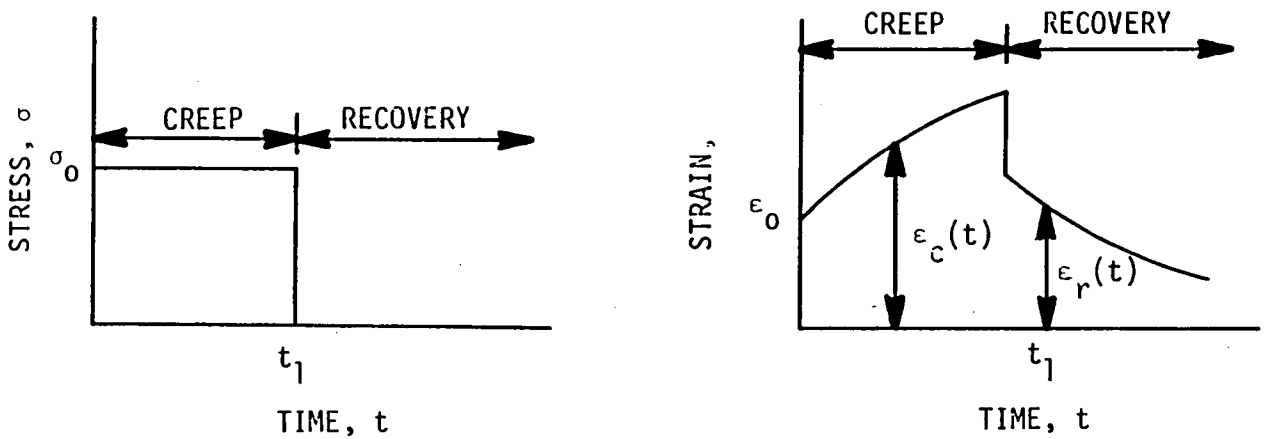

Figure 1. Typical stress-strain response for creep and creep recovery test.

If equation (15) is substituted into equations (13) and (14), the expressions for creep and creep recovery strain become,

$$\varepsilon_c(t) = g_0 D_0 \sigma_0 + C\sigma_0 g_1 g_2 \left(\frac{t}{a_\sigma}\right)^n \tag{16}$$

and

$$\varepsilon_r(t) = \frac{\Delta\varepsilon_1}{g_1}\left[(1 + a_\sigma\lambda)^n - (a_\sigma\lambda)^n\right] \tag{17}$$

where, C and n are material properties which are invariant with stress,

$$\lambda = \frac{t - t_1}{t_1} \tag{18}$$

is a nondimensional time, and

$$\Delta\varepsilon_1 = \varepsilon(t_1) - \varepsilon_0 \tag{19}$$

In Equation (19), $\Delta\varepsilon_1$ represents the transient component of the creep strain just prior to the removal of the stress at $t = t_1$.

Schapery's approach was derived from the theory of irreversible thermodynamics. As a result, each of the stress dependent properties in equation (9) has a thermodynamic origin. Schapery [30] has shown that changes in, g_0, g_1, and g_2, reflect dependence of the Gibbs free energy on the applied stress, while changes in a_σ arise due to a similar stress dependence of both entropy production and free energy.

The greatest advantage of the Schapery approach over the nonlinear theories mentioned previously (excluding Findley) is the relative simplicity of the calculations. This is a result of the simple, single integral form of equation (9). An additional attribute of the method is that, once the nonlinear parameters are determined from tensile creep and creep recovery using equations (16) and (17), they can be

utilized in the more general equation (9) to model a wide variety of loading and unloading situations.

Findley Method

A nonlinear viscoelastic characterization method studied extensively by Findley [57-60] was also incorporated into the current analysis. The basic concept behind the Findley analysis is that for any given creep load, the specimen strain is given by,

$$\varepsilon(t) = \varepsilon_o + m\, t^n \tag{20}$$

where ε_o, m, and n are material properties. Further, the assumptions are made that

n = constant, independent of stress level

$$\varepsilon_o = \varepsilon_o' \sinh \sigma/\sigma_\varepsilon \tag{21}$$

$$m = m' \sinh \sigma/\sigma_m \tag{22}$$

where ε_o', σ_ε, m', and σ_m are material constants for any given temperature, moisture level, etc. The nonlinear effect of stress is accounted for by the hyperbolic sine terms.

It has been shown by Schapery, that his expression for creep strain given by equation (16) is equivalent to the Findley creep expression of equation (20) if

$$g_o = \frac{\sinh \sigma/\sigma_\varepsilon}{\sigma/\sigma_\varepsilon} \tag{23}$$

and

$$\frac{g_1 g_2}{a_\sigma^n} = \frac{\sinh \sigma/\sigma_m}{\sigma/\sigma_m} \tag{24}$$

Determination of the Schapery Parameters

If a viscoelastic material is to be characterized by equations (16) and (17), seven material parameters must be evaluated (n, C, D_o, g_o, g_1, g_2, and a_σ). Schapery suggested a graphical procedure to determine these seven parameters [32]. A brief description of his procedure follows.

First, the exponent, n, is determined from linear creep recovery data. Taking the logarithm of equation (17) gives,

$$\log \bar{\varepsilon}_r = \log \varepsilon_r - \log \frac{\Delta\varepsilon_1}{g_1} = \log [(1 + a_\sigma\lambda)^n - (a_\sigma\lambda)^n] \qquad (25)$$

where $\log \bar{\varepsilon}_r$ is defined as the shifted recovery strain. When $g_1 = a_\sigma = 1$ (linear range), a family of double-logarithmic curves of $[(1 + \lambda)^n - \lambda^n]$ versus λ can be plotted for several values of n (usually $0 < n < 0.5$). Experimentally known values of $\log \varepsilon_r$ can be plotted against λ in the linear range and the shape of the resulting curve can be matched to one of the aforementioned family of curves, thereby determining n. Next, $\log \varepsilon_r$ for each stress level in the nonlinear range can be put on the same graph with the linear data. Since n is independent of stress level, all the curves of $\log \varepsilon_r$ for each stress level can be shifted to form a single continuous creep recovery "master curve." The necessary horizontal shifting for each stress level is $\log a_\sigma$ while the required vertical shifting for each stress level represents $\log \frac{\Delta\varepsilon_1}{g_1}$.

Let equation (16) be represented by,

$$\varepsilon_c(t) = \varepsilon_o + C't^n \qquad (26)$$

where $\varepsilon_o = g_o D_o \sigma_o$ is the initial strain and the creep coefficient, C', is given by,

$$C' = \frac{C\sigma_o g_1 g_2}{(a_\sigma)^n} \tag{27}$$

The quantities ε_o and C' can be obtained for each stress level by solving equation (26) at any two times, t_a and t_b.

At this point the transient creep strain, $\Delta\varepsilon_1$, can be determined for each stress level as,

$$\Delta\varepsilon_1 = C'(t_1)^n \tag{28}$$

As the quantity $\frac{\Delta\varepsilon_1}{g_1}$ is known, g_1 may now be easily determined.

For linear data equation (27) reduces to, $C' = C\sigma_o$, thus the parameter C may be evaluated. The parameter g_2 can be determined for all nonlinear stress levels from equation (27).

The remaining parameter, g_o, is evaluated for each stress level as,

$$g_o = \frac{\varepsilon_o}{D_o \sigma_o} \tag{29}$$

The above graphical procedure is tedious, time consuming, and quite subjective. For this reason, a least squares computer based procedure has been developed at VPI by Hiel [61] and Bertolotti [62]. The method uses a subroutine labeled "ZXSSQ" developed by IMSL, Inc. for an IBM/SINGLE computer. The details of this program are discussed in the following chapter.

Chapter 3

APPROACHES TO DETERMINING MATERIAL PARAMETERS

Computer Modified Schapery Method

Recall that the expressions for uniaxial tensile creep and creep recovery strain were given by,

$$\varepsilon_c(t) = g_o D_o \sigma_o + C\sigma_o g_1 g_2 \left(\frac{t}{a_\sigma}\right)^n \tag{30}$$

and

$$\varepsilon_r(t) = \frac{\Delta\varepsilon_1}{g_1}\left[(1 + a_\sigma\lambda)^n - (a_\sigma\lambda)^n\right] \tag{31}$$

In order to find the seven material parameters in equations (30) and (31) Schapery [32] suggested that creep and creep recovery tests in both the linear and nonlinear range of the material were required. A typical testing program should consist of at least one test in the linear range and several tests in the nonlinear range. The above series of tests would be performed under isothermal (constant temperature) conditions. It should be emphasized that in this procedure the power exponent is determined from creep recovery data. The reason for this is that transient strains are only present in recovery data and these, of course, correspond to the second term in equation (30).

The computer based method of determining the unknown parameters of equations (30) and (31) developed by Heil and Bertolotti [62] incorporates a very powerful subroutine labeled "ZXSSQ" developed by IMSL, Incorporated. This subroutine uses a finite difference Levenberg-Marquardt algorithm to find the minimum sum of squares of the difference between a number of experimental data points and a user defined

function. Convergence is satisfied and execution is terminated if on two successive iterations, the parameter estimates agree, component by component, to three digits.

This subroutine allows the user to define a curve that is to model the data. The unknown parameters are evaluated in such a way as to minimize the error between each experimental data point and the defined curve. A more detailed discussion of this subroutine is given later in this chapter.

The computer program was set up to analyze one set of creep and creep recovery data for each run. The first computer run is made using the linear creep and creep recovery data. In the linear range, by virtue of the fact that $g_1 = a_\sigma = 1$, the creep recovery equation (31) reduces to,

$$\varepsilon_r(t) = \Delta\varepsilon_1[(1 + \lambda)^n - \lambda^n] \tag{32}$$

Subroutine "ZXSSQ" is then used to determine the best fit for $\Delta\varepsilon_1$ and n.

Letting $g_0 = g_1 = g_2 = a_\sigma = 1$ in equation (30), we get,

$$\varepsilon_c(t) = D_0\sigma_0 + C\sigma_0(t)^n \tag{33}$$

where n is now known. Equation (33) can be written as,

$$\varepsilon_c(t) = \varepsilon_0 + C't^n \tag{34}$$

Letting subroutine "ZXSSQ" operate on equation (34), yields best fit values for ε_0 and C', where

$$\varepsilon_0 = D_0\sigma_0 \tag{35}$$

and

$$C' = C\sigma_0 \tag{36}$$

Thus from analysis of the linear data the three parameters, D_o, C and n are now known. These three parameters are assumed to be invariant with stress, and thus will remain constants throughout the nonlinear analysis to follow.

The computer program is now executed with the first set of nonlinear creep and creep recovery data. Subroutine "ZXSSQ" operates on equation (31) with n as a known quantity and determines the quantities $\frac{\Delta\varepsilon_1}{g_1}$ and a_σ. Subroutine "ZXSSQ" then operates on equation (34) with n as a known quantity and determines the best fit for ε_o and C', where

$$\varepsilon_o = g_o D_o \sigma_o \tag{37}$$

and

$$C' = \frac{C\sigma_o g_1 g_2}{(a_\sigma)^n} \tag{38}$$

Realizing that,

$$\Delta\varepsilon_1 = C'(t_1)^n \tag{39}$$

g_1 can be easily determined by,

$$g_1 = \left[\frac{1}{(\Delta\varepsilon_1/g_1)}\right] \cdot C'(t_1)^n \tag{40}$$

From equation (38), g_2 can be determined as,

$$g_2 = \frac{C'(a_\sigma)^n}{C\sigma_o g_1} \tag{41}$$

The last parameter g_o can be determined from equation (37),

$$g_o = \frac{\varepsilon_o}{D_o \sigma_o} \tag{42}$$

The computer program is then reexecuted for each set of nonlinear creep and creep recovery data.

Illustration of Subroutine "ZXSSQ"

The recovery equation (32) will be used as an example to illustrate the numerical process involved in evaluating the unknowns $\Delta\varepsilon_1$ and n. Subroutine "ZXSSQ" requires that the right hand side of equation (32) be written as,

```
X(1)*((1.+XLAB(I)**X(2)-XLAB(I)**X(2))                    (43)
```

Let,

```
F(I)=REC(I)-X(1)*((1.+XLAB(I)**X(2)-XLAB(I)**X(2))        (44)
```

where,

X(1) and X(2) -- parameters to be evaluated (X(1) replaces $\Delta\varepsilon_1$ and X(2) replaces n)

REC(I) -- array containing the experimental creep recovery strains

XLAB(I) -- array containing the reduced time values

F(I) -- array containing the error between the experimental creep recovery strains and the recovery equation (43)

A DO LOOP around equation (44) evaluates the values of the array, F(I). Each of these values is squared and all elements are summed. Thus for every value of X(1) and X(2) there is an associated value of the sum of squres error, ΣR^2. If a series of values of X(1) and X(2) and their associated error, ΣR^2, are plotted on a 3-D graph, an error surface is formed (Figure 2).

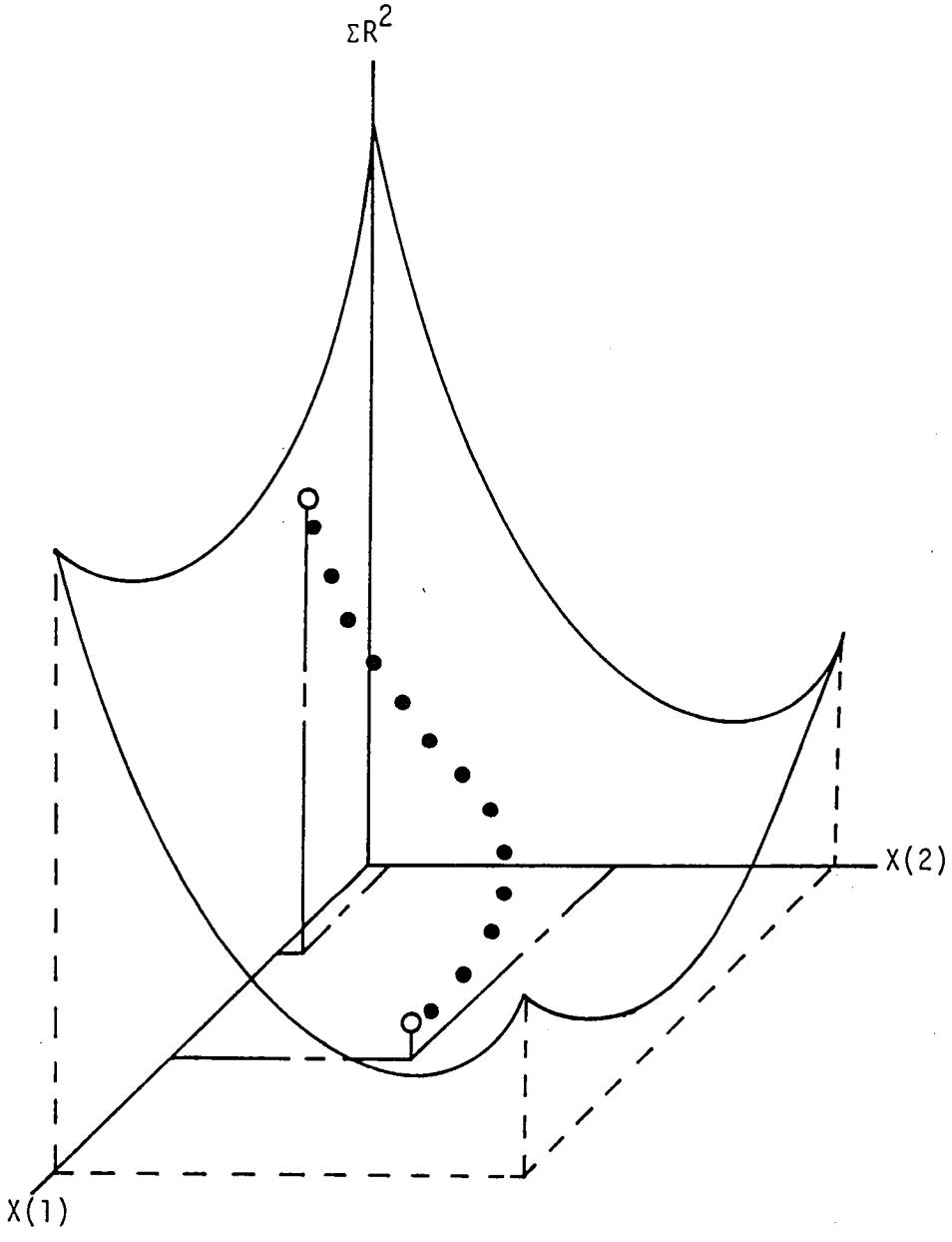

Figure 2. ΣR^2 error surface and computer approximation path.

The unknown parameters X(1) and X(2) must be given initial values by the user. Subroutine "ZXSSQ" begins searching for the best fit values of X(1) and X(2) by examining the initial guesses. The subroutine calculates the value of the normal to the gradient for the initial values of X(1) and X(2), and finds the direction of steepest descent. New values of X(1) and X(2) are found in the direction of the steepest descent line, and the normal to the gradient is calculated again. This process continues until the parameter estimates of two successive iterations agree to three digits. The procedure just described is illustrated in Figure 2.

Computer Modified Findley Approach

As will be discussed in a later chapter, the computer method described above did not always result in stable values for n and C. As a result, a Findley based approach to the determination of these parameters which uses only creep data was utilized. The computer program to so determine n and C was developed by Yen [63] using the same subroutine, "ZXSSQ." This modified approach is in fact equivalent to that employed by Peretz and Weitsman [33] and determines the three parameters, C, n and D_o, from linear creep data as discussed below.

Recall that the creep strain can be written as,

$$\varepsilon_c(t) = \varepsilon_o + C't^n \tag{45}$$

Letting subroutine "ZXSSQ" perform a three parameter fit on equation (45), will yield the best fit values of ε_o, C' and n, where

$$\varepsilon_o = D_o\sigma_o \tag{46}$$

and

$$C' = C\sigma_o \tag{47}$$

Thus from analysis of the linear creep data only, the three parameters, D_o, C and n can be determined. These parameters then remain invariant throughout the nonlinear analysis.

The nonlinear analysis remains as was previously detailed. Specifically, the quantities $\frac{\Delta\epsilon_1}{g_1}$ and a_σ are determined from a two parameter fit of equation (31) and the quantities ϵ_o and C' are fit from equation (34). The three nonlinear parameters, g_o, g_1 and g_2 are then determined from equations (42), (40) and (41), respectively.

The inconsistencies between the two procedures and the results obtained will be discussed in detail in Chapter 5.

Chapter 4

EXPERIMENTAL PROCEDURES

Cure Cycle and Specimen Preparation

The two adhesives investigated in this study were FM-73 and FM-300. Both adhesives are produced by the American Cyanamid Company of Havre de Grace, Maryland. Both FM-73 and FM-300 are manufactured and distributed in the form of a thin film supported by a polyester carrier. These thin films (plies) of adhesive material were formed into bulk adhesive panels at NASA-Langley Research Center. The cure cycles employed by NASA-Langley are given in Table 1.

The final bulk adhesive panels were approximately 12 x 12 x 0.05 inches. Dog bone specimens whose dimensions are given in Figure 3, were machined from each panel.

Equipment

All tests were performed on an ATS (Applied Test Systems) Model 2330 lever arm creep test machine with automatic draw head and releveler. Loading or unloading required approximately 10 seconds. Since this time was less than 1% of the total test time, the experiment was considered to be a good approximation of instantaneous (step) loading.

The creep machine was equipped with an ATS series 2912 oven and a series 230 temperature controller. This control unit maintained an oven temperature within ±2°F (±1°C) of the desired temperature.

Table 1. Adhesive Cure Cycles

FM-73

7 plies -- 10 mils per ply

full vacuum

Temperature	Time
150°F (65.5°C)	
200°F (93.3°C)	1 hour at each temperature
250°F (121.1°C)	

Viton Dam & Plus -- Nylon Sheet each side

Sealant on base to retain resin (adhesive)

FM-300

6 plies -- 16 mils per ply

full vacuum

Temperature	Time
250°F (121.1°C)	
300°F (148.9°C)	1 hour at each temperature
350°F (176.7°C)	

Viton Dam & Plus - Nylon Sheet on each side

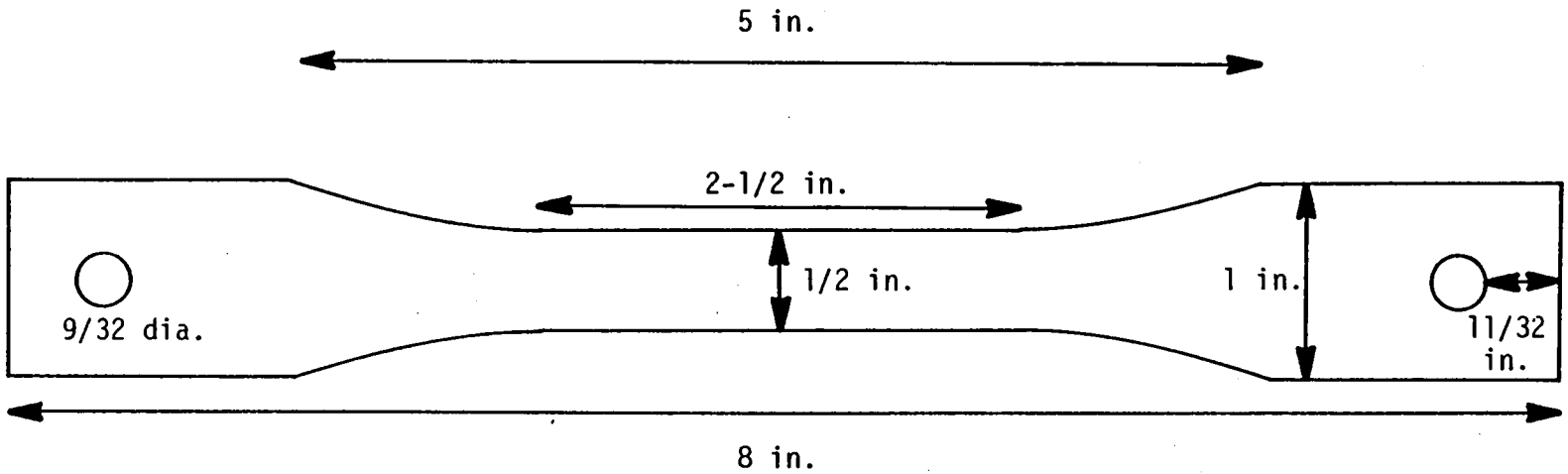

Figure 3. Tensile dogbone specimen.

Temperature was monitored by thermocouples and a Doric 412A Trendicator digital thermometer.

The more desirable procedure of using back to back gages was not utilized due to the small thickness (and the corresponding cross sectional area) of the test specimens. It was felt that the back to back gage arrangement would produce a significant stiffening of the specimen. The small specimen thickness also tends to minimize the induced bending effects caused by eccentricities in loading. It is this induced bending which usually necessitates the use of the back to back gage arrangement. Caplan [64] conducted tests on polycarbonate using the back to back gage arrangement. He found the difference between the two strain gage readings to be negligible. It was thus determined that back to back gages were both unnecessary and undesirable in the present situation. For all tests, strain was measured using a single strain gage. These gages were Micro-Measurements EP-08-125BB-120, 120 ohm gages with pre-attached lead wires. Gages with pre-attached lead wires were used to eliminate soldering directly on the specimen surface. Surface preparation was performed according to recommended Micro-Measurements procedures. Gages were bonded with M-Bond 600 adhesive and cured according to the manufacturer's specifications. An unstrained specimen with a "dummy" (compensating) gage was used in a half-bridge arrangement to compensate for strain due to fluctuations in temperature. A voltage of 2V was used to minimize induced strains due to gage heating effects in the 120 ohm gages. A 2120 Vishay System was used to condition the strain gage output. The conditioned strain data was read from an MTS 408.31 digital voltmeter.

The specimens were pin loaded using serrated metal grips bolted around the specimen ends.

Moisture Content

Moisture content is known to have a significant effect on the strength and stiffness of polymers. Absorption of moisture is known to have an effect similar to increasing the temperature [65]. It has been shown [32] that even a small change in humidity can affect specimen response appreciably. Therefore, moisture content could be a major factor in creep studies. However, for the purposes of the present study, it seemed reasonable to characterize the bulk adhesives in the as-received condition. Therefore all specimens were stored and tested under normal laboratory conditions.

Mechanical Conditioning

It became apparent very early in the study that repeatable creep and creep recovery curves could not be obtained from a specimen which had not been "conditioned." It was also observed that a specimen which had not been conditioned would not return to a state of zero strain after the load was removed. The reason for this permanent strain (damage) was assumed to be the occurrence of crack and damage growth during the loading phase [32,33]. It was felt that if the specimen was repeatedly loaded and unloaded (mechanically conditioned), a constant damage state would be reached and repeatable results could then be obtained [32,33]. This was found to be the case.

Following a procedure similar to Peretz and Weitsman [33], the gaged dog bone specimens were mechanically conditioned by subjecting

them to several loading and unloading cycles at approximately 80% of their ultimate strength. A particular creep load was applied to a specimen and maintained for approximately 20 seconds and then removed. This process was repeated about ten times or until satisfactory stress-strain reproducibility was attained. It should be noted that even though a specimen may have been conditioned previously, if the specimen was to be used at a higher temperature than that at which it was conditioned, the conditioning process was repeated. This was done because polymeric materials often "heal" themselves upon unloading and the healing process is accelerated by an increase in temperature.

Testing Program

A series of creep and creep recovery tests were performed at various temperatures and stress levels. The test temperatures selected were, room temperature, 40°C (104°F), 55°C (131°F), 70°C (158°F), 85°C (185°F), and 100°C (212°F). Similar to Peretz and Weitsman [33], the lowest stress level used at each temperature was assumed to be in the linear range of the material, even though FM-73 and FM-300 are linear only for exceedingly small stresses and strains, if they are linear at all. The assumption of linearity was necessary because of the difficulty of obtaining accurate strain values associated with small stress levels.

Although a multitude of creep and creep recovery tests have been performed to date, and the results have been reported and discussed by many authors, there is no consensus at the present time as to the ideal length of a creep and creep recovery experiment. Lou and

Schapery [32] used a test program consisting of one hour of creep and two hours of recovery. Peretz and Weitsman [33], with the aid of a data acquisition system were able to perform the nonlinear viscoelastic characterization of FM-73 by collecting only 15 minutes of creep data and 5 minutes of recovery data. Based upon creep tests performed by Caplan [64] on polycarbonate, it was decided that a test program consisting of 30 minutes of creep and 60 minutes of creep recovery would be sufficient for the present study.

Inasmuch as the purpose of the present effort was to determine the feasibility of using a nonlinear viscoelastic characterization procedure for FM-73 and FM-300 and not to determine statistically valid properties, the testing program needed to determine the nonlinear parameters described in the preceding chapters was conducted on a single specimen. However, the two short term experiments performed to predict the creep and creep recovery response of FM-300 under an arbitrary temperature and stress situation were performed with a "fresh" specimen, as were the two long term creep experiments.

Chapter 5

RESULTS AND DISCUSSION

FM-73 Adhesive Characterization

The modified epoxy adhesive, FM-73, exhibited viscoelastic creep and creep recovery phenomena at all temperature levels. Isochronous stress-strain results for 30°C (86°F) are shown in Figure 4. The lowest stress level employed, 493 psi (3.45 MPa), was assumed to be the upper limit of linear viscoelastic material response. The reason for this assumption of linearity was explained in the preceding chapter. Since this initial stress level is less than 10% of the ultimate stress of the material the assumption seems justifiable.

The Schapery parameters necessary to characterize the viscoelastic response of FM-73 at 30°C (86°F) were obtained via the computer approach described in Chapter 3. The stress invariant parameters, n, C, and D_0, were determined to be, 0.151, 0.219, and 1.569, respectively. The stress dependent material parameters, g_0, g_1, g_2, and a_σ, are plotted in Figures 5-7. With the seven Schapery parameters known, the complete creep and creep recovery response of FM-73 at 30°C (86°F) can be described by equations (16) and (17) respectively.

The vertical shift parameter, $(\Delta\varepsilon_1/g_1)$, is plotted as a function of stress in Figure 8. Use of this parameter greatly facilitates the application of equation (17) to describe the recovery response. As mentioned previously, the creep response given by equation (16) can be stated in a simpler fashion by equation (26). The instantaneous creep

Pages missing from the original document

Pages missing from the original document

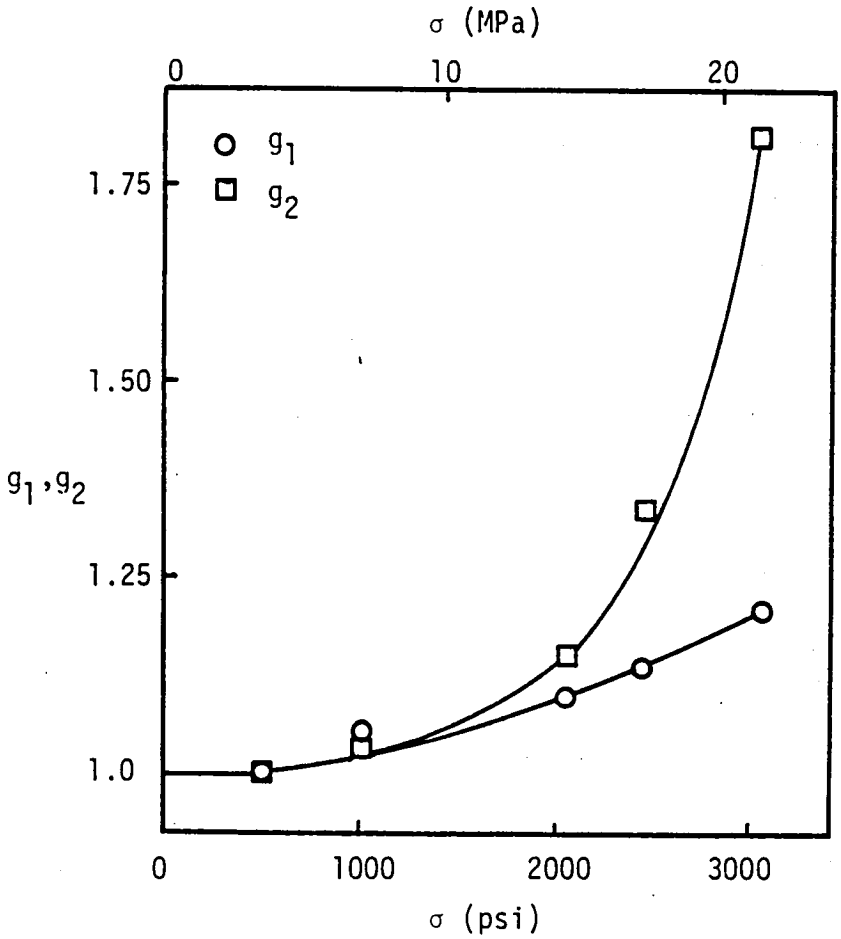

Figure 6. Nonlinear parameters, g_1 and g_2 vs. stress, T = 30°C (86°F).

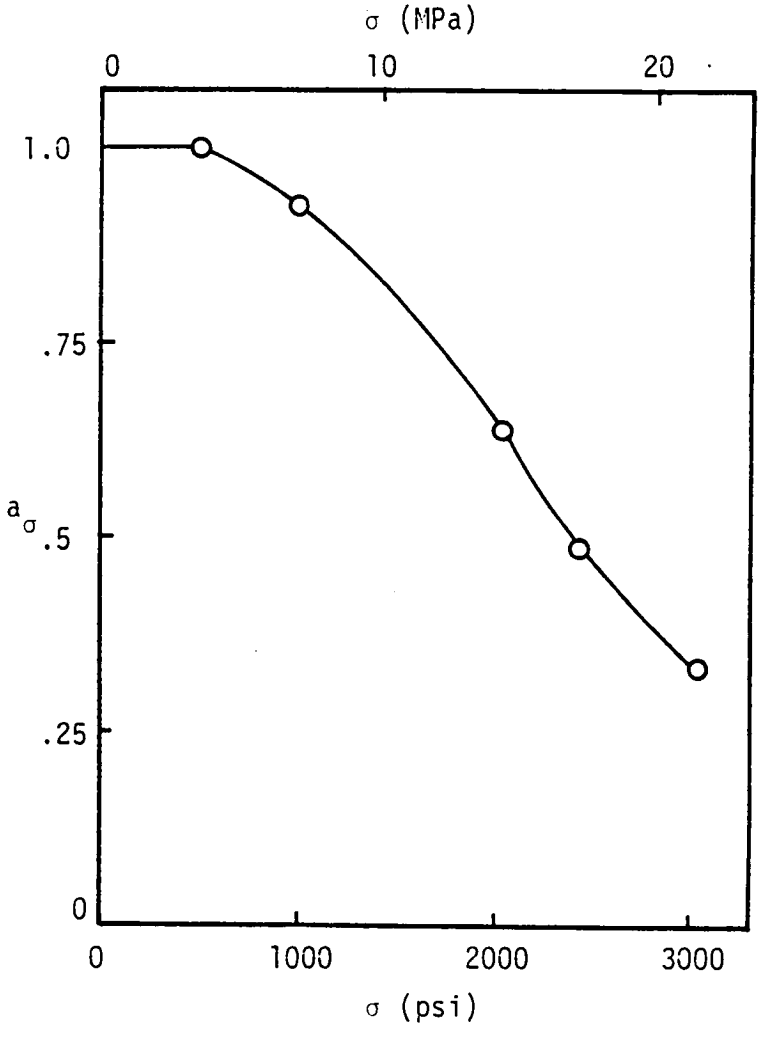

Figure 7. Horizontal shift function, a_σ vs. stress, T = 30°C (86°F).

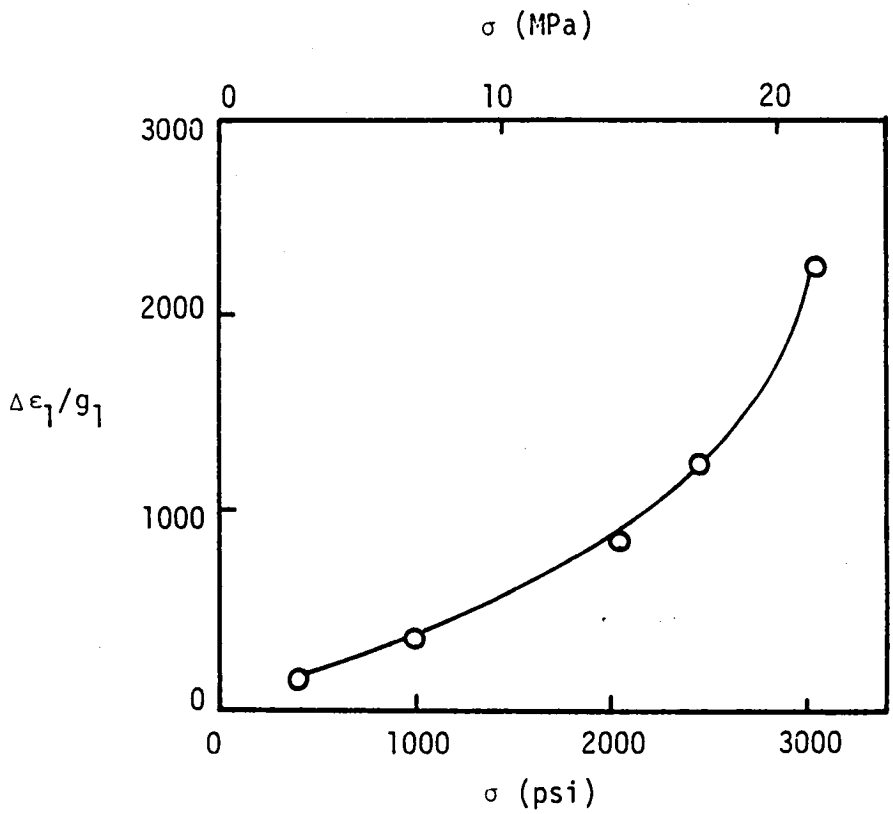

Figure 8. Vertical shift function, $\Delta\varepsilon_1/g_1$ vs. stress, T = 30°C (86°F).

strain, ε_0, and the creep coefficient, C', both plotted as a function of stress level, are given in Figures 9 and 10, respectively.

A comparison of experimental creep data and the corresponding Schapery fit of the data for several stress levels at 30°C (86°F) is given in Figure 11. A similar comparison for recovery data is given in Figure 12. Inspection of Figure 12 shows that the Schapery fit yields strain values lower than the experimental values as the length of recovery time increases. This trend in the Schapery recovery curve fit was apparent throughout the current research.

A master creep recovery curve for FM-73 at 30°C (86°F) is given in Figure 13. This "master curve" is included here to illustrate the accuracy with which the computer based procedure determines the horizontal and vertical shift factors, a_σ and $(\Delta\varepsilon_1/g_1)$. In the past, when the Schapery procedure was performed graphically, the shift factors, a_σ and $(\Delta\varepsilon_1/g_1)$, were defined as the amount of horizontal and vertical shifting, respectively, necessary to form a smooth master curve from the log-log plot of recovery strain vs. λ for the various stress levels. The master curve of Figure 13 was generated in the reverse manner. The computer determined values for a_σ and $(\Delta\varepsilon_1/g_1)$ were used to shift the recovery strain vs. λ curves for the various stress levels. Inspection of Figure 13 reveals that this shifting did result in a smooth creep recovery master curve, thus illustrating the accuracy of the computer based technique.

It was attempted at this point to perform the same characterization procedure as described above, for FM-73 at 40°C (104°F). A complete set of creep and creep recovery data was collected at this

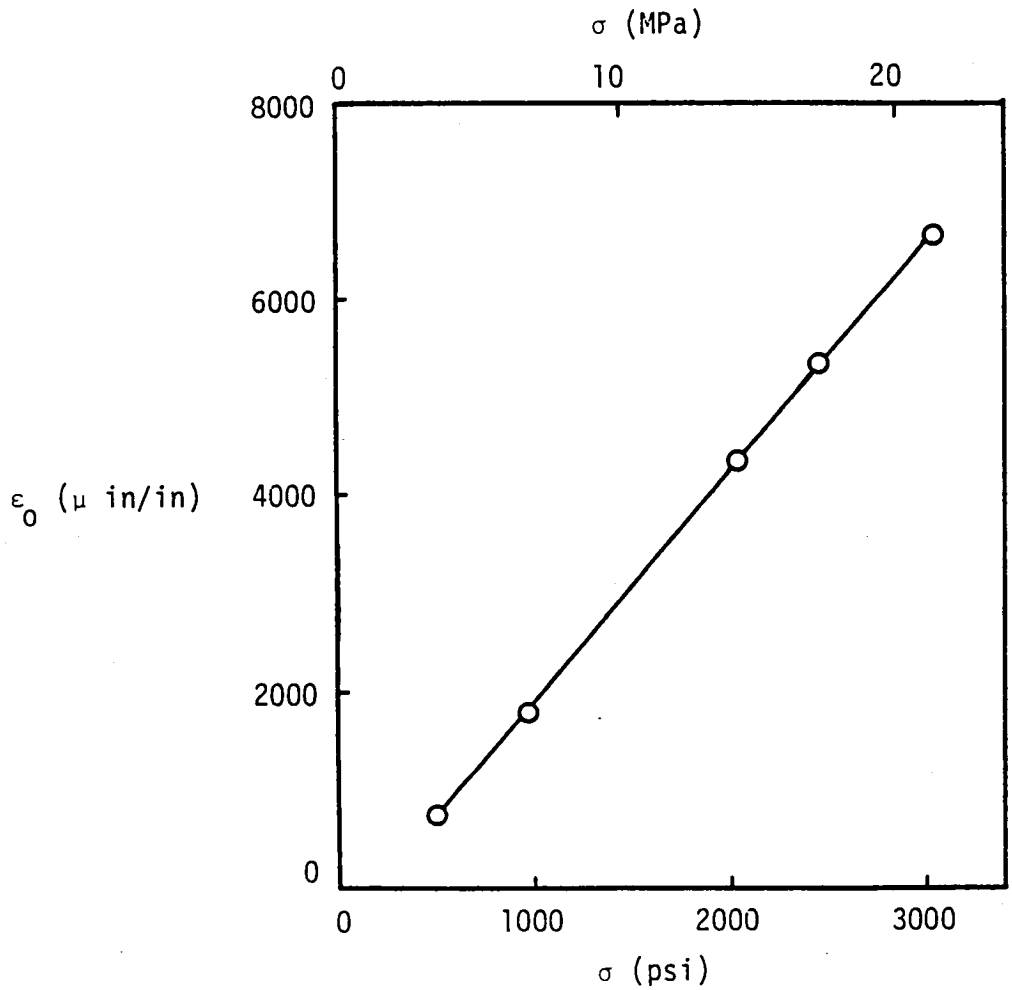

Figure 9. Instantaneous creep strain, ε_o vs. stress, T = 30°C (86°F).

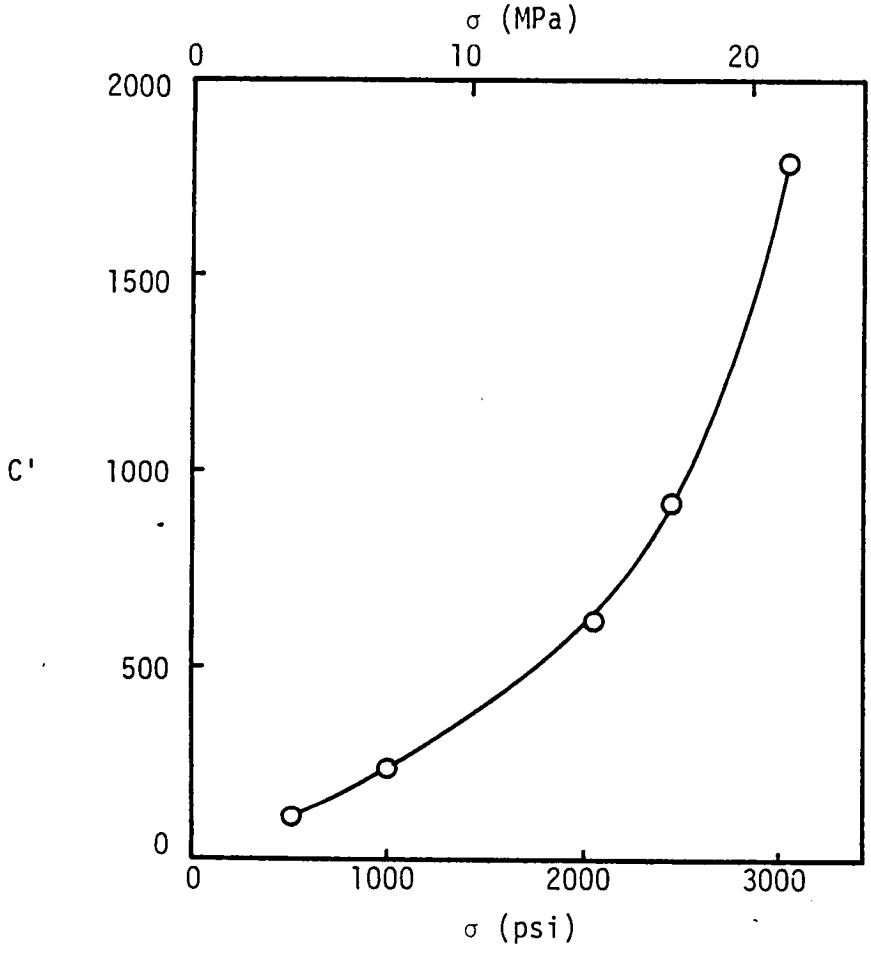

Figure 10. Creep coefficient, C' vs. stress, T = 30°C (86°F).

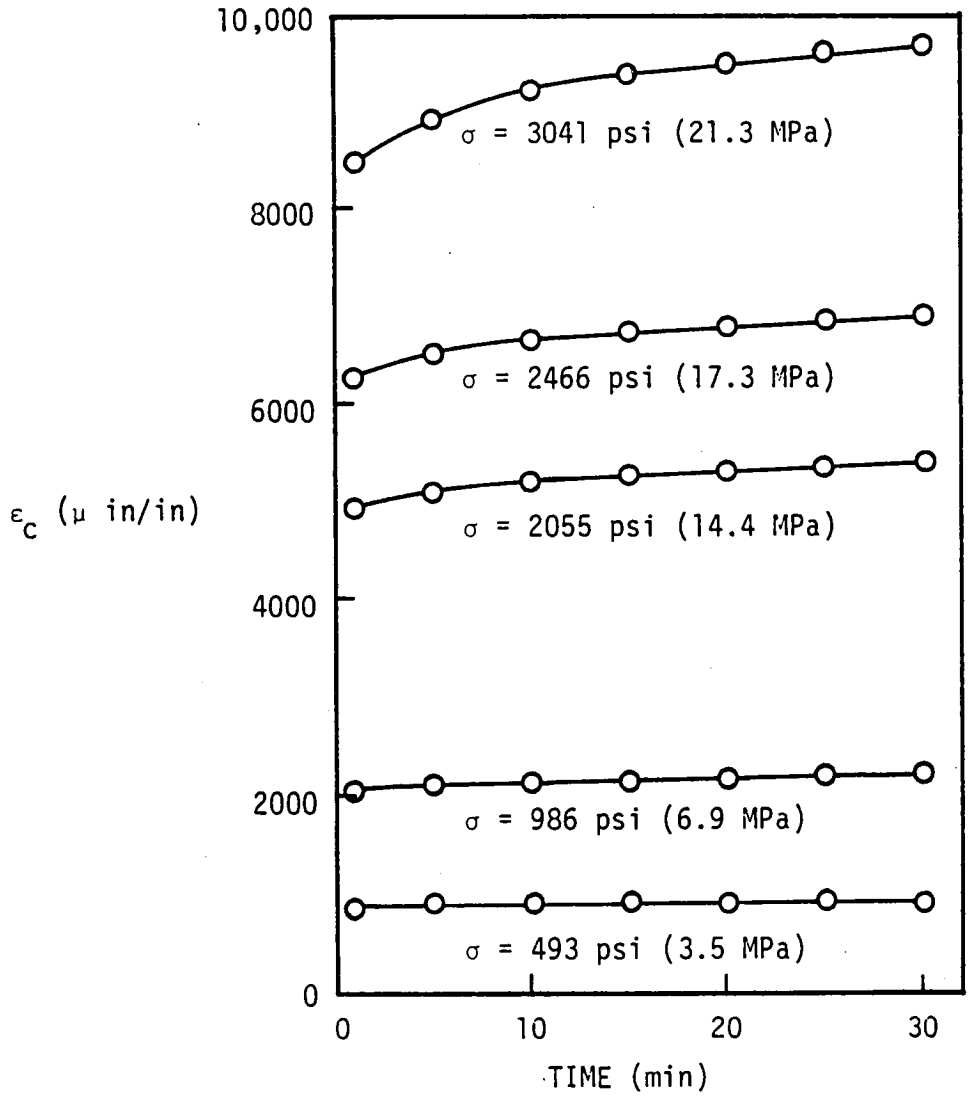

Figure 11. Experimental creep data (symbols) and the corresponding Schapery fit of the data (solid lines) for several stress levels at T = 30°C (86°F).

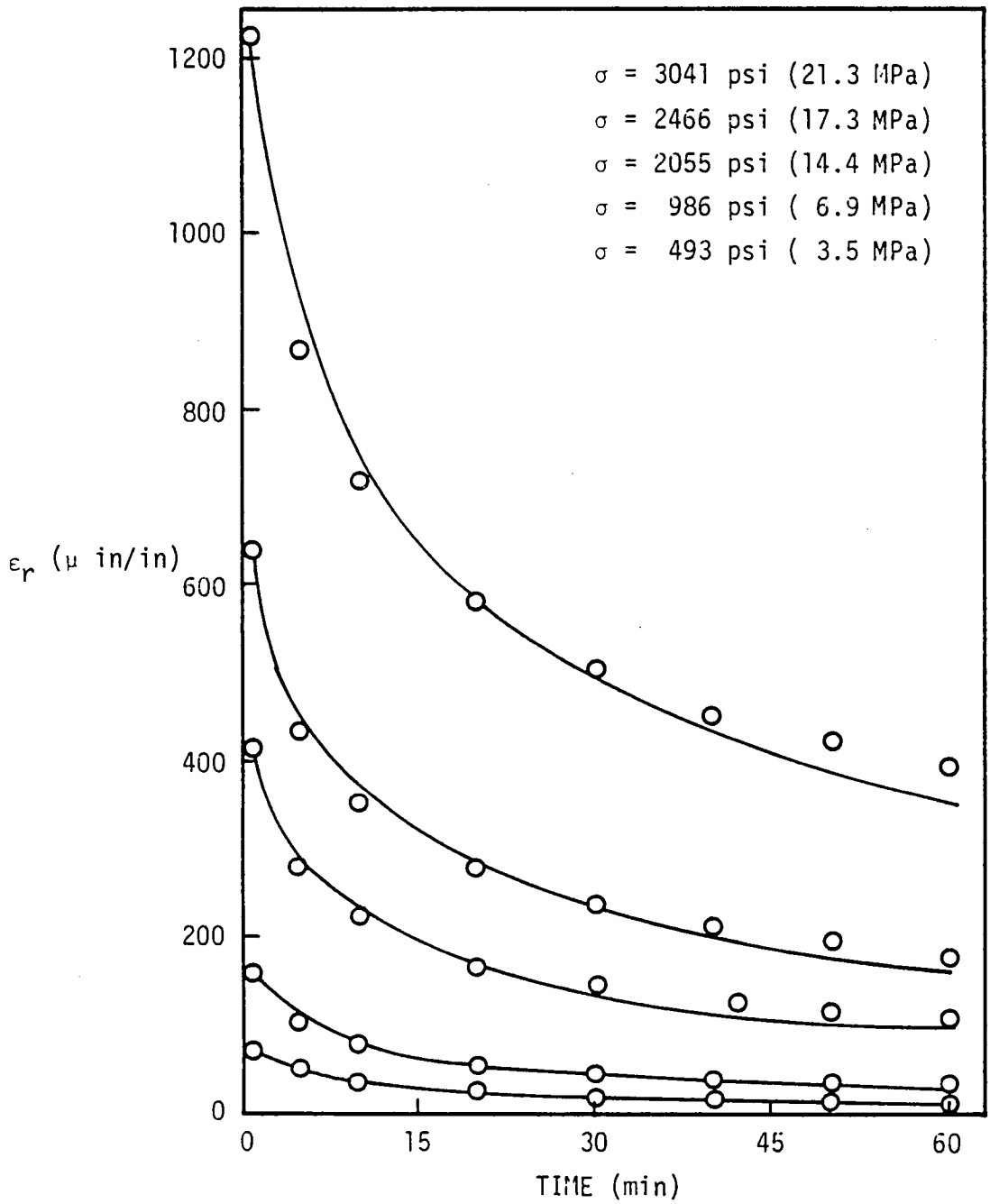

Figure 12 Experimental creep recovery data (symbols) and the corresponding Schapery fit of the data (solid lines) for several stress levels at T = 30°C (86°F).

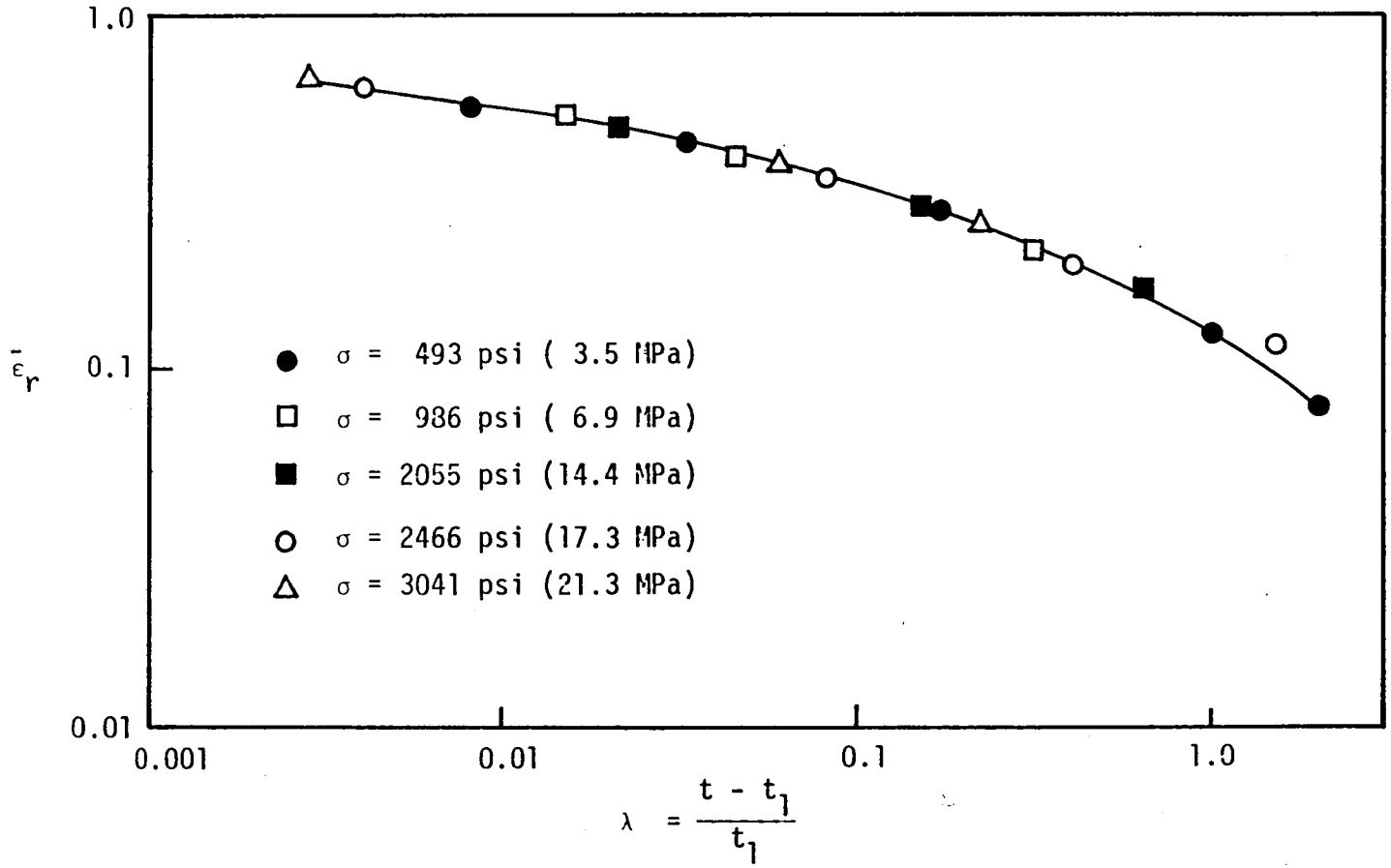

Figure 13. FM-73 master creep recovery curve, T = 30°C (86°F).

temperature. The data was analyzed and the seven material parameters were evaluated. Plots of these parameters obtained at this temperature exhibited large amounts of scatter, so much scatter in fact that fitting a curve to the results was not possible. Upon further investigation it was discovered that the creep and creep recovery strain values for any particular stress level at this temperature could not be reproduced with the desired accuracy.

There are many possible reasons that could account for the scatter mentioned above. These might be enumerated as;

- Fluctuations in temperature from test to test or during a test
- Absorption or evaporation of moisture between tests or during a test
- Experimental error
- Data reduction error

In fact, the scatter might be attributable to a combination of all of these items. For example, it is well known that moisture may lower the T_g by a substantial amount. If such were the case, test temperatures of 50 or 60°C could be in or near the transition region of the material where the modulus varies by a large amount, giving rise to errors in measurement. Also, as a test progresses, the specimen is continually drying out, thereby essentially raising the transition point and inducing further error. In addition, the Schapery method requires high accuracy in measuring transient response. Thus, the problems might be attributable to the accuracy involved in obtaining recovery strains and the data reduction related thereto.

Modified Schapery Approach for FM-300 Adhesive Characterization

The modified epoxy adhesive, FM-300, was found to exhibit viscoelastic creep and creep recovery phenomena at all temperature levels. Isochronous stress-strain results for FM-300 at 26°C (79°F) are given in Figure 14. For reasons presented previously, the lowest stress level employed, 452 psi (3.17 MPa), was assumed to be the upper limit of linear response for each of the six temperatures considered.

Note that according to both the Schapery and Findley methods the instantaneous value of the creep strain, ε_0, is a curve fitting parameter which may be evaluated by our computer program and is not an experimental data point. Figure 15 shows the variation of the "theoretical" transient creep strain, $\Delta\varepsilon_1$, with temperature, where $\Delta\varepsilon_1$ is defined as the creep strain at 30 minutes (ε_{30}) minus the initial creep strain (ε_0), as determined by the computer program. Inspection of Figure 15 will verify that ε_0 is a curve fitting parameter only, inasmuch as the results for $\Delta\varepsilon_1$ do not follow observed experimental trends such as that of Figure 16. Figure 16 shows the variation of the "approximate experimental" transient creep strain, $\Delta\varepsilon$, with temperature, where $\Delta\varepsilon$ is defined as the creep strain at 30 minutes (ε_{30}) minus the creep strain at 15 seconds ($\varepsilon_{0.25}$). Figure 16 indicates an increase in transient creep strain with an increase in temperature for a given stress level. This result is in agreement with well known behavior of viscoelastic materials.

It was mentioned in Chapter 3 that the original computerized Schapery procedure in which the power law exponent, n, is determined from linear recovery data was found to give inconsistent results.

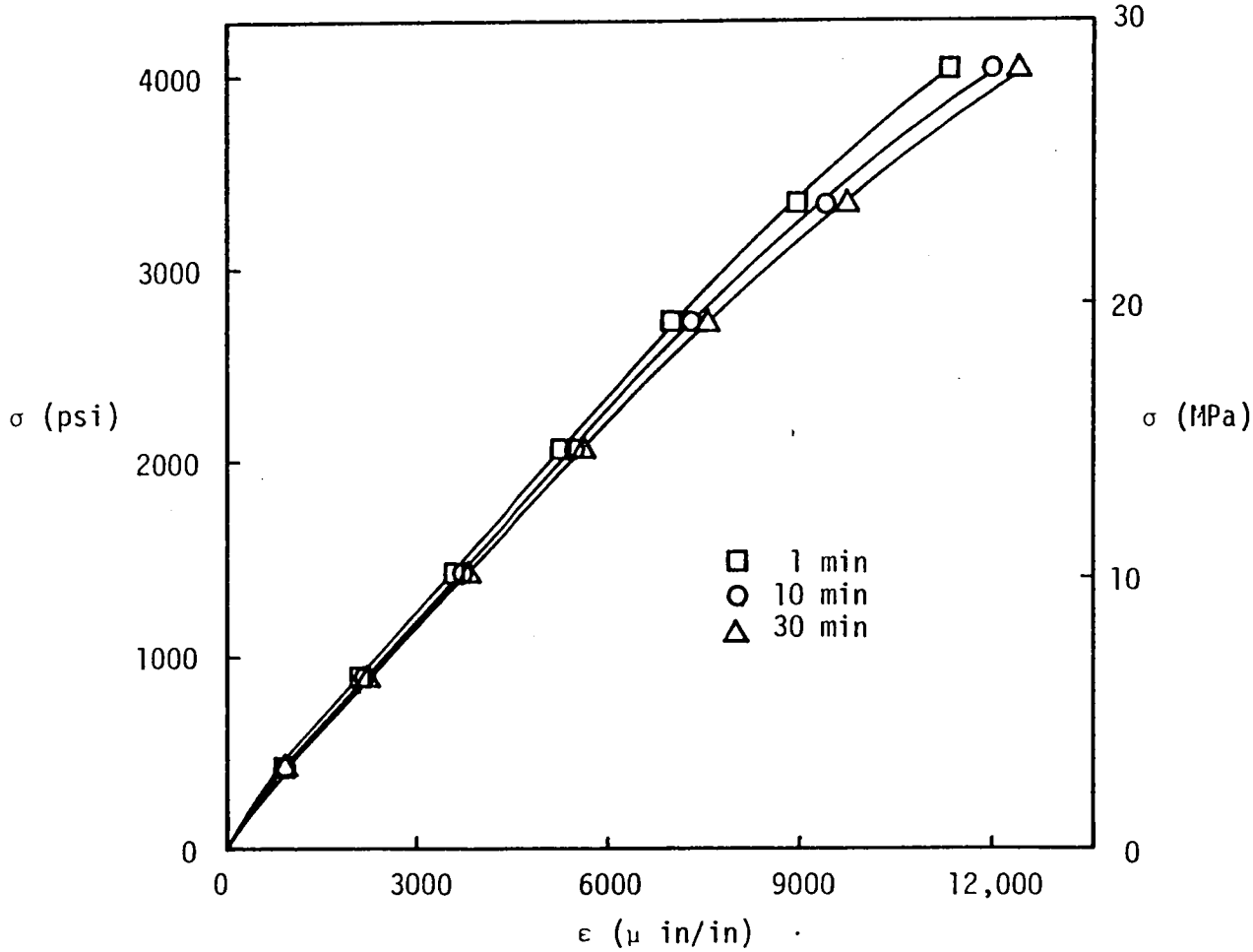

Figure 14. FM-300 isochronous stress-strain plot, T = 26°C (79°F).

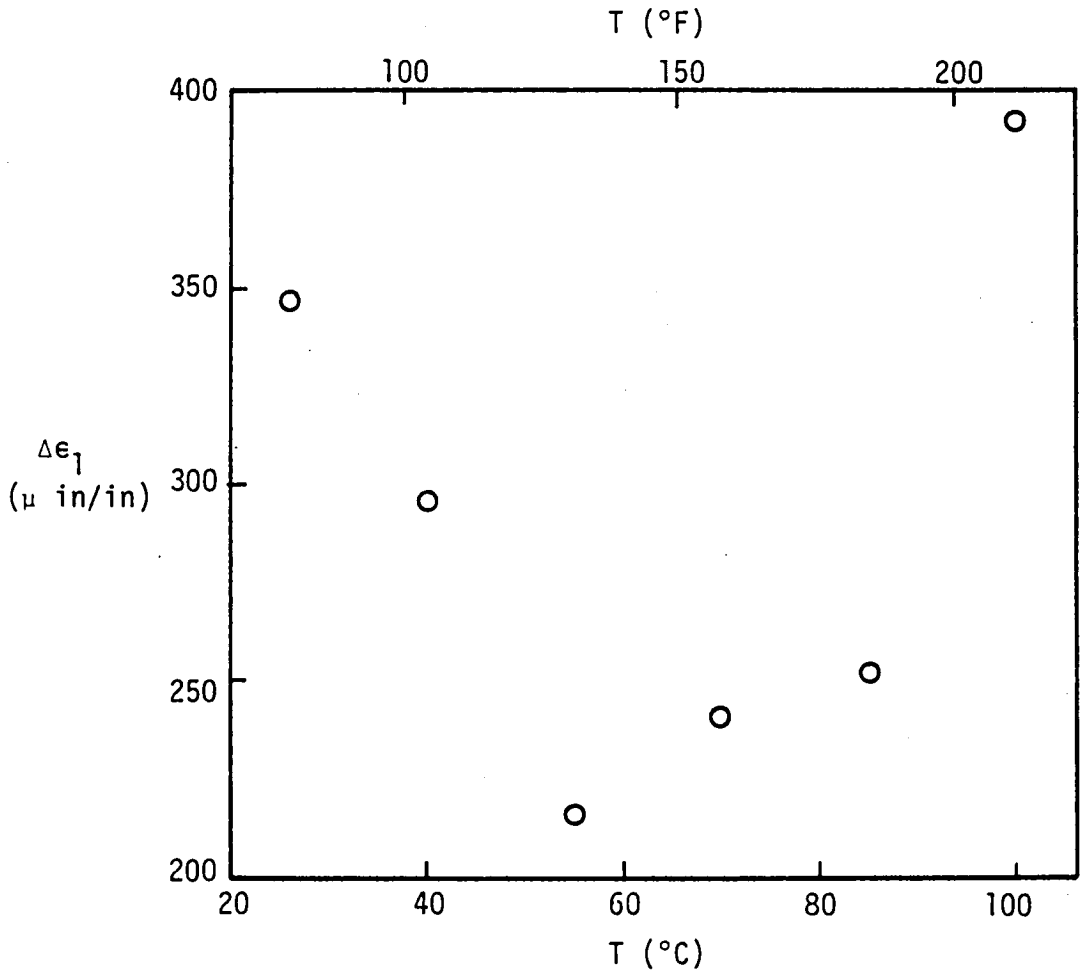

Figure 15. Theoretical transient creep strain, $\Delta\epsilon_1$ vs. temperature, σ = 452 psi (3.17 MPa).

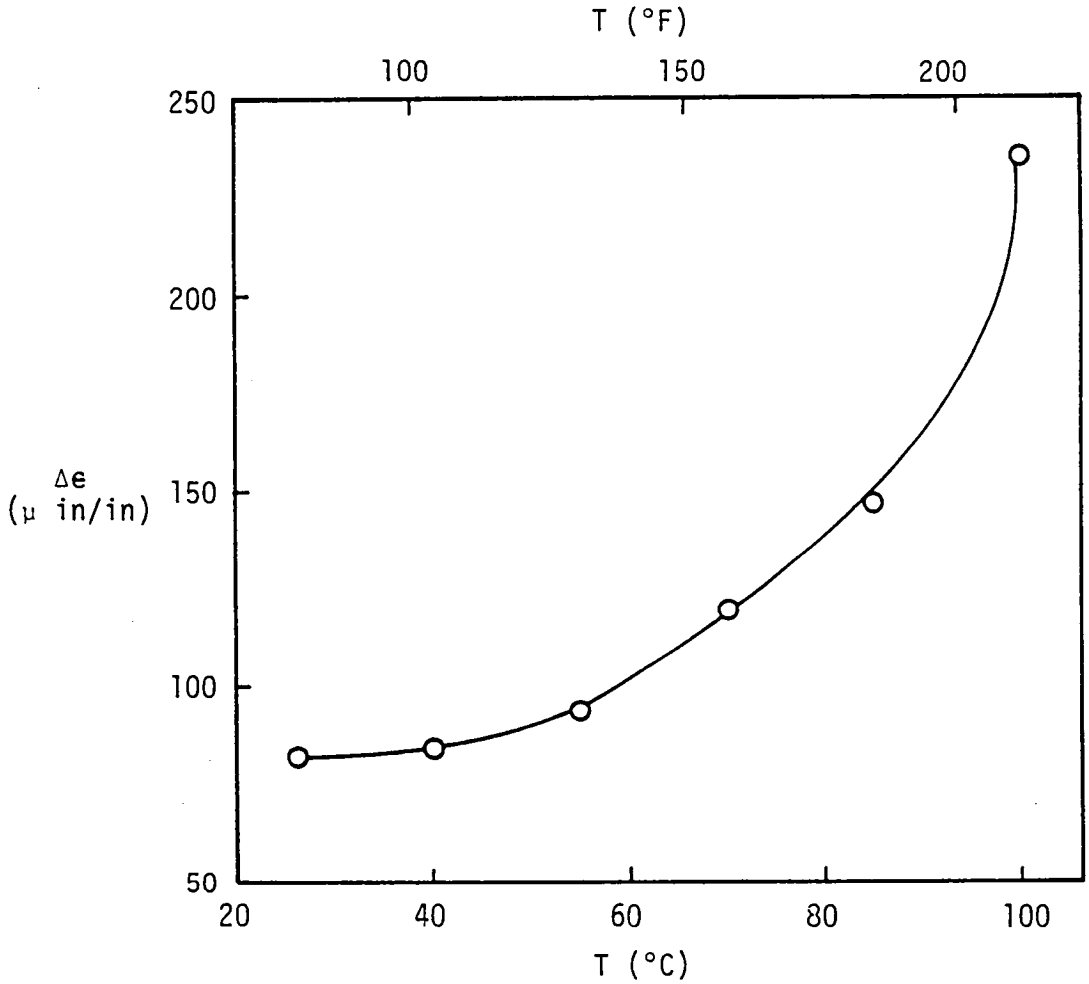

Figure 16. Approximate transient creep strain, $\Delta\varepsilon$ vs. temperature, σ = 452 psi (3.17 MPa).

The two stress invariant parameters, n and C, so determined, are plotted as a function of temperature in Figures 17 and 18, respectively. The fluctuation of the parameters was so severe that passing a curve through these results was not attempted. Since the goal of the current study was to be able to predict the Schapery parameters for a given temperature and stress level, it is obvious that this degree of fluctuation in the results was intolerable.

Further investigation revealed even greater inconsistencies. It was discovered that the n-value increased as the length of recovery data increased for a given length of creep. It was also determined that the n-value increased as the length of creep increased for a given length of recovery. In short, the power law exponent, n, is a function of both the length of creep and the length of recovery data analyzed. This fact is quite distressing, for it implies that no unique value of the power law exponent, n, exists. This observation could be in fact consistent with the Schapery analysis wherein the reduced time parameters ψ and ψ' might be functions of time.

The author wishes to emphasize that the discussion of the difficulties with the power law used in the computerized version of the "conventional" Schapery procedure is relevant only for the FM-300 material system considered herein, and is in no way a statement of the accuracy of the numerical algorithm itself. The computerized "conventional" Schapery method has been used successfully by Hiel [61] for the characterization of a 934 "neat epoxy resin" used in making composite laminates. He also characterized the viscoelastic properties of a unidirectional T300/934 graphite/epoxy laminate in the same study.

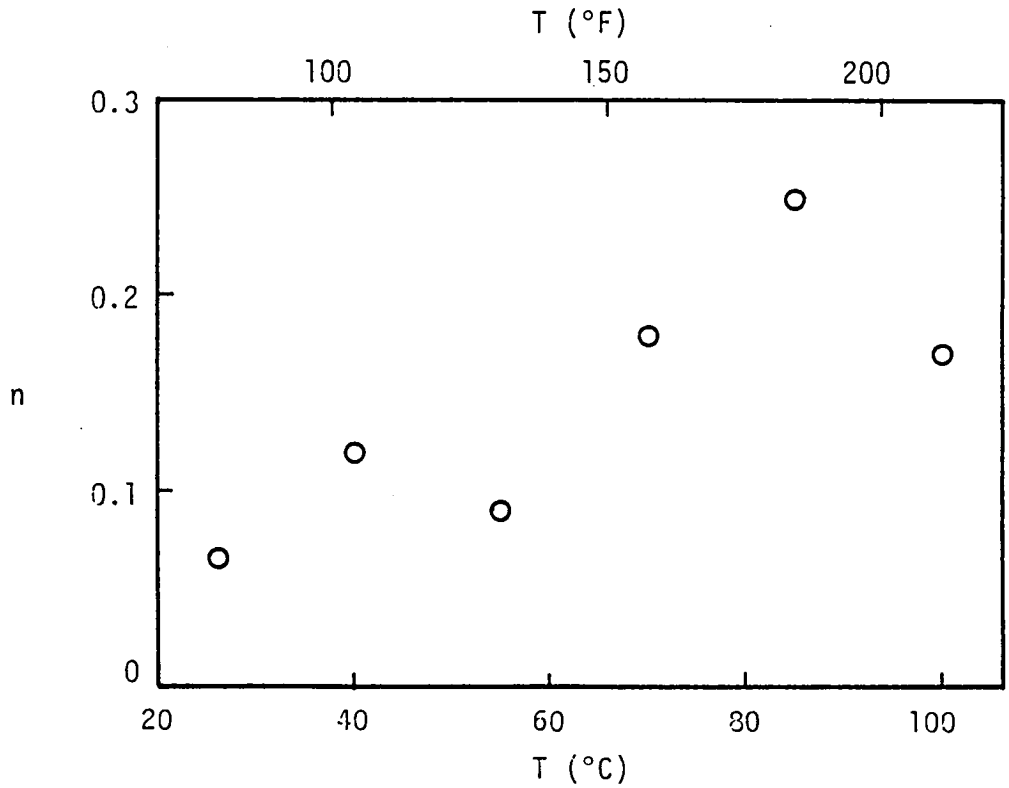

Figure 17. Power law exponent, n vs. temperature, as determined via the "conventional" Schapery procedure, σ = 452 psi (3.17 MPa).

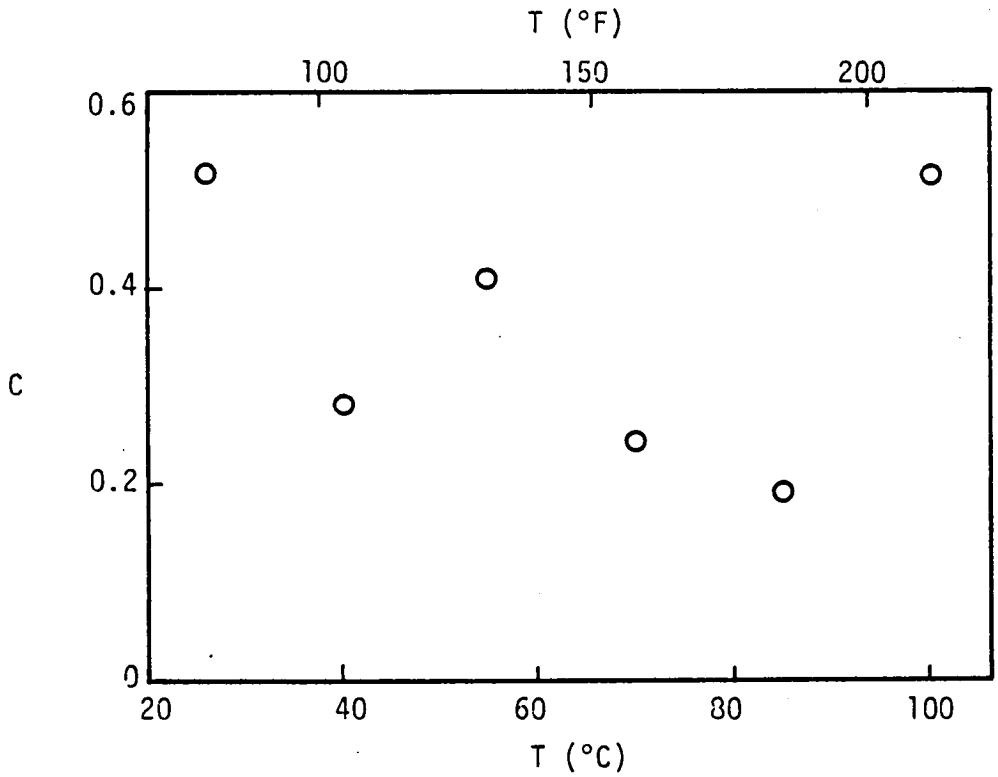

Figure 18. Stress invariant parameter, C vs. temperature, as determined via the "conventional" Schapery procedure, σ = 452 psi (3.17 MPa).

Modified Findley Approach for FM-300 Characterization

In order to stabilize the variation of the n-value with temperature, the "modified" Findley computer approach given in Chapter 3 was employed. That is, the power law exponent was determined from creep rather than recovery data. The variation of the parameters, n, C, and ε_0, with temperature, as determined by this approach, are shown in Figures 19-21, respectively. The variation of the n-value with temperature of Figure 19 is obviously more acceptable than that of Figure 17. From this point on, Figure 19 is to be used for determining the n-value for a given temperature.

All of the remaining parameters necessary to evaluate the creep and creep recovery response of FM-300 within the temperature range between room temperature and 100°C (212°F) are plotted in Figures 22-45. The instantaneous creep strain, ε_0, is plotted as a function of stress for each of the six temperature levels considered in Figures 22-27. Recall that ε_0 is a curve fitting parameter only and has no experimental verification. The creep coefficient, C', plotted as a function of stress for the six temperature levels, is shown in Figures 28-33. Variation of the vertical shift factor, $\Delta\varepsilon_1/g_1$, is shown in Figures 34-39, while the behavior of the horizontal shift factor, a_σ, is detailed in Figures 40-45.

The nonlinear parameters, g_0, g_1, and g_2, are shown plotted as a function of stress for various temperatures in Figures 46-57. These figures are included for inspection purposes only, as they are not utilized in any of the numerical calculations in the next section.

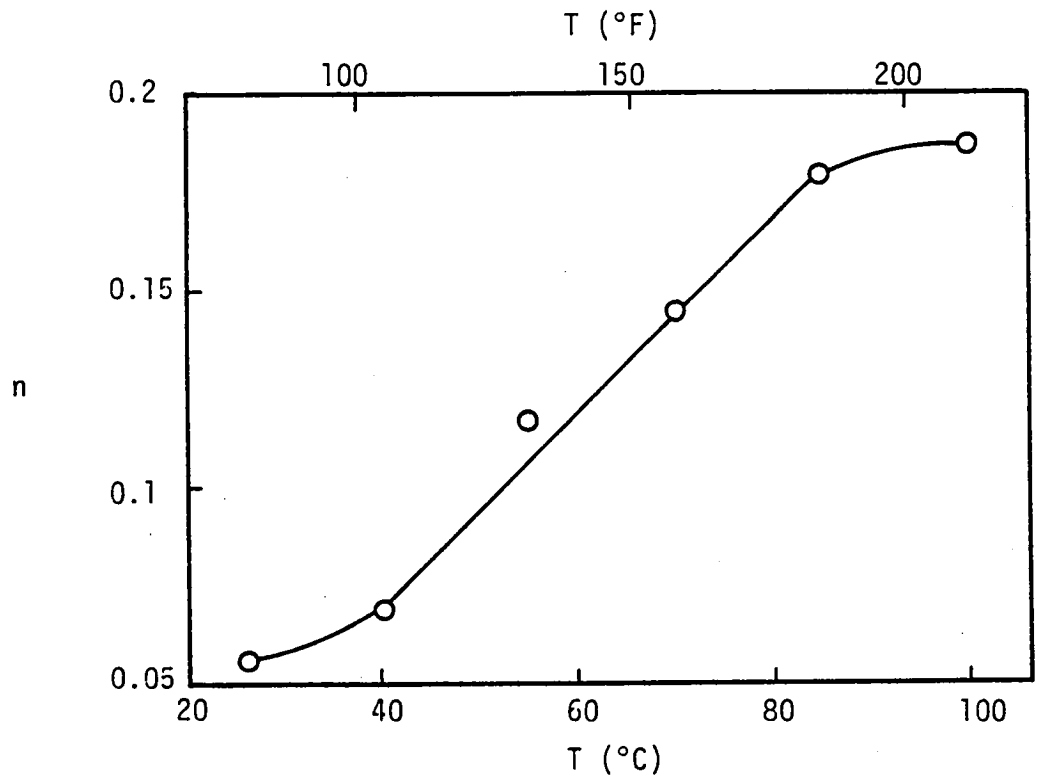

Figure 19. Power law exponent, n vs. temperature, as determined via the "modified" Schapery procedure, σ = 452 psi (3.17 MPa).

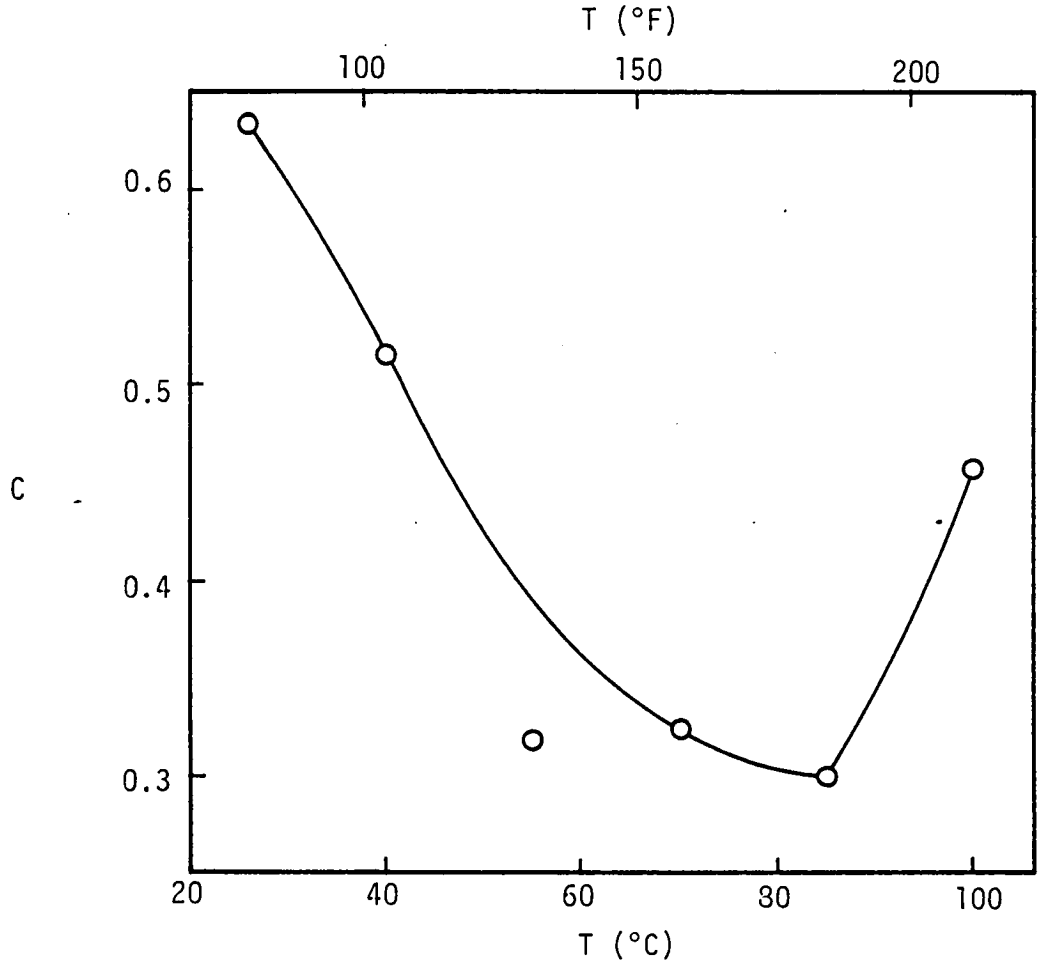

Figure 20. Stress invariant parameter, C vs. temperature, as determined via the "modified" Schapery procedure, σ = 452 psi (3.17 MPa).

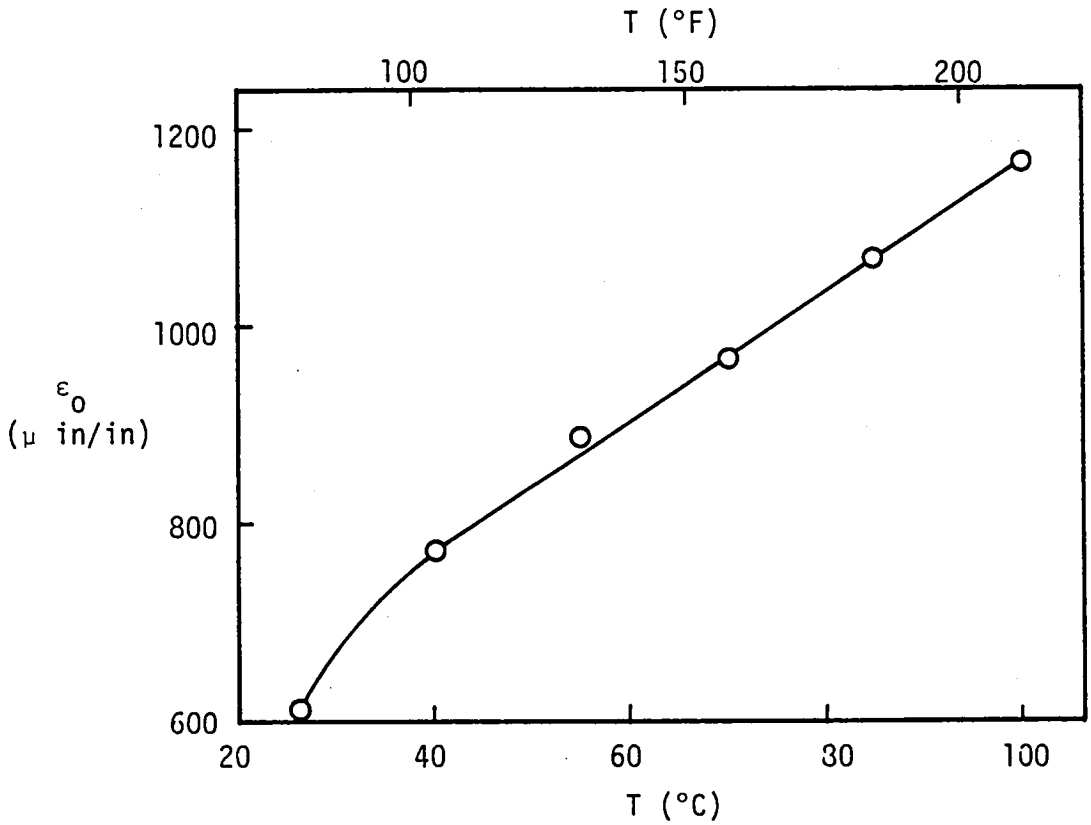

Figure 21. Instantaneous creep strain, ε_o vs. temperature, σ = 452 psi (3.17 MPa).

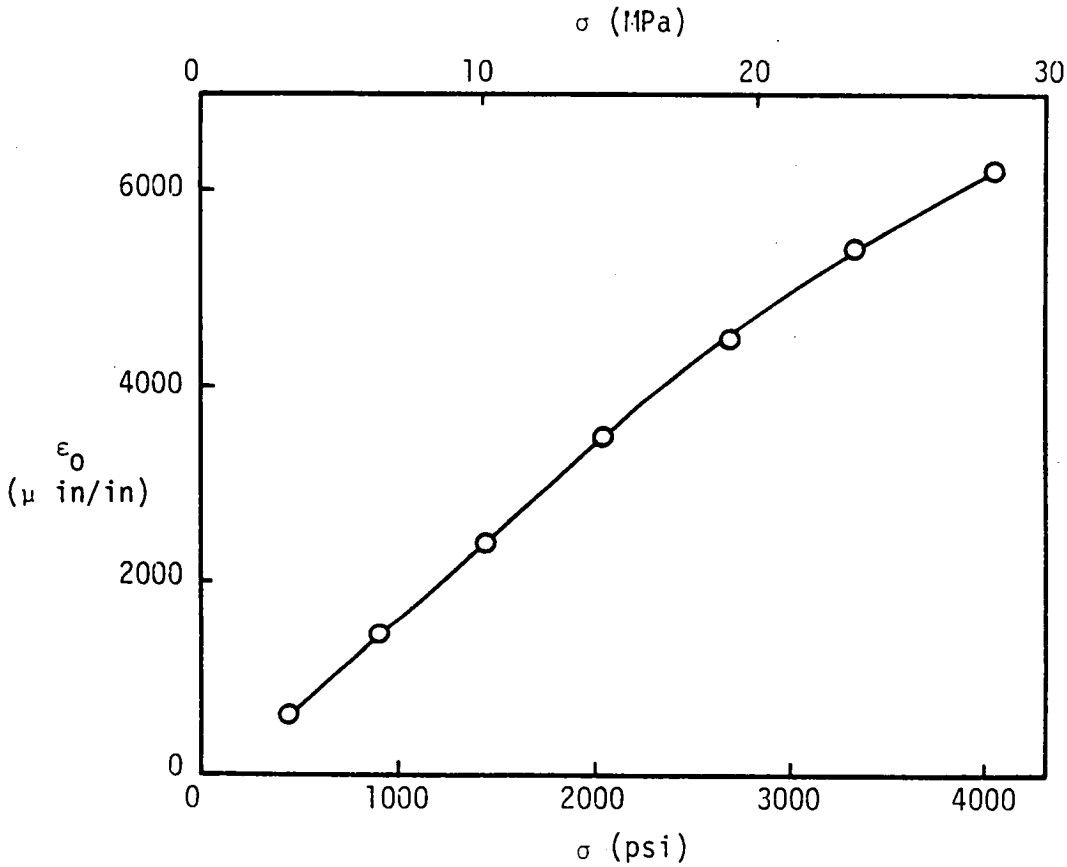

Figure 22. Instantaneous creep strain, ε_o vs. stress, T = 26°C (79°F).

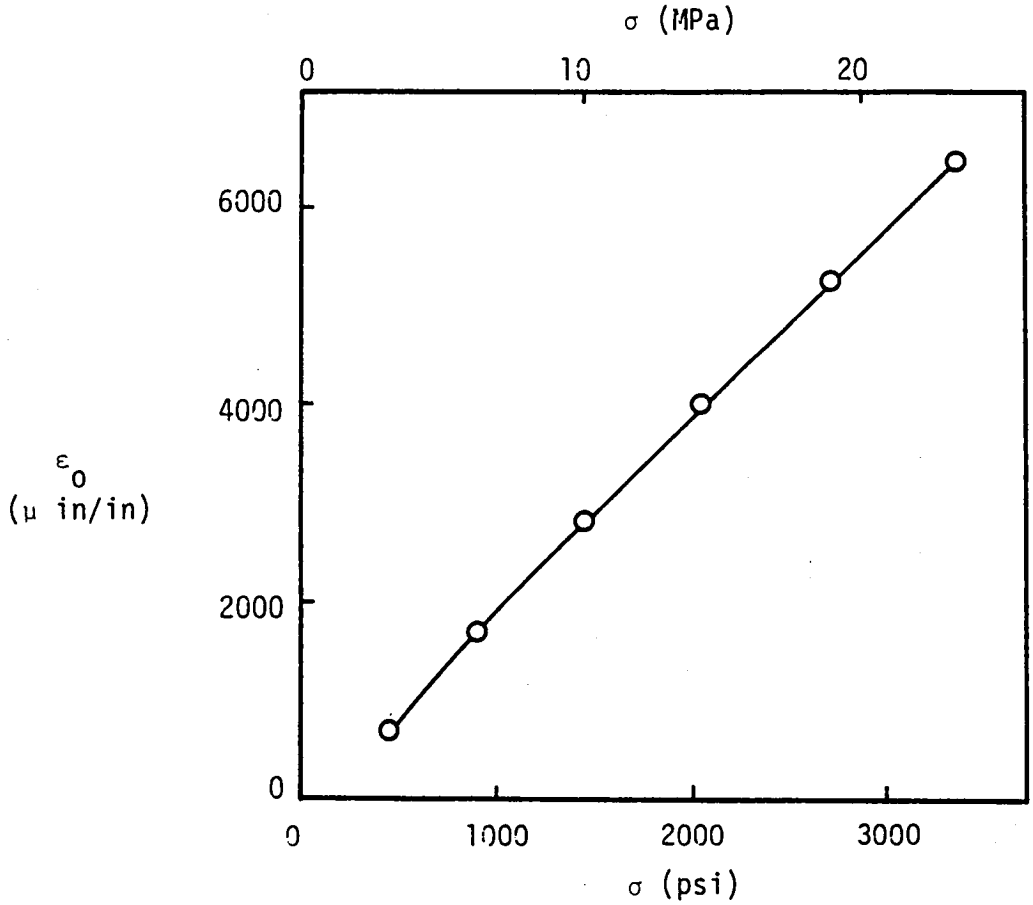

Figure 23. Instantaneous creep strain, ε_o vs. stress, T = 40°C (104°F).

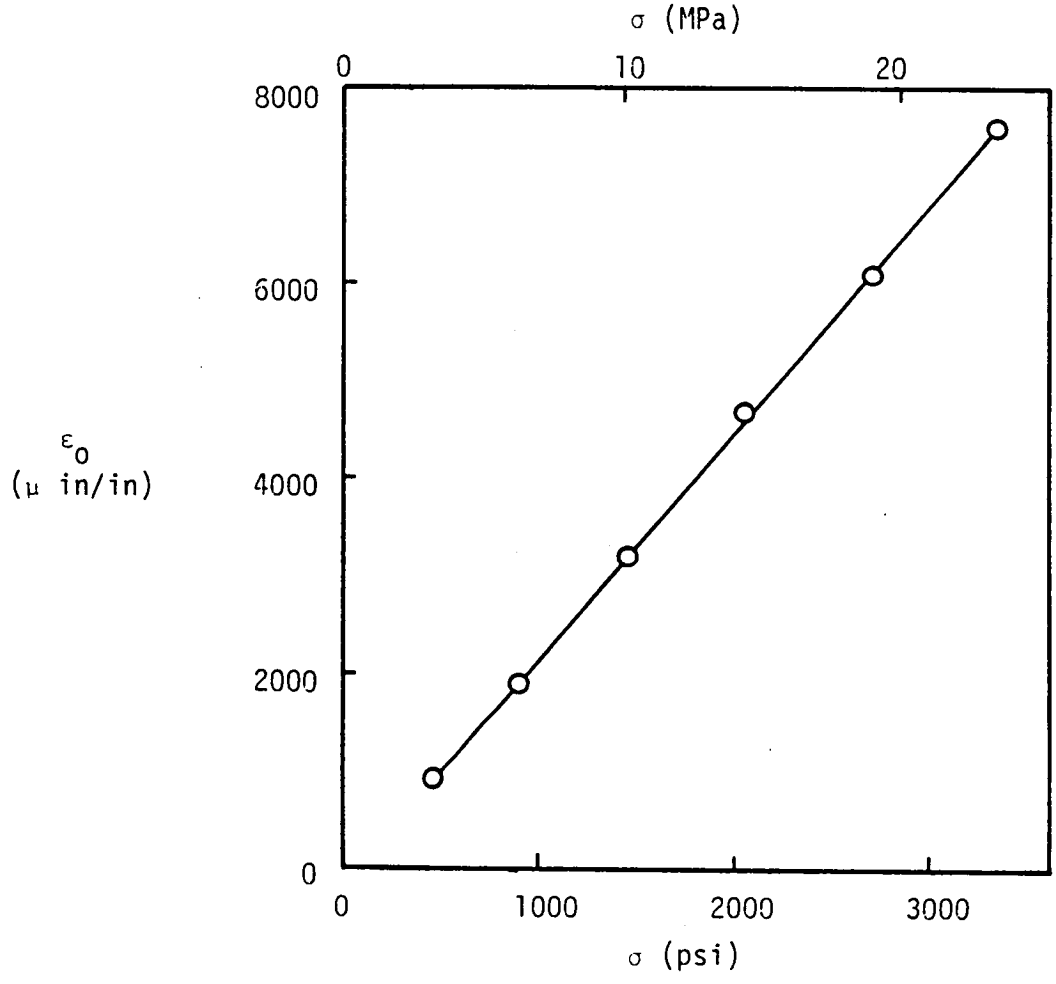

Figure 24. Instantaneous creep strain, ε_o vs. stress, T = 55°C (131°F).

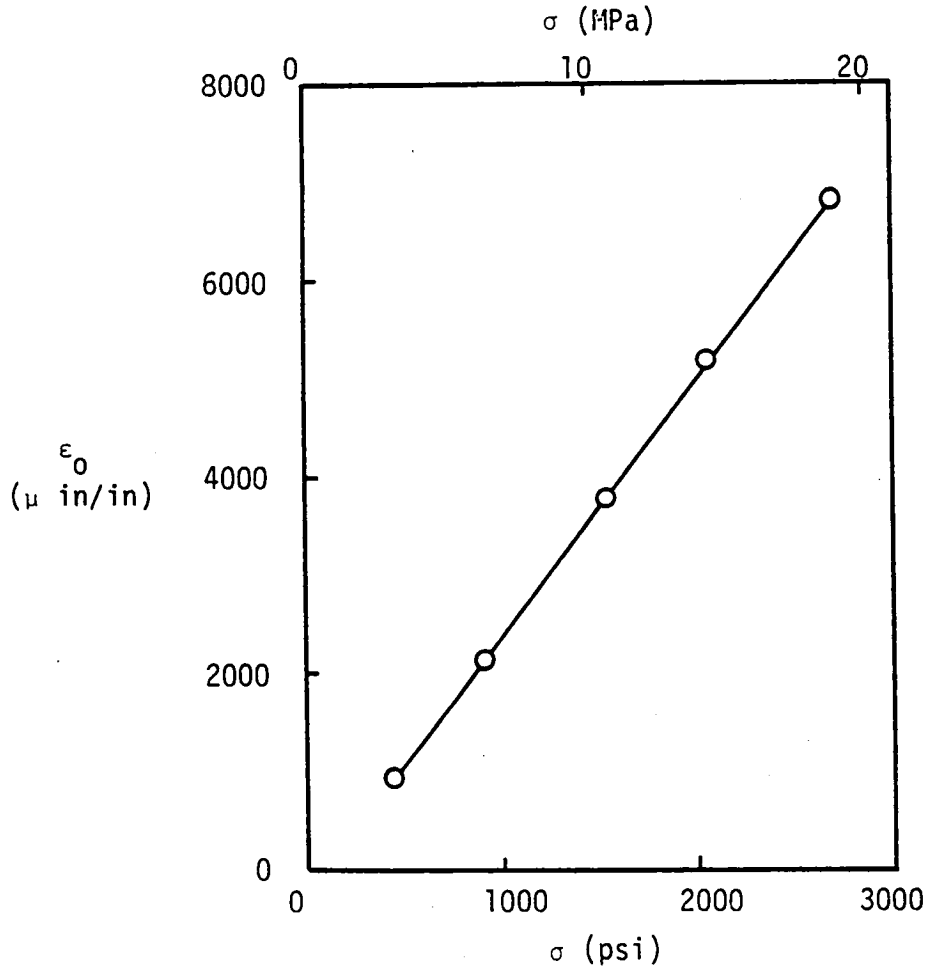

Figure 25. Instantaneous creep strain, ε_o vs. stress, T = 70°C (158°F).

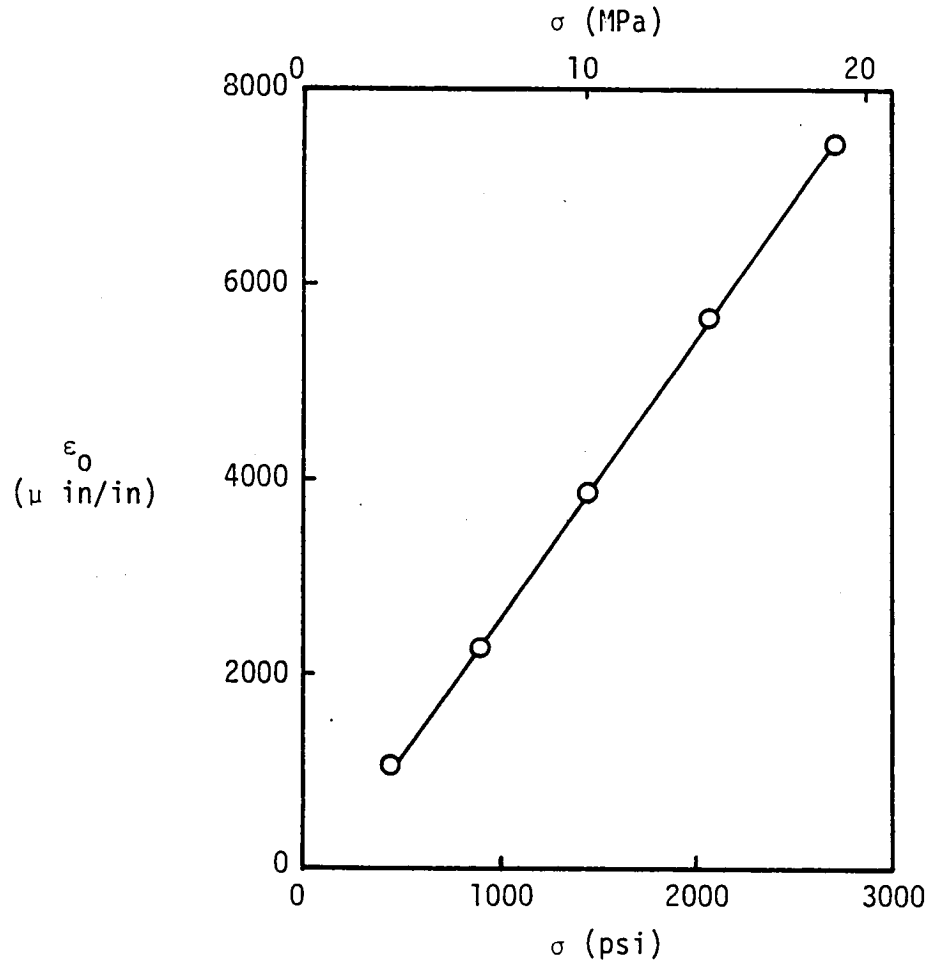

Figure 26. Instantaneous creep strain, ε_o vs. stress, T = 85°C (185°F).

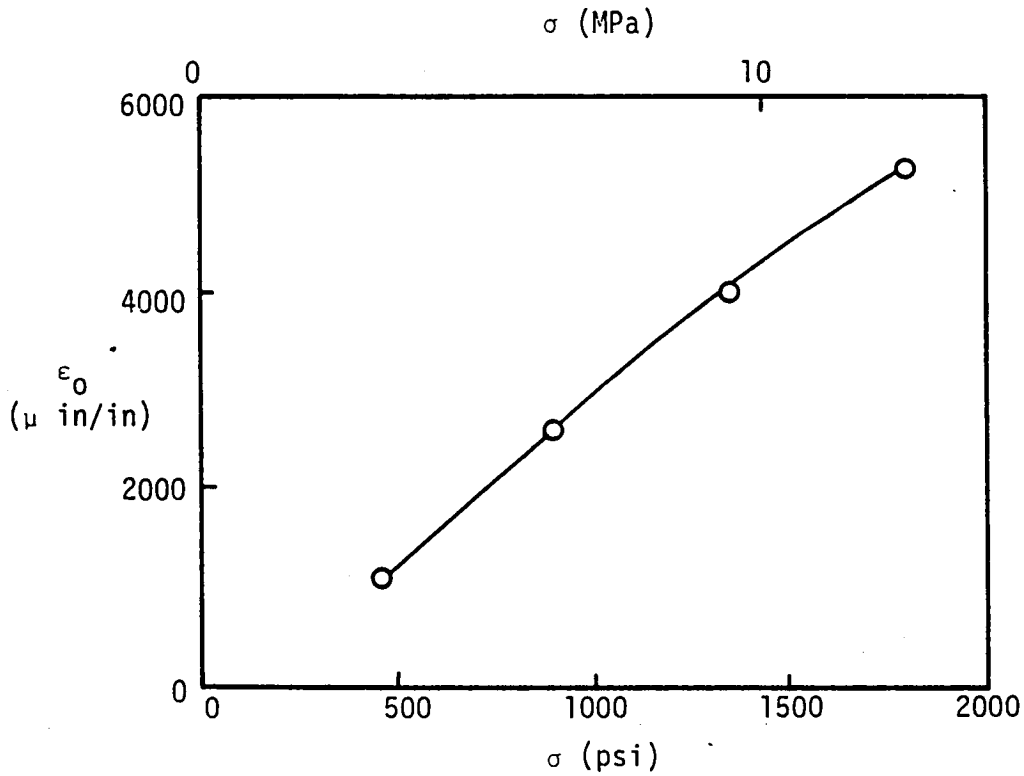

Figure 27. Instantaneous creep strain, ε_o vs. stress, T = 100°C (212°F).

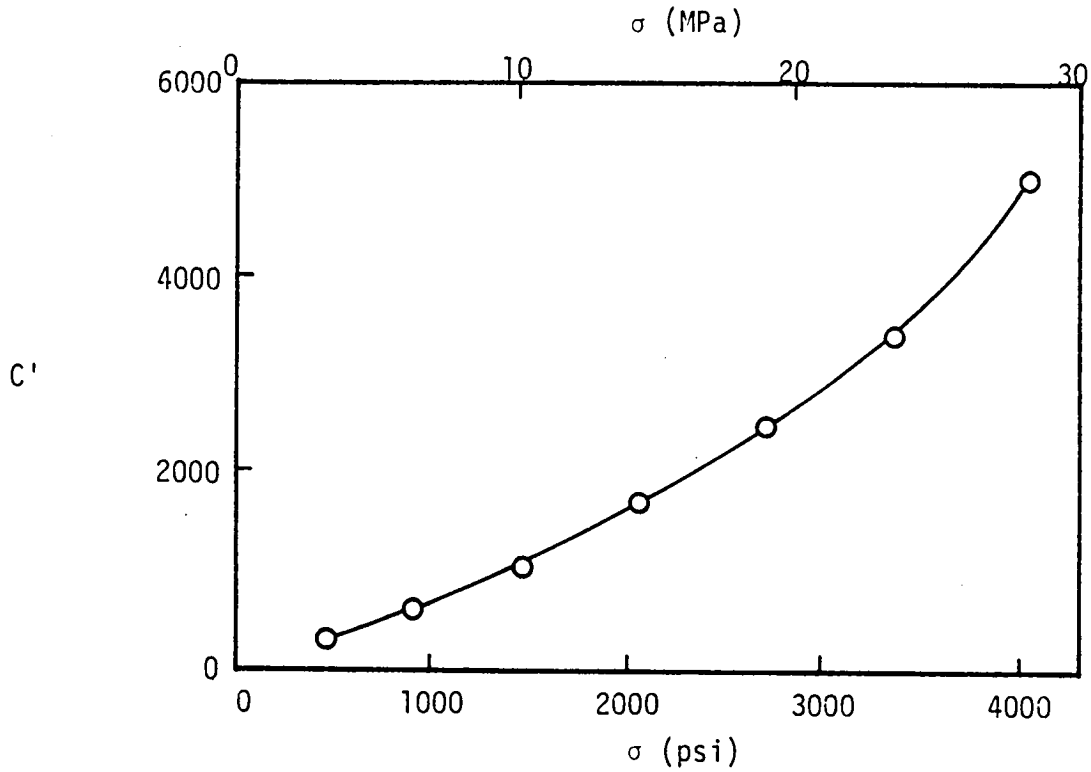

Figure 28. Creep coefficient, C' vs. stress, T = 26°C (79°F).

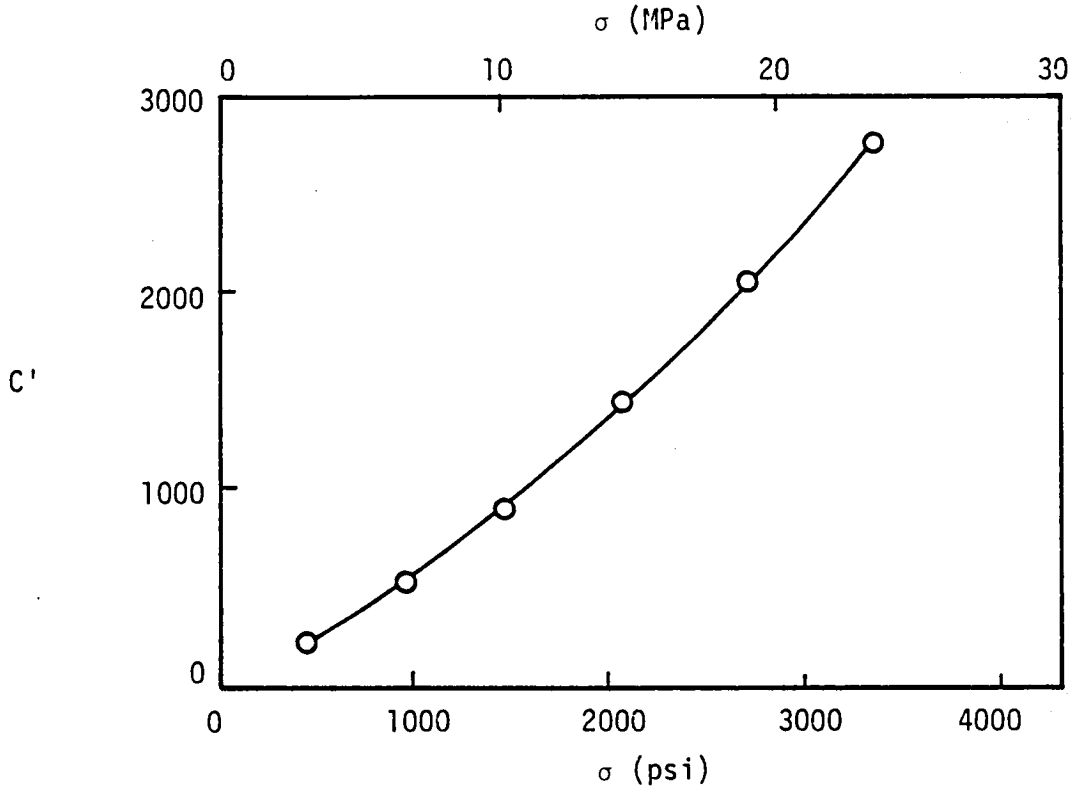

Figure 29. Creep coefficient, C' vs. stress, T = 40°C (104°F).

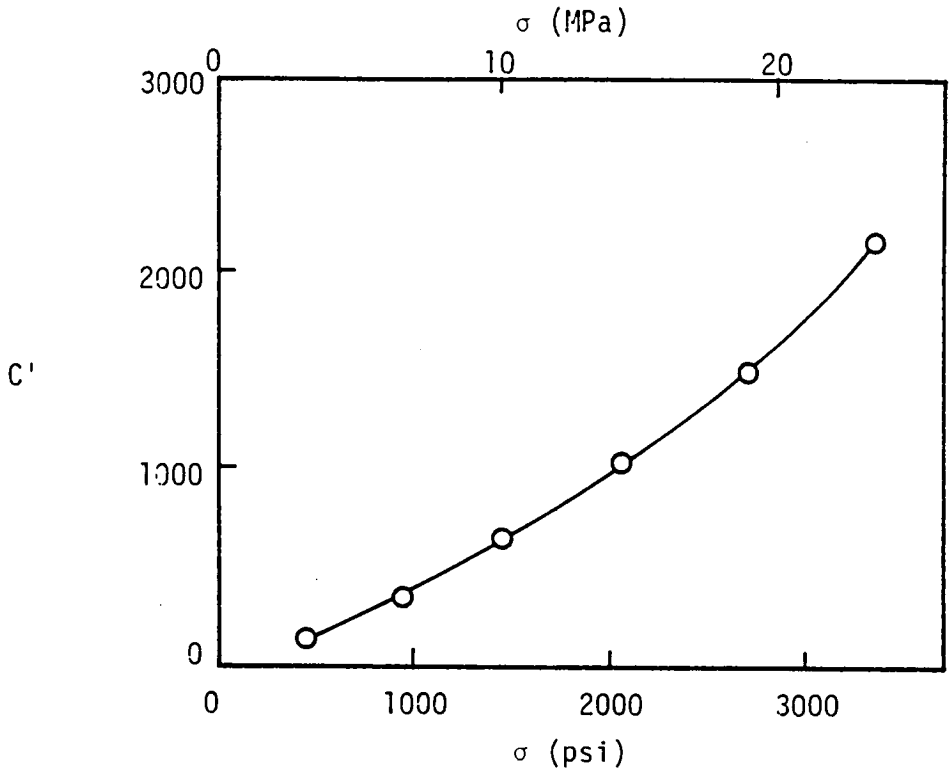

Figure 30. Creep coefficient, C' vs. stress, T = 55°C (131°F).

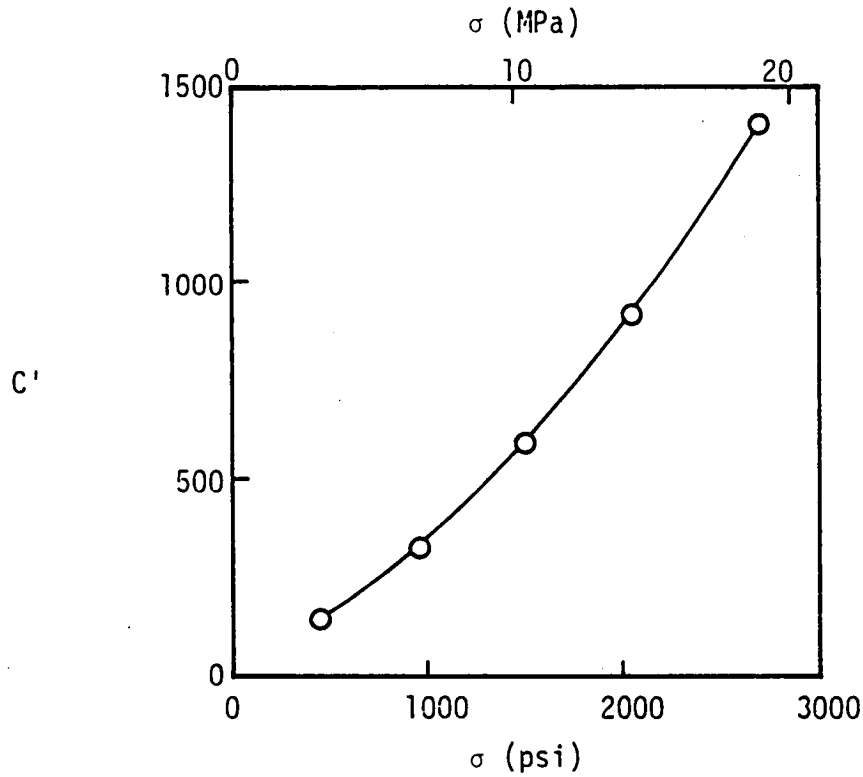

Figure 31. Creep coefficient, C' vs. stress, T = 70°C (158°F).

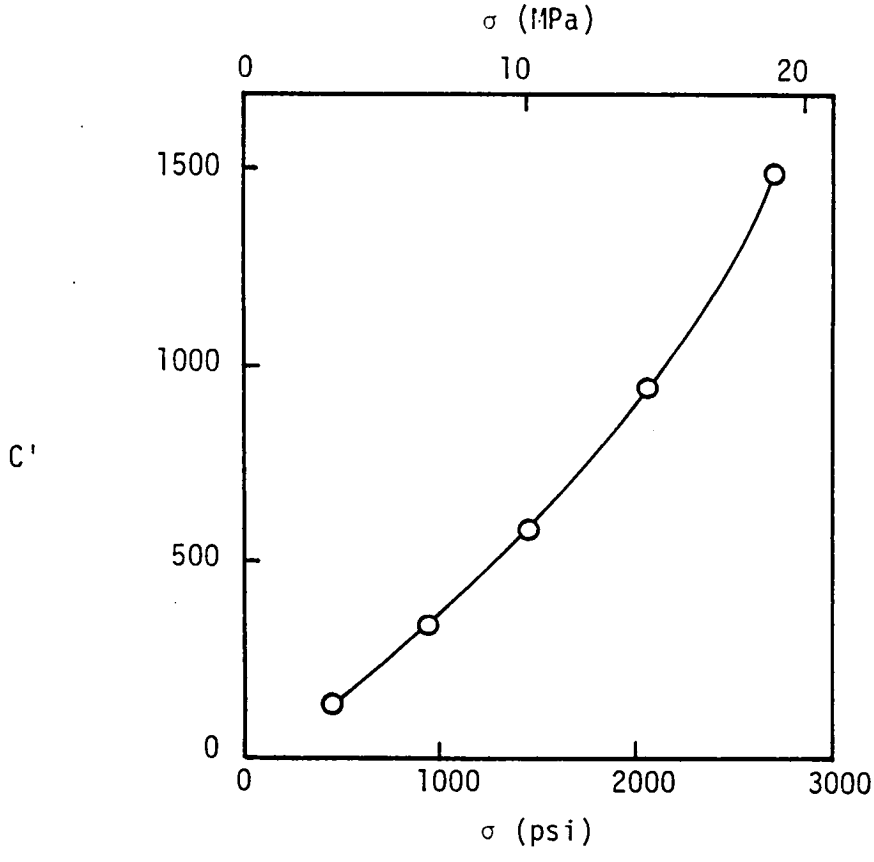

Figure 32. Creep coefficient, C' vs. stress, T = 85°C (185°F).

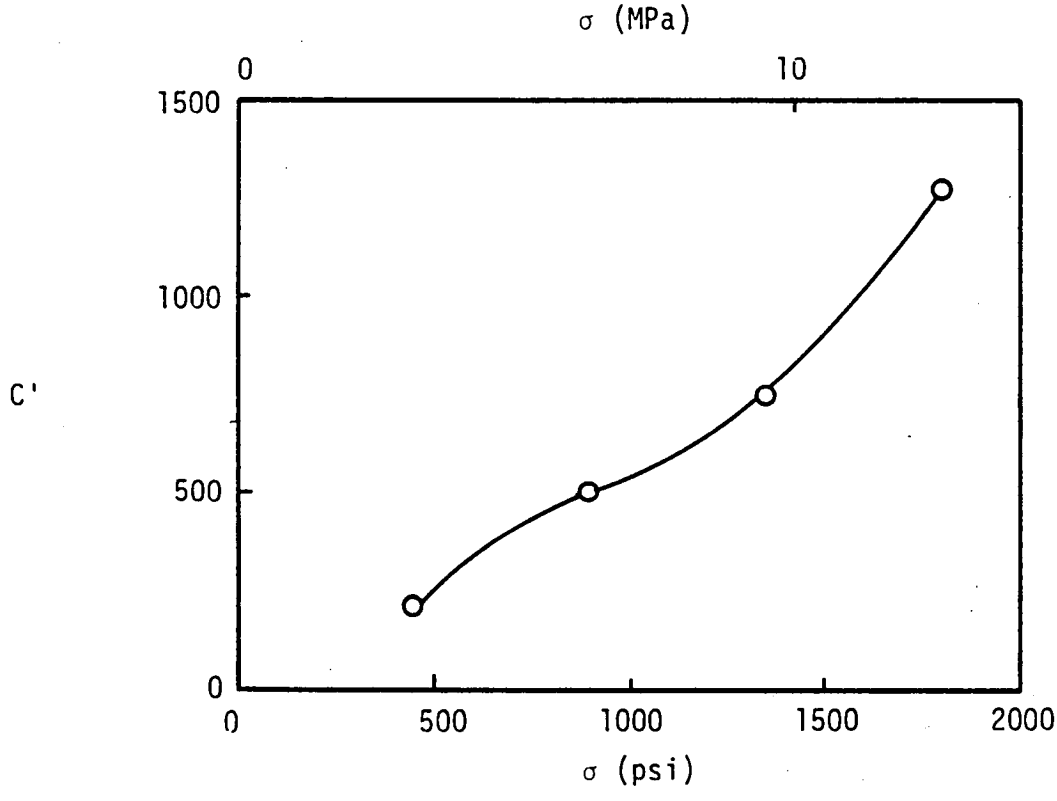

Figure 33. Creep coefficient, C' vs. stress, T = 100°C (212°F).

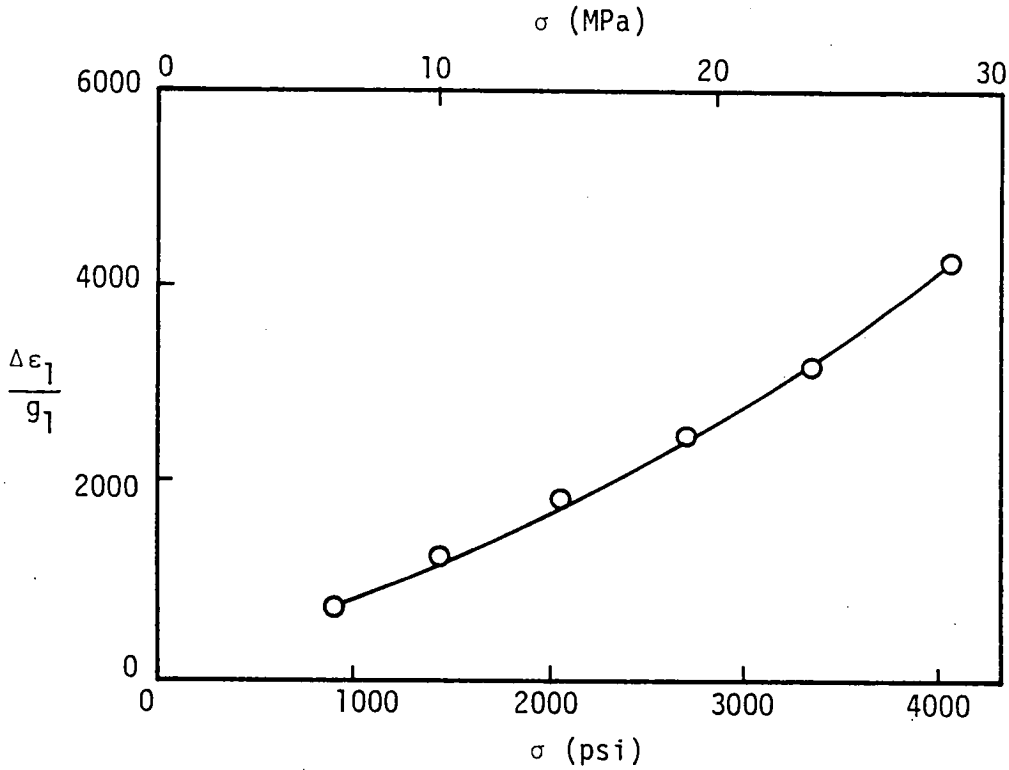

Figure 34. Vertical shift function, $\Delta\varepsilon_1/g_1$ vs. stress, T = 26°C (79°F).

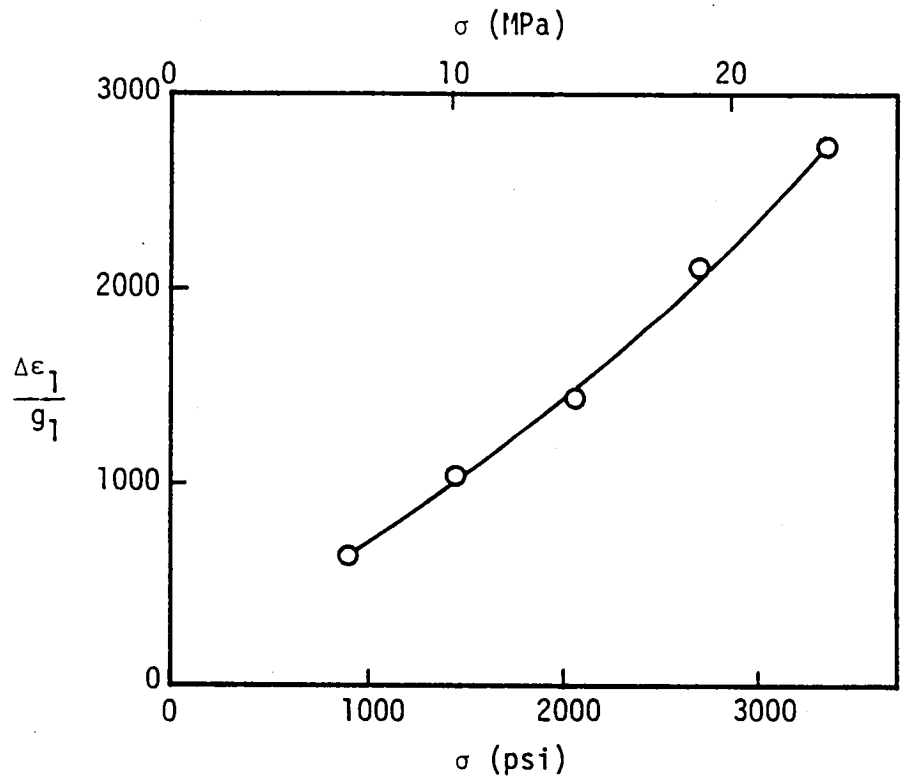

Figure 35. Vertical shift function, $\Delta\epsilon_1/g_1$ vs. stress, T = 40°C (104°F).

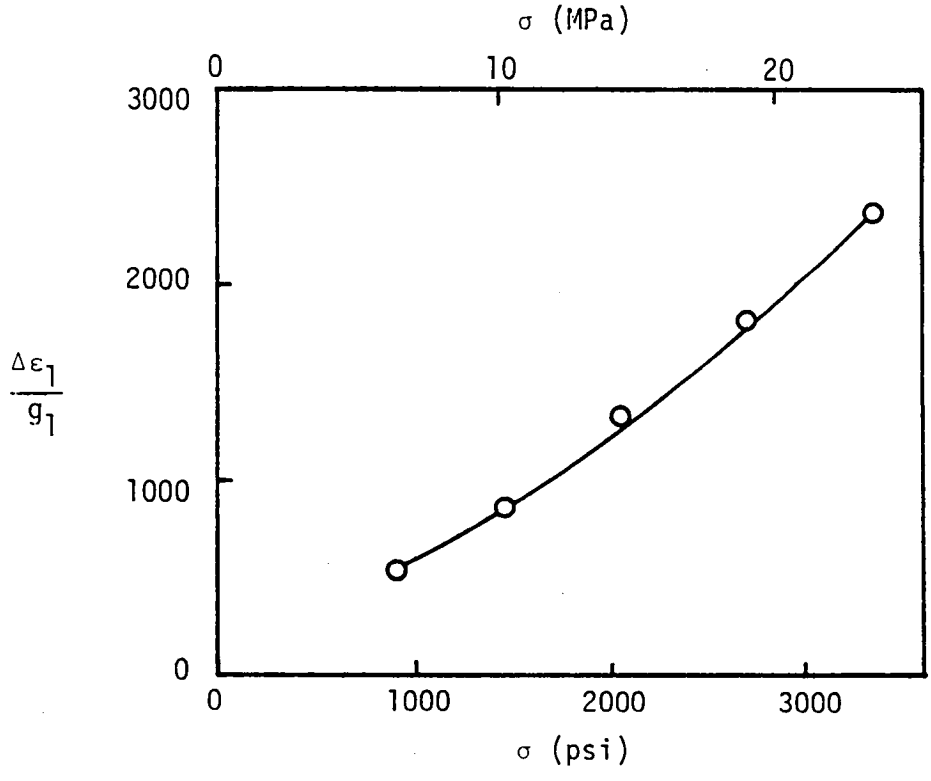

Figure 36. Vertical shift function, $\Delta\varepsilon_1/g_1$ vs. stress, T = 55°C (131°F).

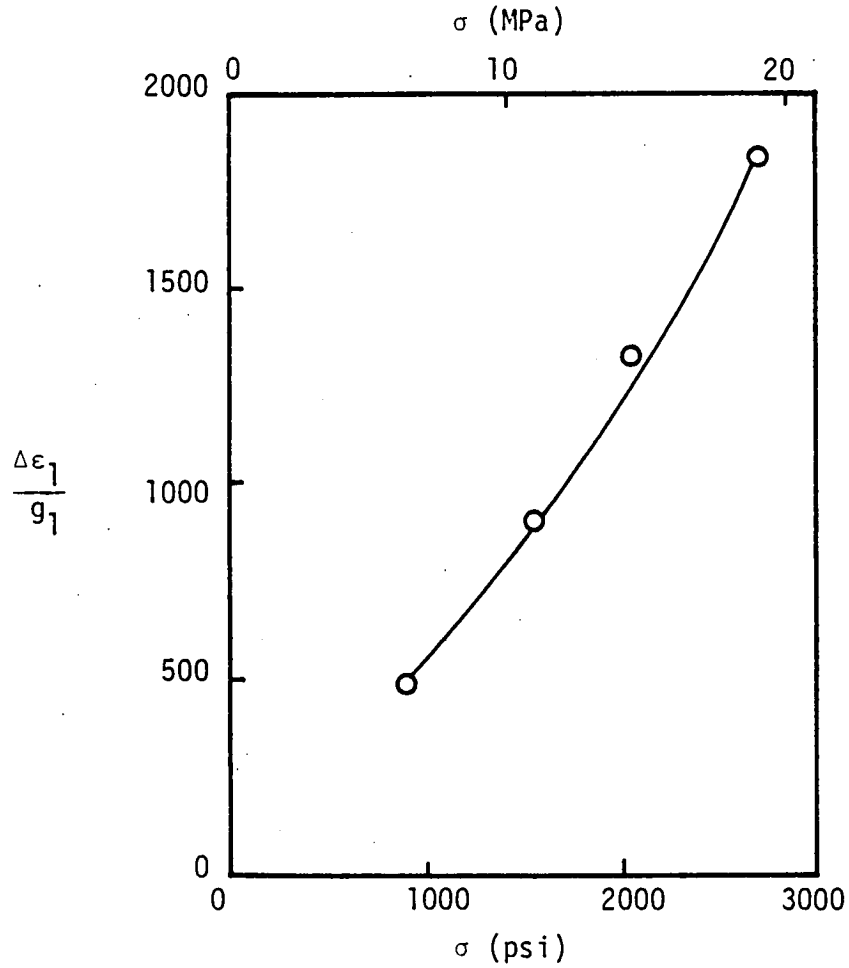

Figure 37. Vertical shift function, $\Delta\varepsilon_1/g_1$ vs. stress, T = 70°C (158°F).

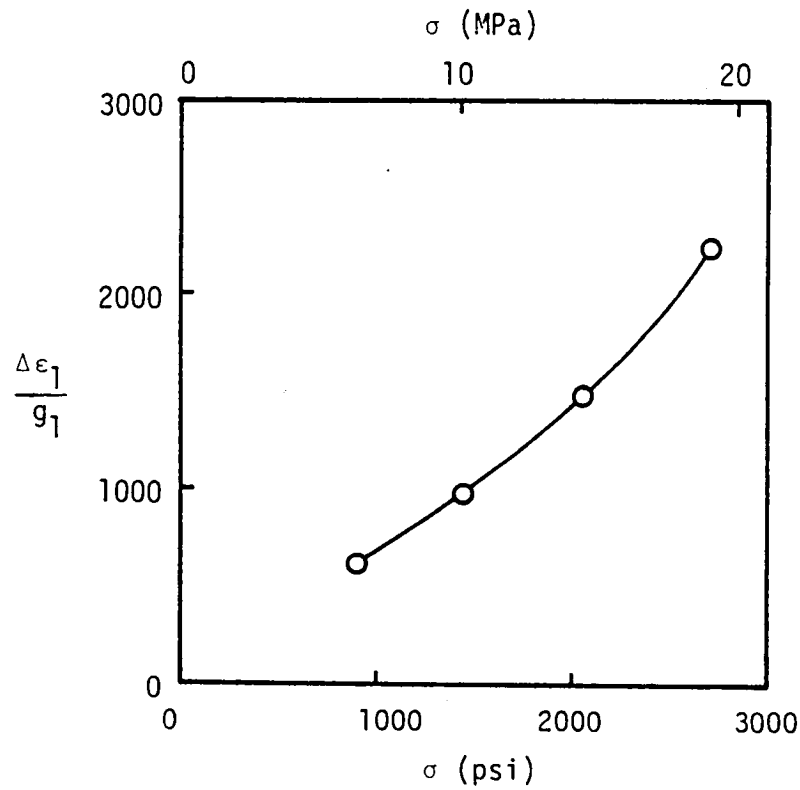

Figure 38. Vertical shift function, $\Delta\varepsilon_1/g_1$ vs. stress, T = 85°C (185°F).

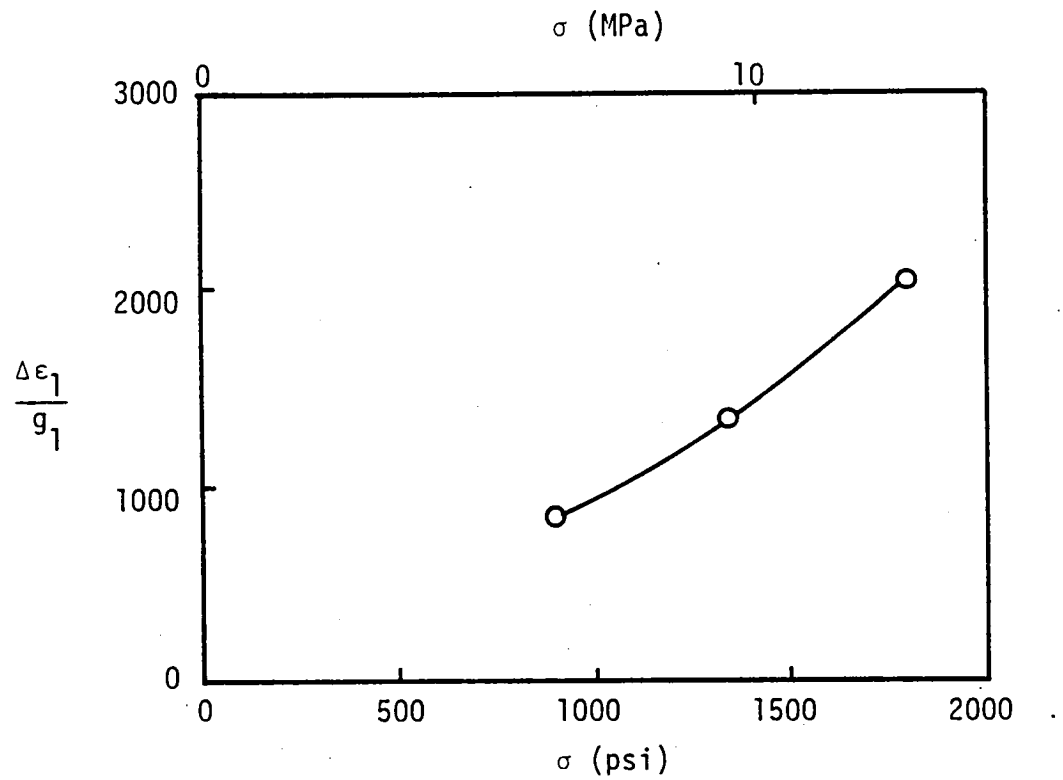

Figure 39. Vertical shift function, $\Delta\varepsilon_1/g_1$ vs. stress, T = 100°C (212°F).

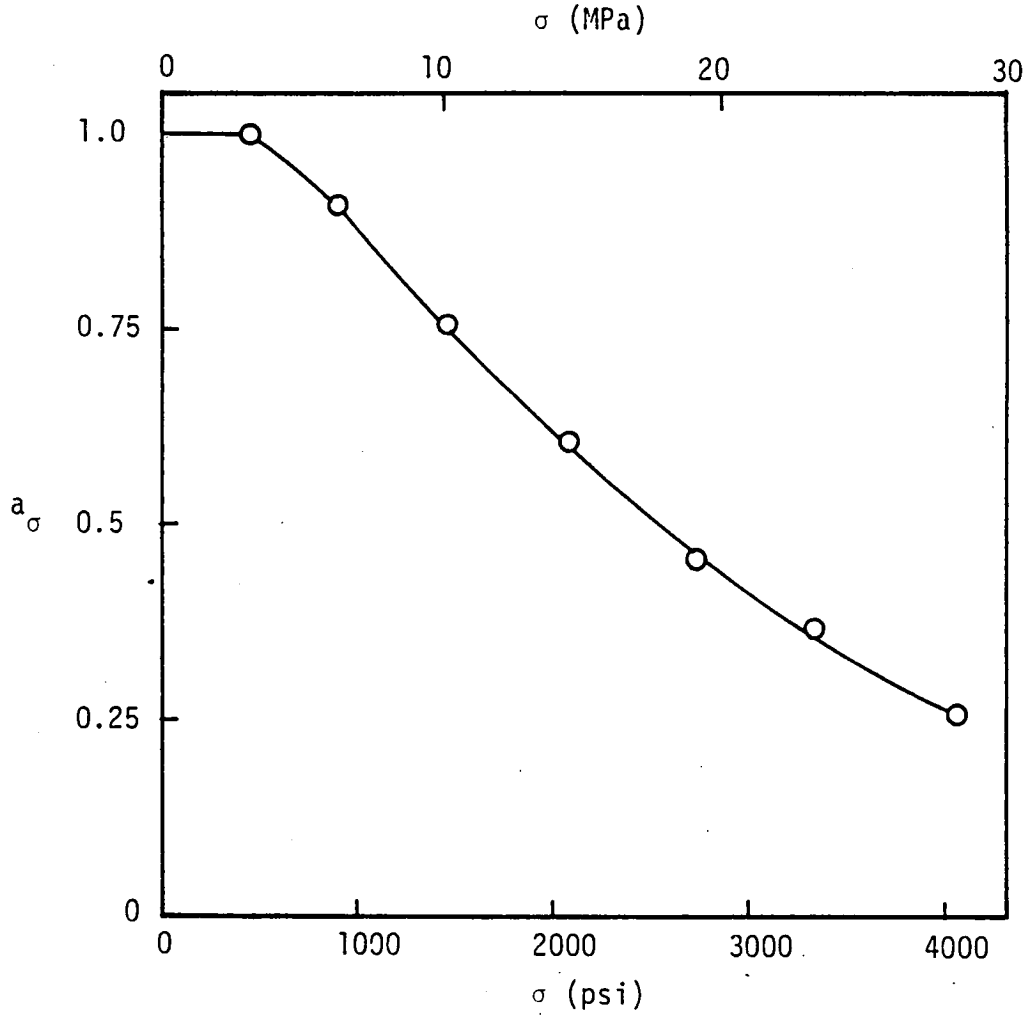

Figure 40. Horizontal shift function, a_σ vs. stress, T = 26°C (79°F).

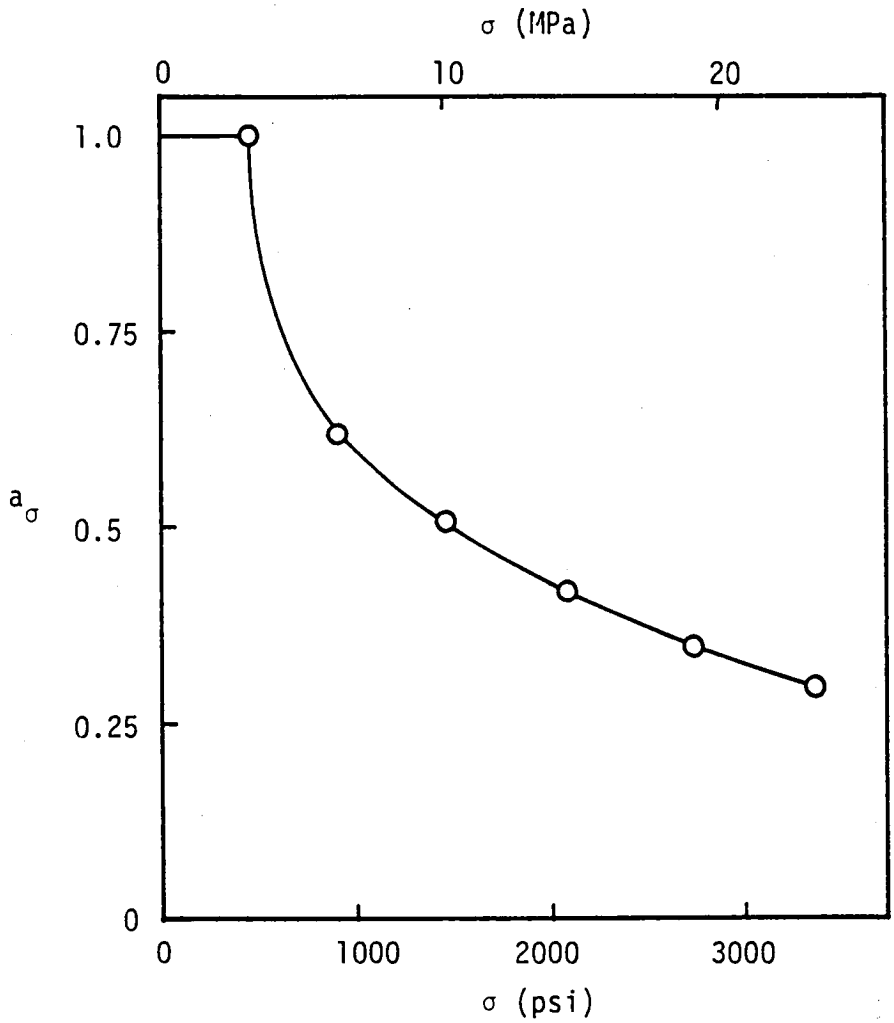

Figure 41. Horizontal shift function, a_σ vs. stress, T = 40°C (104°F).

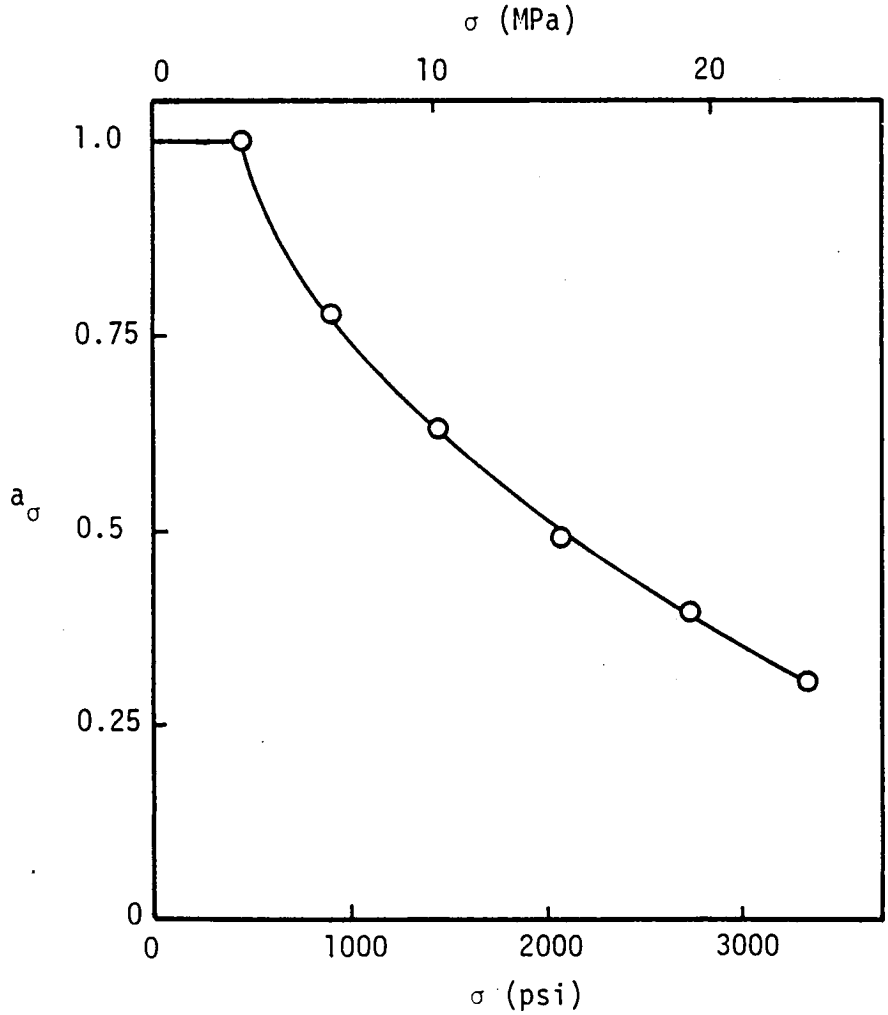

Figure 42. Horizontal shift function, a_σ vs. stress, T = 55°C (131°F).

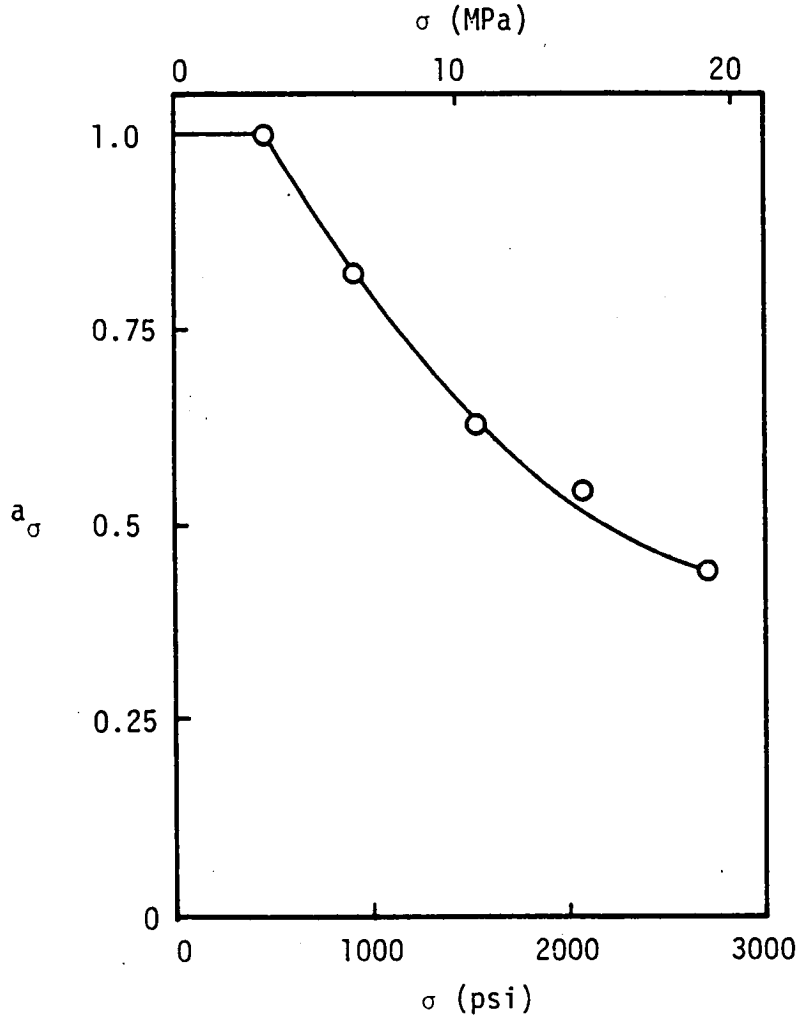

Figure 43. Horizontal shift function, a_σ vs. stress, T = 70°C (158°F).

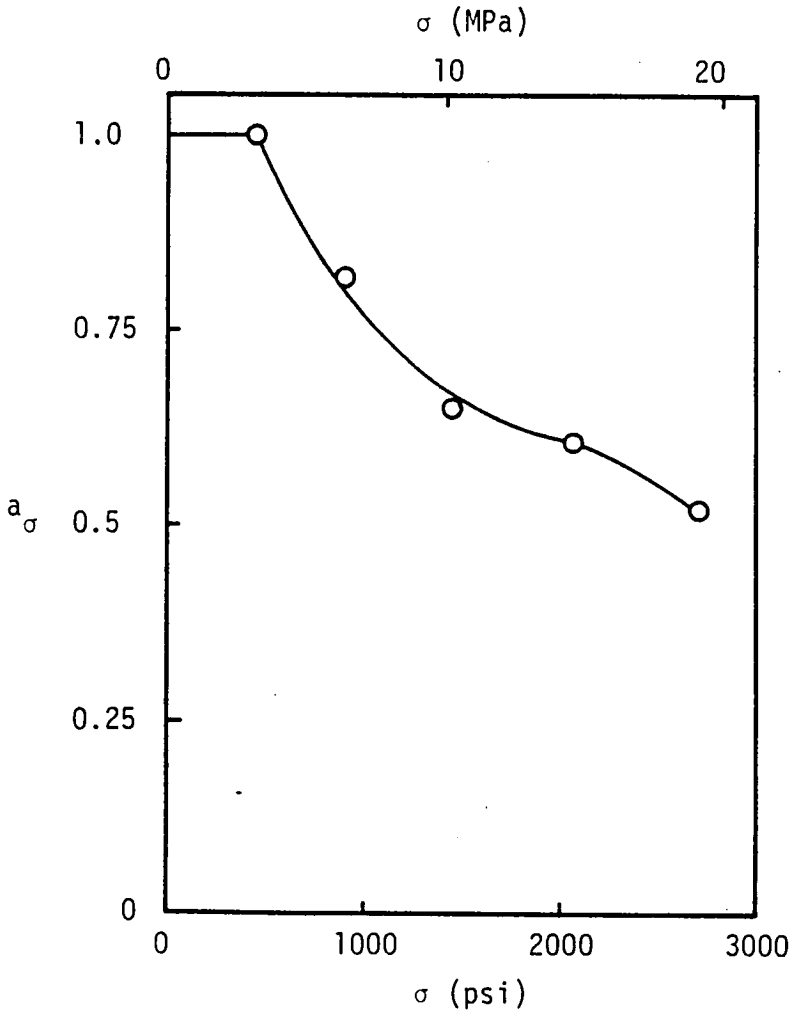

Figure 44. Horizontal shift function, a_σ vs. stress, T = 85°C (185°F).

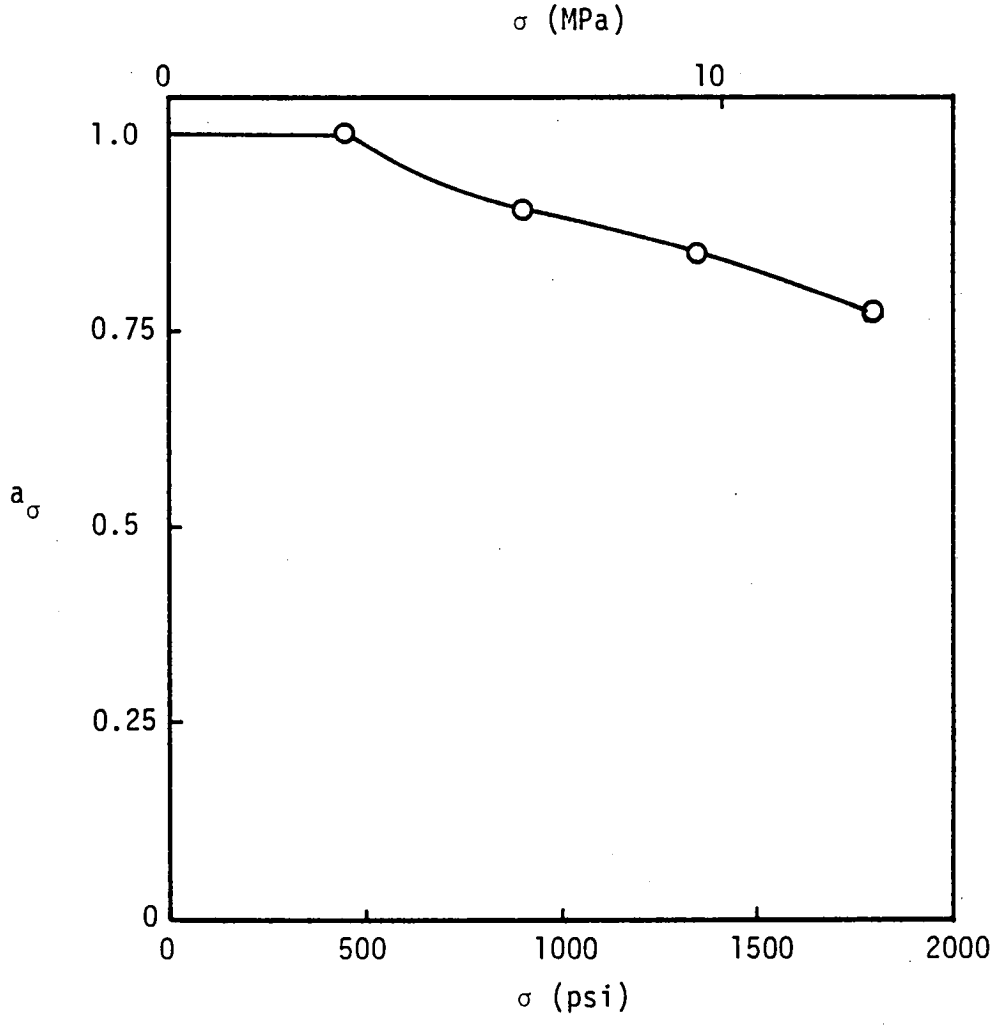

Figure 45. Horizontal shift function, a_σ vs. stress, T = 100°C (212°F).

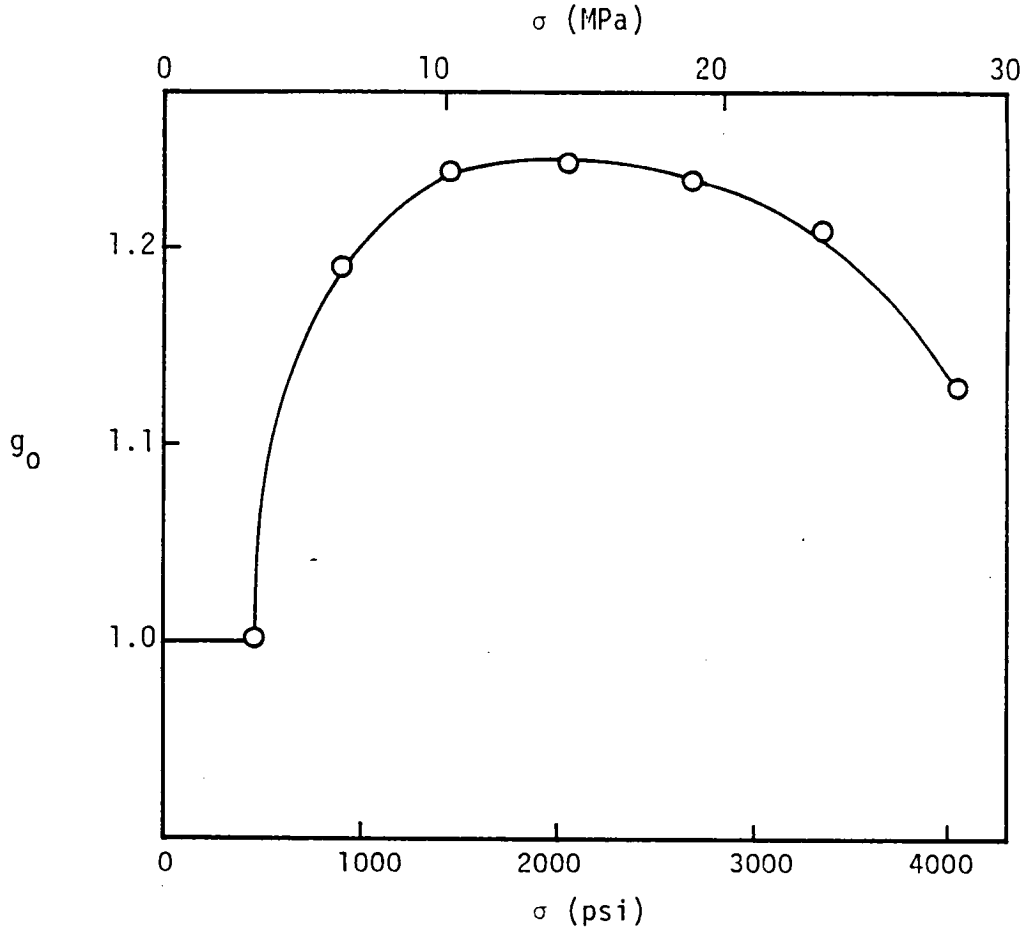

Figure 46. Nonlinear parameter, g_o vs. stress, T = 26°C (79°F).

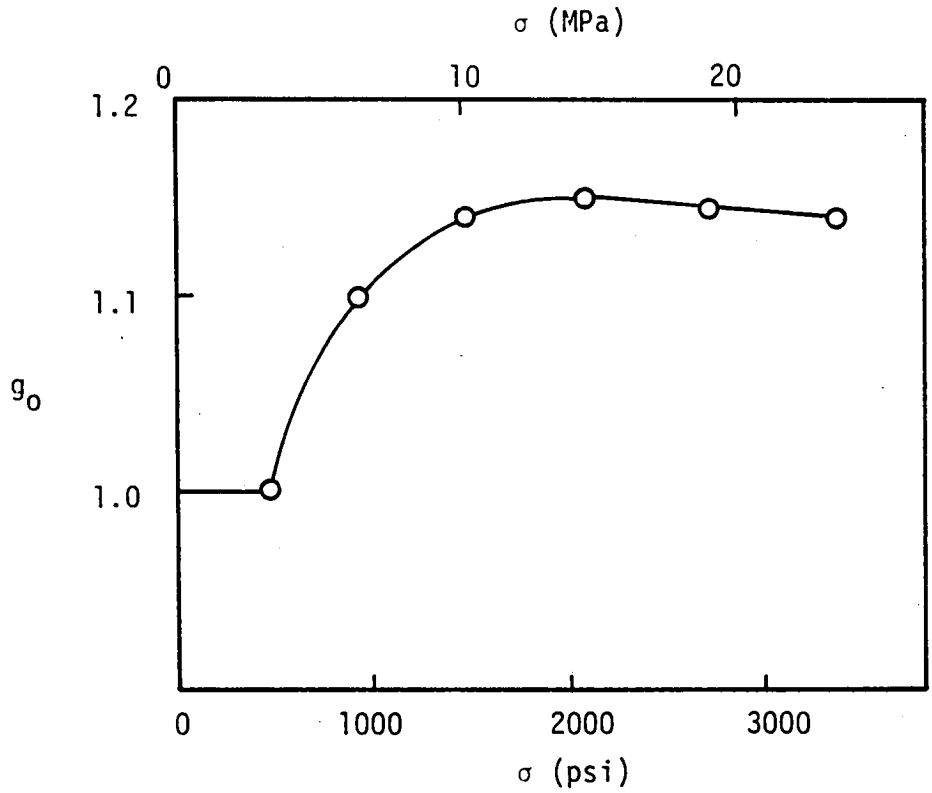

Figure 47. Nonlinear parameter, g_o vs. stress, T = 40°C (104°F).

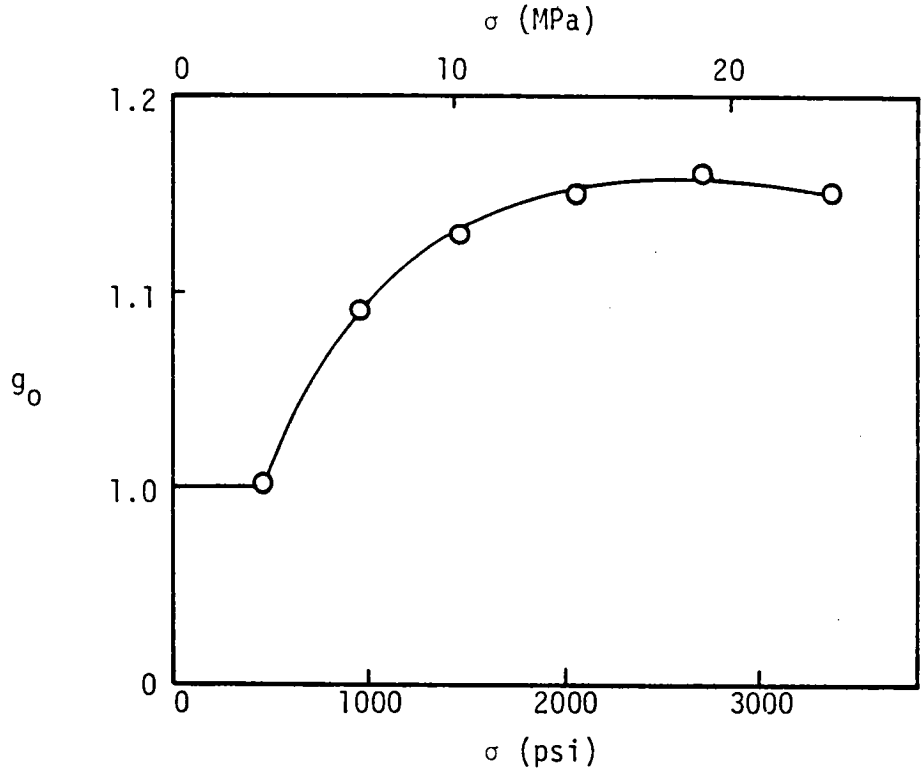

Figure 48. Nonlinear parameter, g_o vs. stress, T = 55°C (131°F).

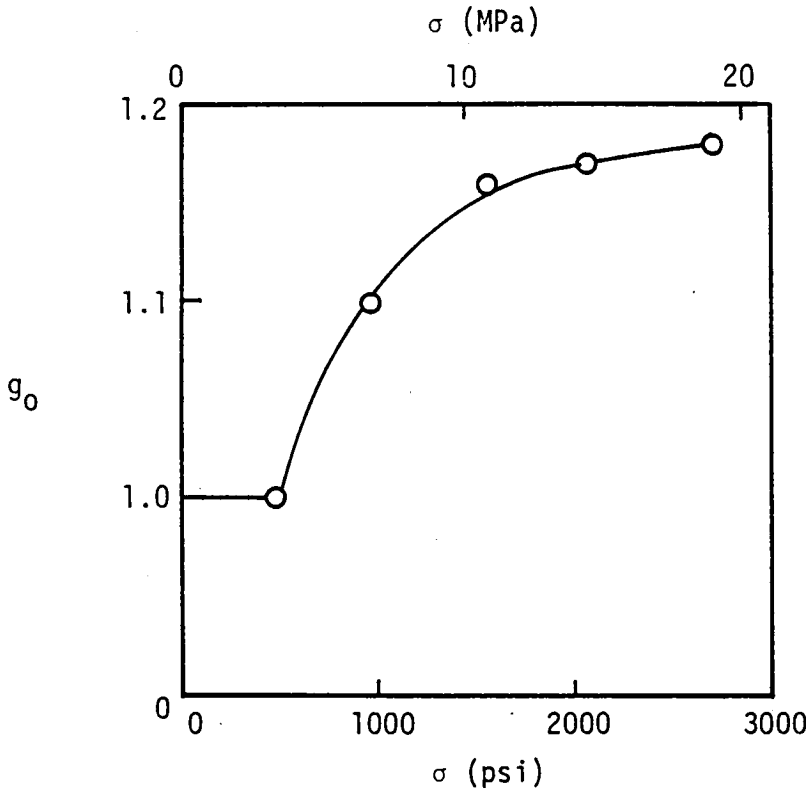

Figure 49. Nonlinear parameter, g_o vs. stress, T = 70°C (158°F).

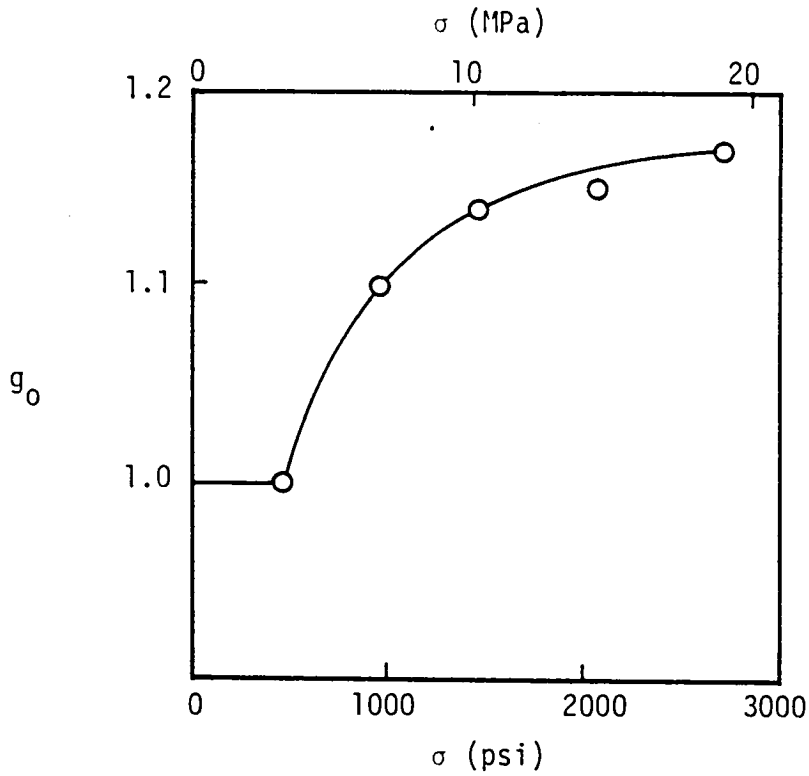

Figure 50. Nonlinear parameter, g_o vs. stress, T = 85°C (185°F).

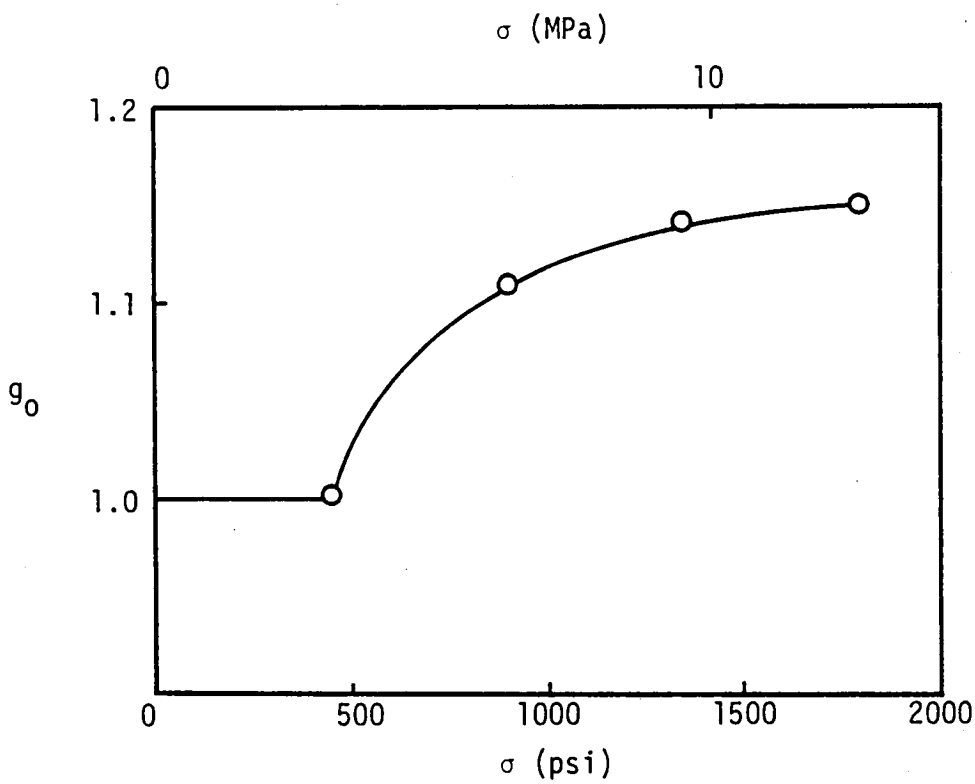

Figure 51. Nonlinear parameter, g_o vs. stress, T = 100°C (212°F).

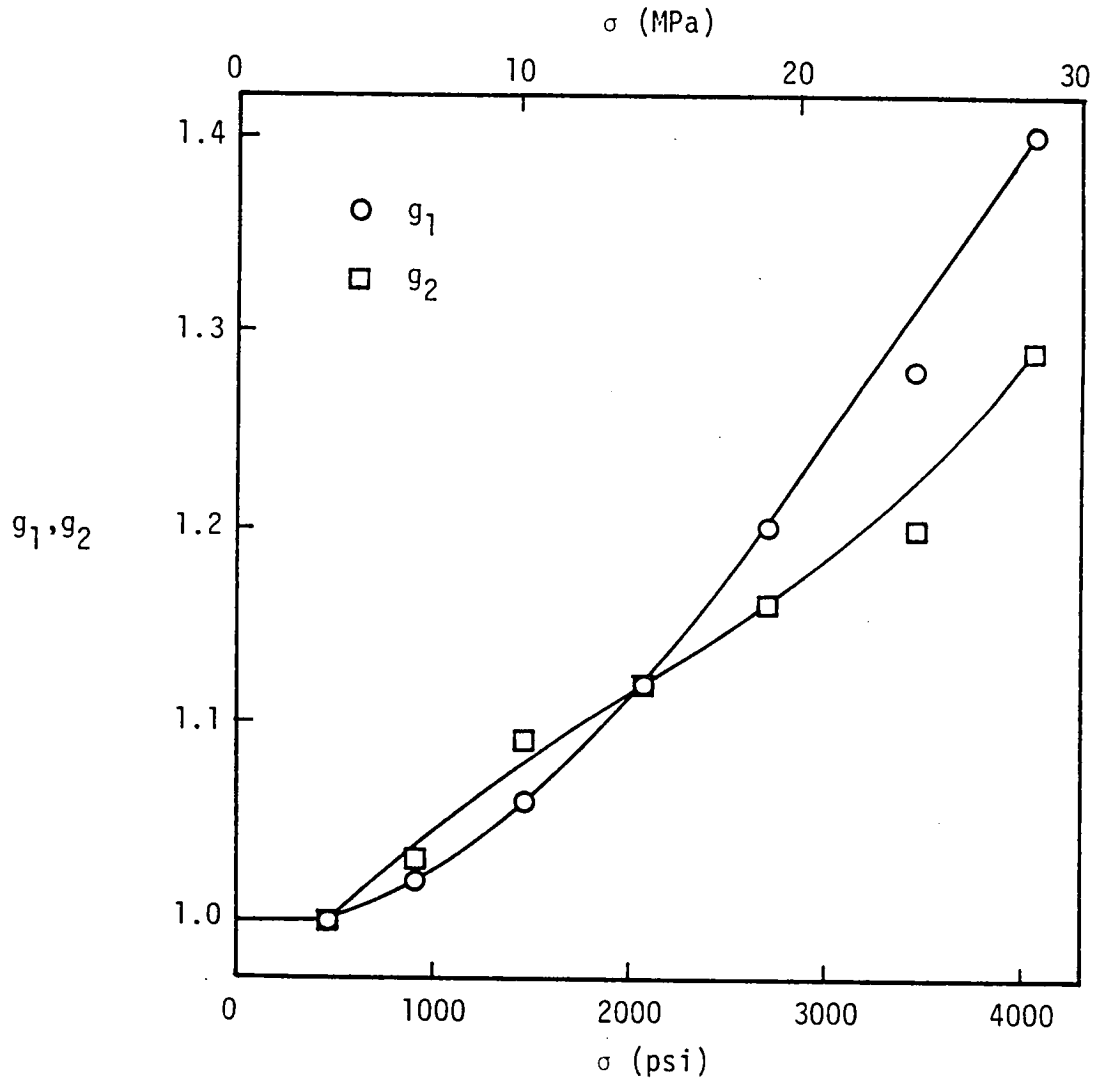

Figure 52. Nonlinear parameters, g_1 and g_2 vs. stress, T = 26°C (79°F).

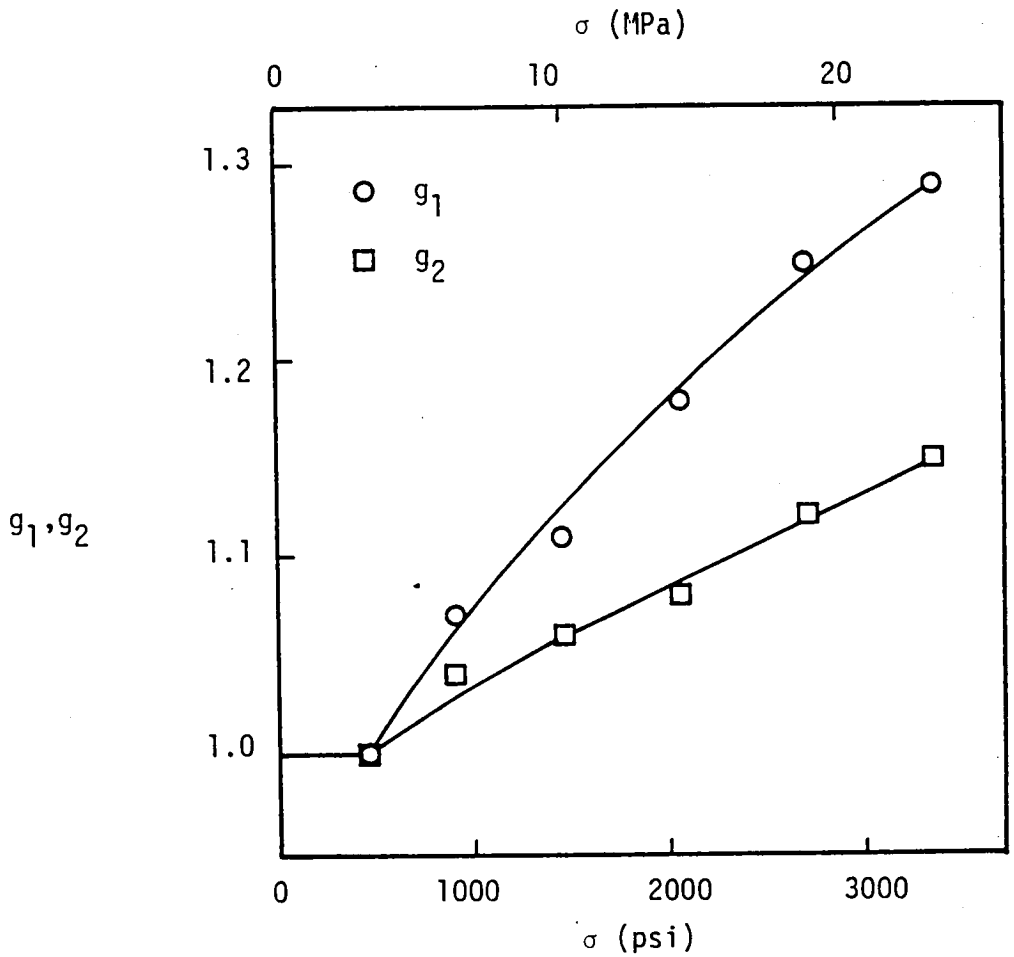

Figure 53. Nonlinear parameters, g_1 and g_2 vs. stress, T = 40°C (104°F).

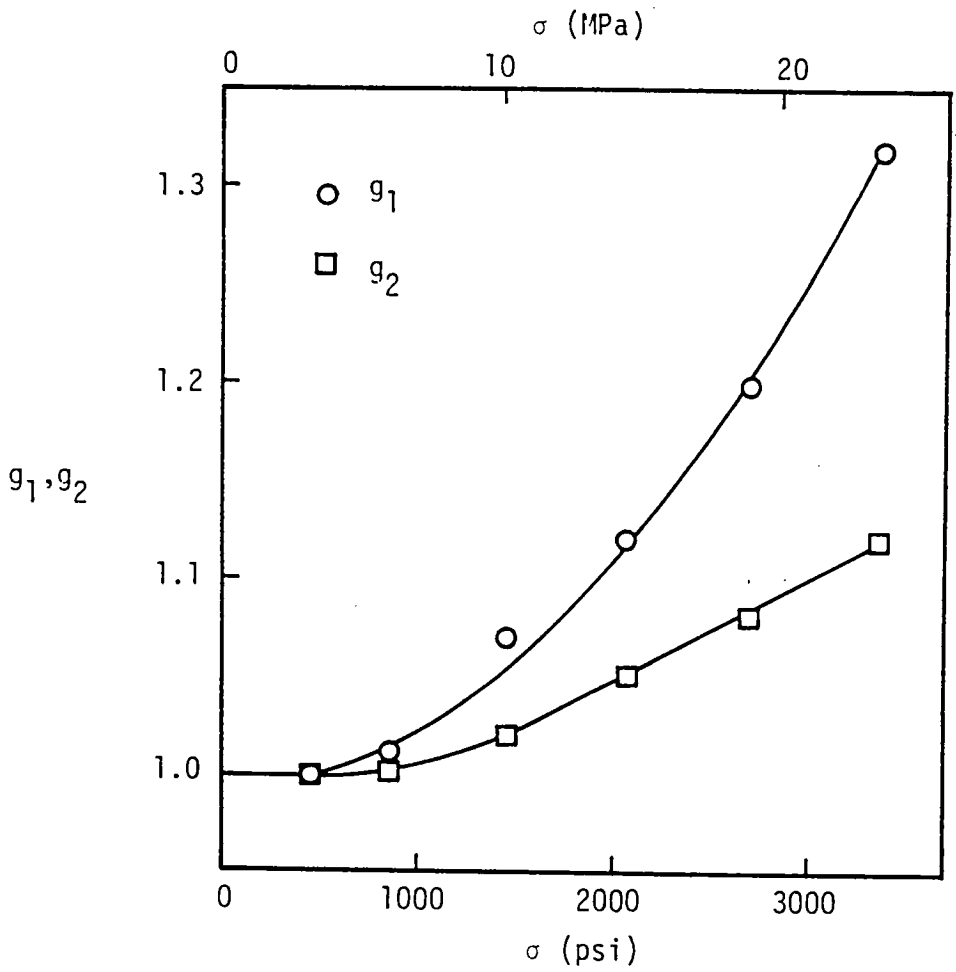

Figure 54. Nonlinear parameters, g_1 and g_2 vs. stress, T = 55°C (131°F).

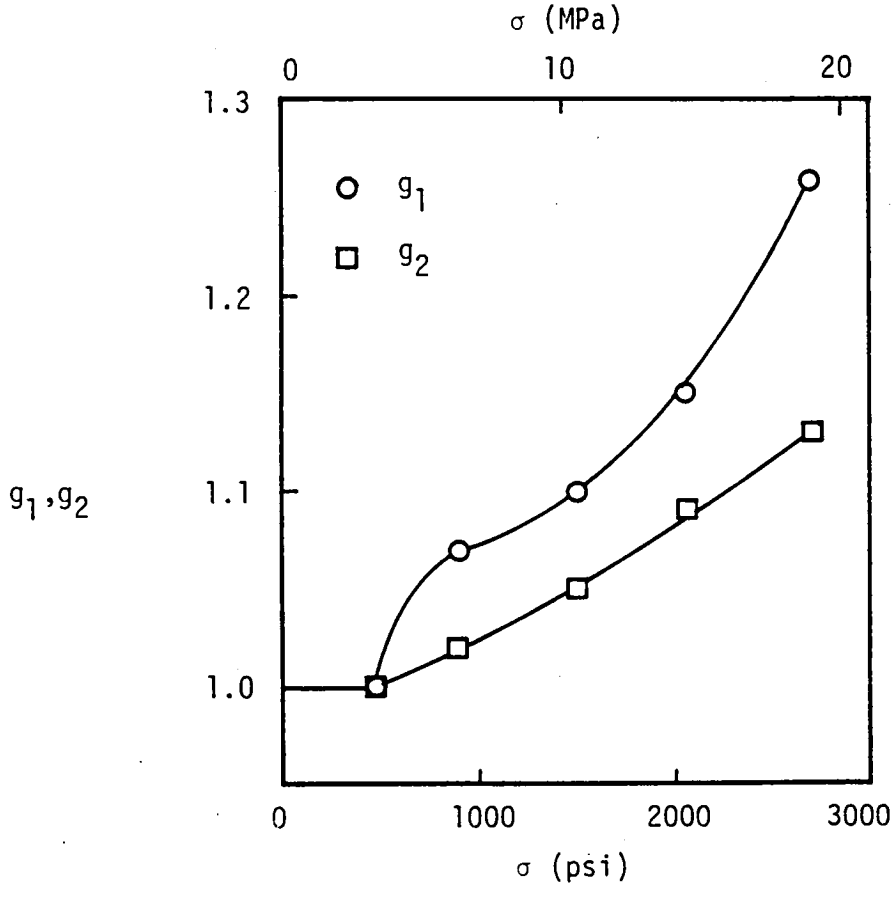

Figure 55. Nonlinear parameters, g_1 and g_2 vs. stress, T = 70°C (158°F).

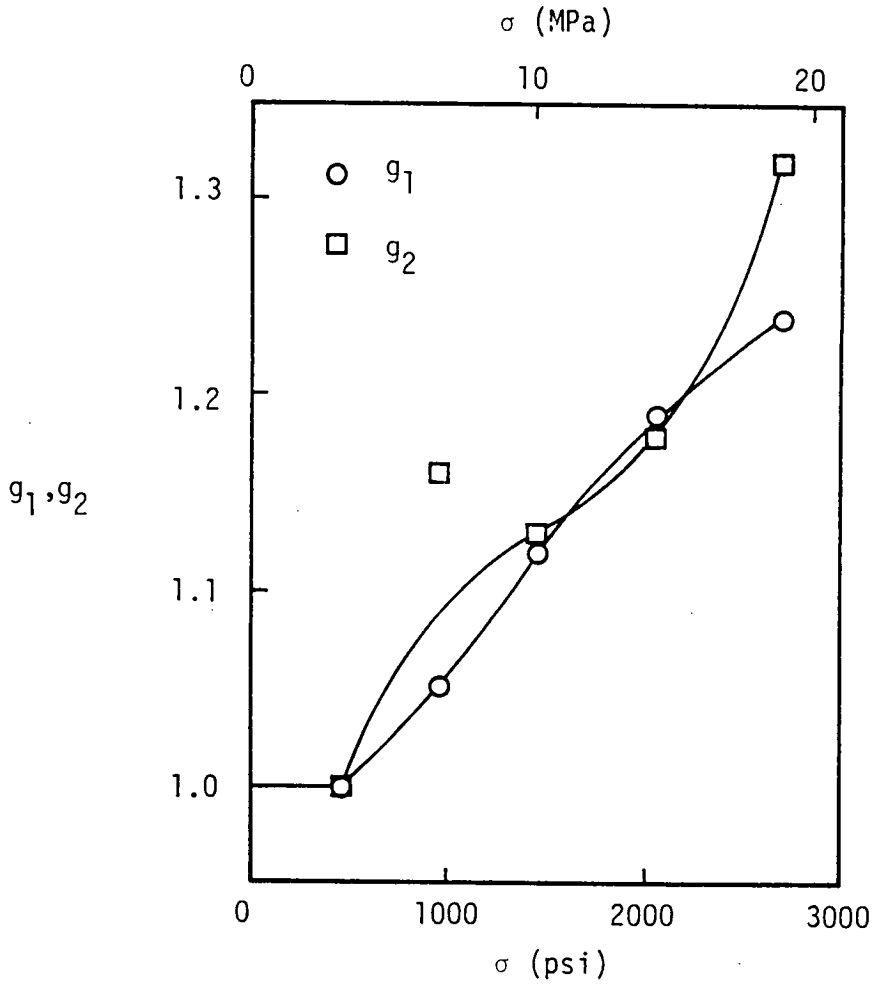

Figure 56. Nonlinear parameters, g_1 and g_2 vs. stress, T = 85°C (185°F).

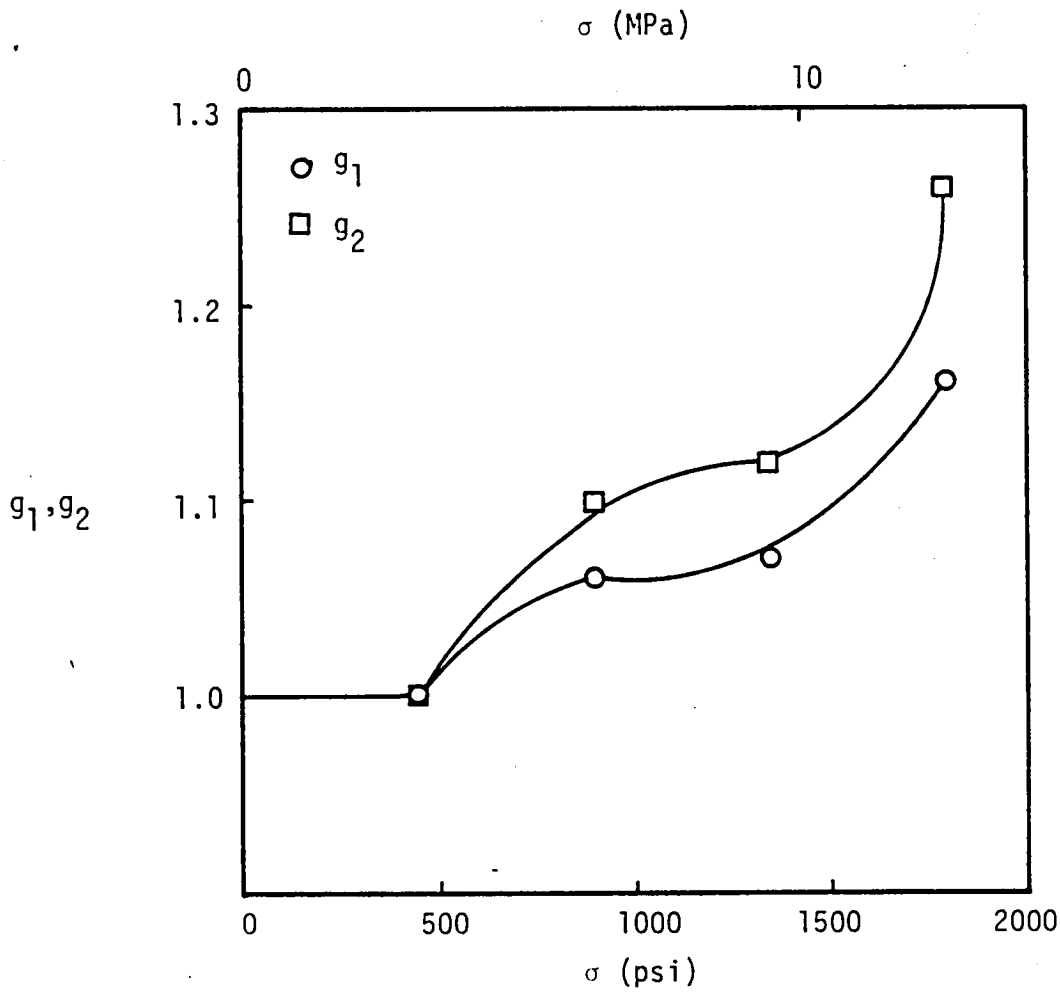

Figure 57. Nonlinear parameters, g_1 and g_2 vs. stress, T = 100°C (212°F).

Creep and Creep Recovery Response of FM-300 Under an Arbitrary Temperature and Stress Situation

Before investigating the creep and creep recovery response of FM-300 under arbitrary conditions, it seems appropriate to pause for an inspection of Figures 58 and 59. Figure 58 shows experimental creep strain data at room temperature for several stress levels along with the associated fit of the data. Figure 59 shows experimental creep recovery strain data at room temperature for the same stress levels along with the Schapery fit of the data. As before, note that the Schapery fit under-predicts the recovery strain as time increases.

This brings us to the point where the most critical question of the current study may be asked. Can the creep and creep recovery response of FM-300 be accurately predicted for any arbitrary temperature under the application of any arbitrary stress? Two arbitrary creep and creep recovery tests were performed in order to answer this question.

The first test was performed at a temperature of 145°F (62.8°C) with an applied stress of 2260 psi (15.58 MPa). The n-value corresponding to this temperature was predicted from Figure 19 as 0.126. The instantaneous strain, ε_0, was determined by using linear interpolation with respect to temperature between Figure 24 and Figure 25, resulting in a value of 5412. Similar linear interpolations with respect to temperature, between the appropriate figures, yielded the remaining necessary parameters. The creep coefficient, C', was found to be 1118, while the values for the horizontal and vertical shifts, a_σ and $\Delta\varepsilon_1/g_1$, were determined to be equal to 0.48 and 1414,

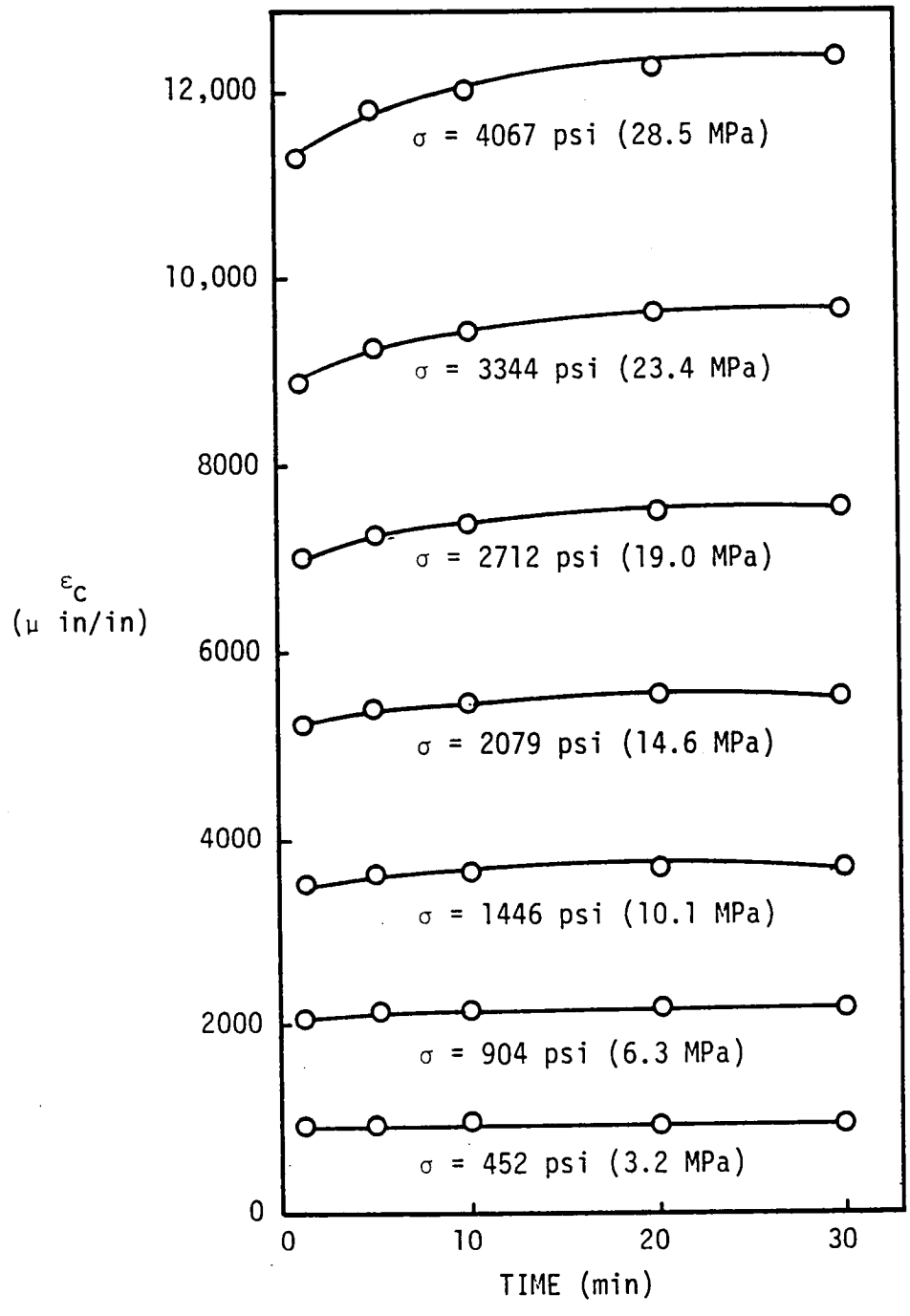

Figure 58. Experimental creep data (symbols) and the corresponding Schapery fit of the data (solid lines) for several stress levels at T = 26°C (79°F).

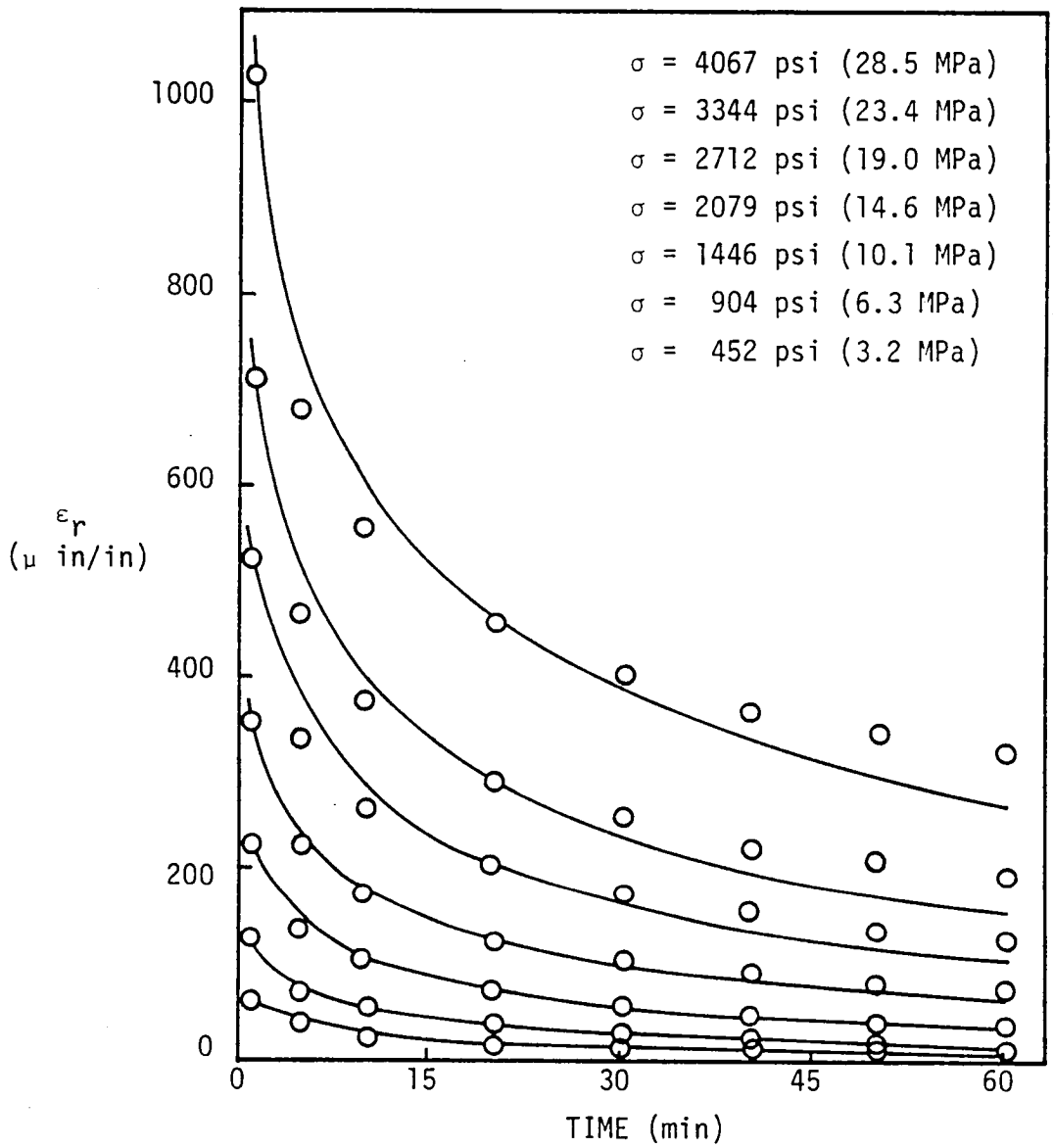

Figure 59. Experimental creep recovery data (symbols) and the corresponding Schapery fit of the data (solid lines) for several stress levels at T = 26°C (79°F).

respectively. The creep and creep recovery response was predicted using equations (34) and (31), respectively. Figure 60 shows a comparison between the predicted creep strain via equation (34) and the actual creep strain data, while Figure 61 gives a comparison between the predicted recovery strain via equation (31) and the actual recovery strain data. The experimental creep and creep recovery data is given in Table 2.

The second arbitrary test was performed at a temperature of 173.7°F (78.7°C) with an applied stress of 1808 psi (12.47 MPa). The five necessary parameters were evaluated by the same procedure as was used in the first test. The n-value, the instantaneous strain, ε_0, and the creep coefficient, C', were evaluated as, 0.165, 4711, and 776, respectively. The values for the horizontal and vertical shifts, a_σ and $\Delta\varepsilon_1/g_1$, were evaluated as, 0.60 and 1166, respectively. As before, the creep and creep recovery response was predicted using equations (34) and (31). Figure 62 gives a comparison between the predicted creep strain and the actual creep strain, while Figure 63 shows the comparison between the predicted recovery strain and the actual recovery strain. The experimental creep and creep recovery data is given in Table 3.

Inspection of Figures 60-63 reveals that the predicted creep and creep recovery response was quite close to the actual creep and creep recovery response for both of the arbitrary tests performed. The results of these two experiments are quite encouraging, for they indicate that the prediction of the creep and creep recovery response of FM-300 under an arbitrary temperature and stress situation is indeed possible.

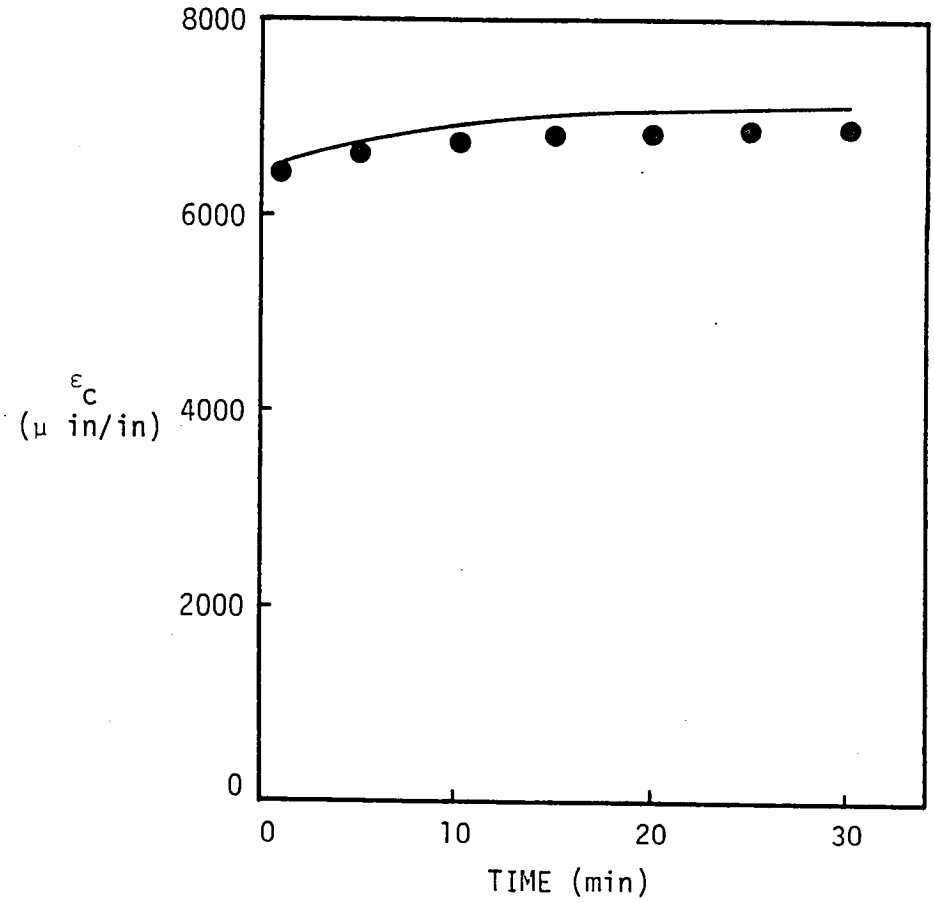

Figure 60. Comparison between the predicted creep strain (solid line) and the actual creep strain (symbols) for FM-300, σ = 2260 psi (15.58 MPa) and T = 145°F (62.8°C).

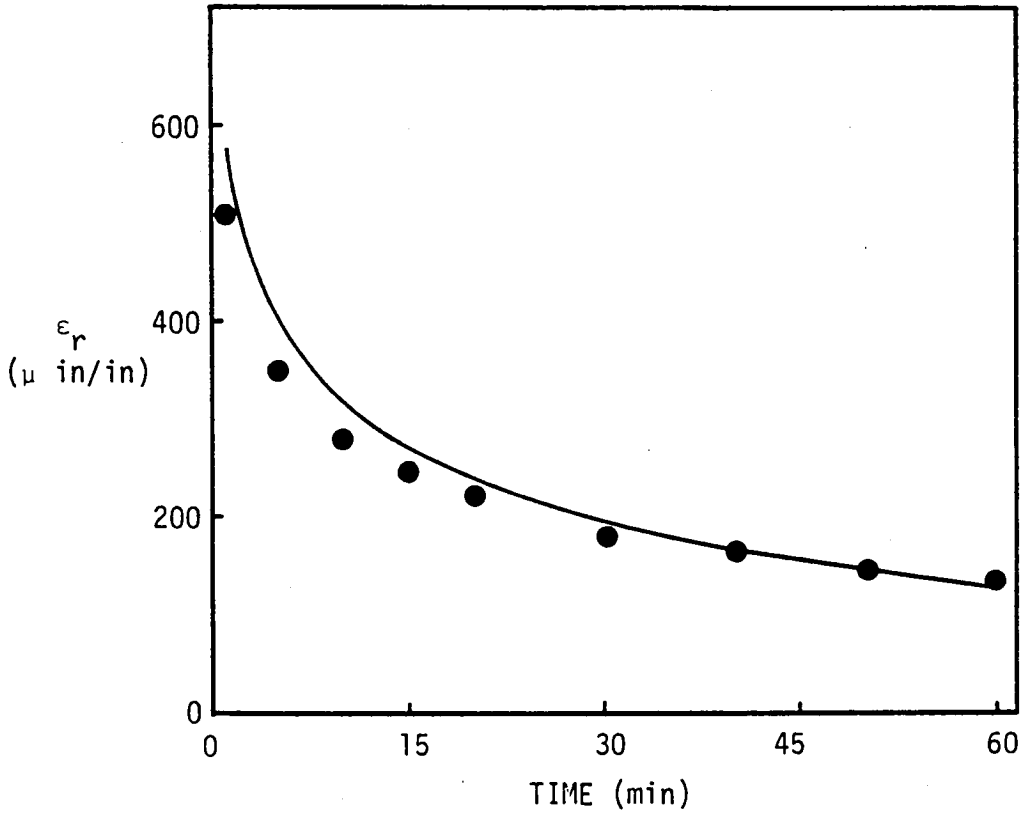

Figure 61. Comparison between the predicted creep recovery strain (solid line) and the actual creep recovery strain (symbols) for FM-300, σ = 2260 psi (15.58 MPa) and T = 145°F (62.8°C).

Table 2. Experimental creep and Creep Recovery Data for FM-300 at σ = 2260 psi (15.58 MPa) and T = 145°F (62.8°C).

Time (min)	Creep Strain (μin/in)	Time (min)	Recovery Strain (μin/in)
.25	6257	.25	646
.50	6331	.50	584
.75	6382	.75	542
1.0	6417	1.0	513
1.25	6444	1.25	489
1.5	6470	1.5	473
1.75	6490	1.75	458
2.0	6504	2.0	444
2.25	6521	2.25	431
2.5	6536	2.5	421
2.75	6548	2.75	411
3.0	6562	3.0	400
3.5	6582	3.5	385
4.0	6604	4.0	370
4.5	6621	4.5	358
5.0	6634	5.0	349
6.0	6664	6.0	327
7.0	6689	7.0	318
8.0	6712	8.0	305
9.0	6725	9.0	291
10.0	6746	10.0	278
12.0	6772	12.0	262
15.0	6816	15.0	246
17.0	6831	17.0	231
20.0	6865	20.0	222
25.0	6904	25.0	199
30.0	6943	30.0	182
		40.0	167
		50.0	149
		60.0	136

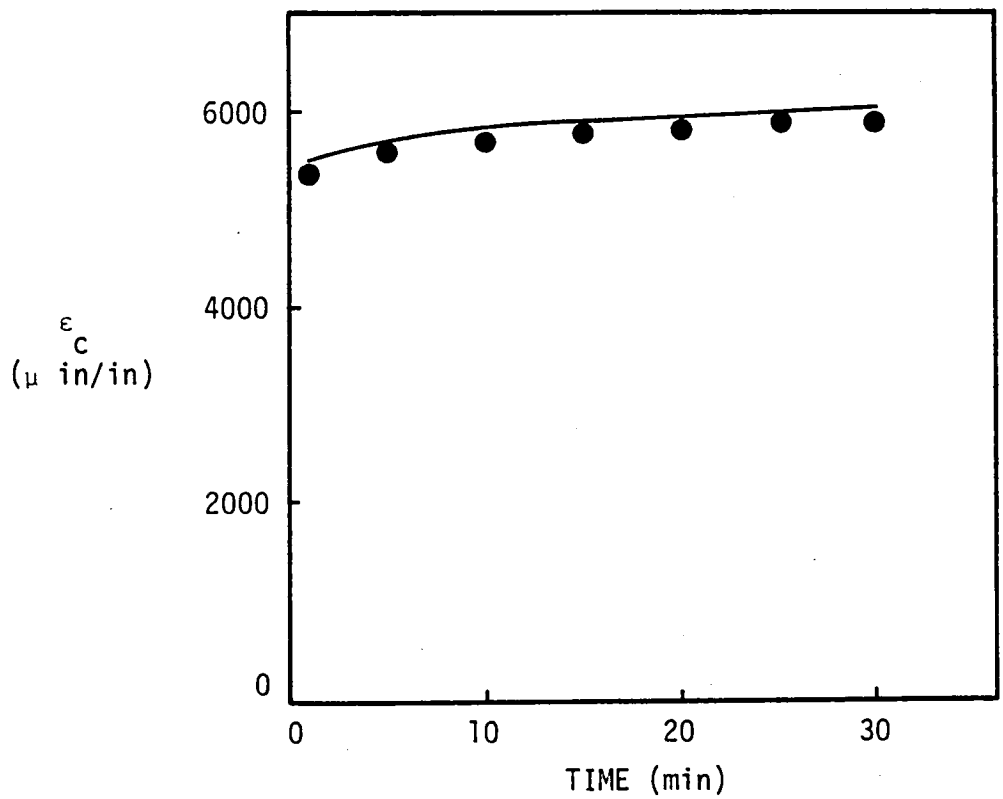

Figure 62. Comparison between the predicted creep strain (solid line) and the actual creep strain (symbols) for FM-300, σ = 1808 psi (12.47 MPa) and T = 173.7°F (78.7°C).

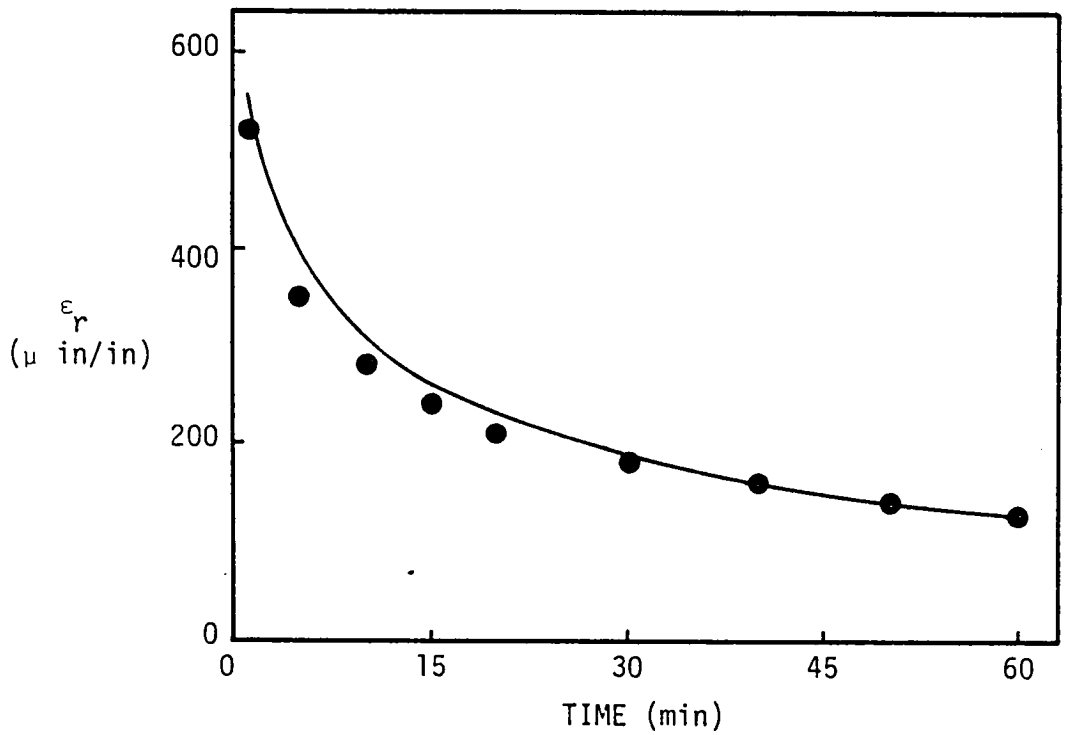

Figure 63. Comparison between the predicted creep recovery strain (solid line) and the actual creep recovery strain (symbols) for FM-300, σ = 1808 psi (12.47 MPa) and T = 173.7°F (78.7°C).

Table 3. Experimental Creep and Creep Recovery Data for FM-300 at σ = 1801 psi (12.47 MPa) and T = 173.7°F (78.7°C).

Time (min)	Creep Strain (μ/in/in)	Time (min)	Recovery Strain (μin/in)
.25	5236	.25	661
.50	5308	.50	594
.75	5354	.75	554
1.0	5384	1.0	523
1.25	5415	1.25	500
1.5	5440	1.5	475
1.75	5458	1.75	456
2.0	5473	2.0	445
2.25	5488	2.25	433
2.5	5500	2.5	420
2.75	5514	2.75	413
3.0	5526	3.0	401
3.5	5545	3.5	385
4.0	5568	4.0	372
4.5	5585	4.5	360
5.0	5599	5.0	350
6.0	5627	6.0	331
7.0	5655	7.0	312
8.0	5672	8.0	302
9.0	5696	9.0	287
10.0	5709	10.0	279
12.0	5742	12.0	258
15.0	5787	15.0	242
17.0	5810	17.0	229
20.0	5839	20.0	212
25.0	5880	25.0	195
30.0	5910	30.0	181
		40.0	162
		50.0	141
		60.0	130

Material Parameter Surfaces

In the preceding section, the desired material parameters were determined by linear interpolation with respect to temperature between the appropriate figures. Determination of the material parameters in this manner implies the existence of a material "parameter surface" for each of the four necessary stress dependent material parameters, ε_0, C', a_σ, and $\Delta\varepsilon_1/g_1$. The existence of the material "parameter surface" was discussed recently by Hiel [61], while a similar concept, the lamina property surface was discussed previously by Brinson and Dillard [42].

The "parameter surface" is a three dimensional illustration showing the variation of a given material parameter as a function of both stress level and temperature. The "surface" for the instantaneous strain, ε_0, is shown in Figure 64. Similarly, surfaces could also be drawn for the three remaining parameters, C', a_σ, and $\Delta\varepsilon_1/g_1$. Possession of an accurate description of these "parameter surfaces" would make the prediction of the creep and creep recovery response of FM-300 under arbitrary conditions almost trivial.

Prediction of Long Term Creep Response Based on Short Term Testing

It is well documented [61,63,66] that the n-value derived via a three parameter fit of linear creep data increases as the length of the creep data increases, before reaching an asymptotic value at approximately 10^3 minutes. Although it was known in advance that predictions based on the parameters which were derived from only 30 minutes of creep data would under-predict the long term creep strain, it was of interest to verify this fact. Two long term (10^4 minutes) creep tests

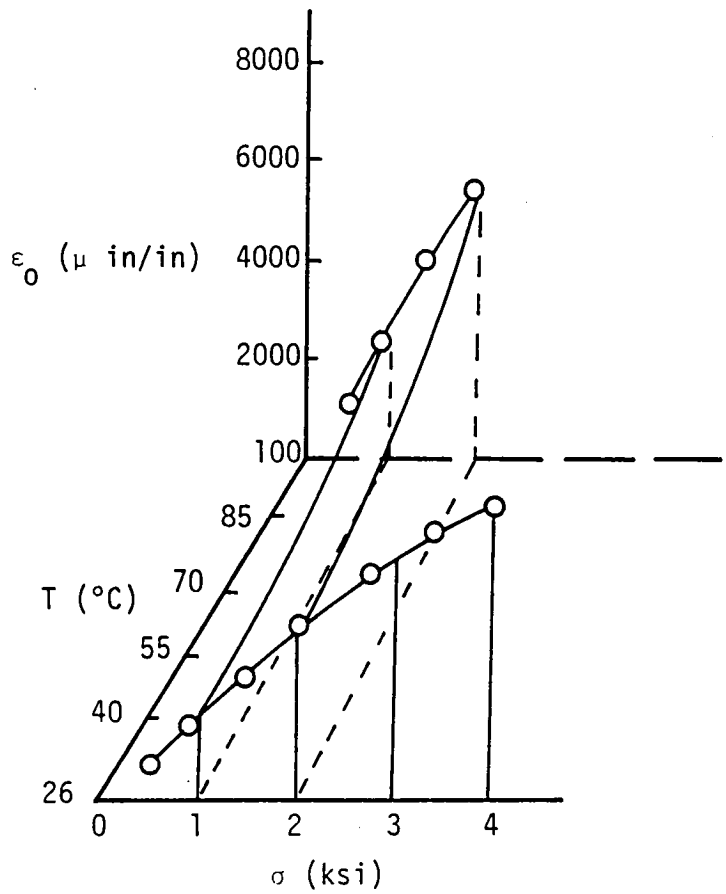

Figure 64. Parameter surface for the instantaneous strain, ε_o.

were performed in order to obtain the bounds on the accuracy of the long term predictions.

The first long term test was performed at room temperature under an applied stress of 452 psi (3.12 MPa). The 30 minute creep parameters (ε_o = 610, C' = 287, n = 0.056) were substituted into equation (34) and the creep response through 10^4 minutes was calculated. The comparison between the predicted creep response and the actual creep response is shown in Figure 65. The actual long term experimental creep data is given in Table 4. Note that the actual creep strain exceeded the predicted creep strain by only 3.0% at 10,200 minutes.

The second long term test was performed at a temperature of 212°F (100°C) under an applied stress of 1356 psi (9.35 MPa). As before, the 30 minute creep parameters (ε_o = 4012, C' = 767, n = 0.187) were substituted into equation (34) and the creep response through 10^4 minutes was calculated. The comparison between the predicted and the actual creep response is shown in Figure 66. Table 5 gives the actual long term experimental creep data. In this case, the actual creep strain exceeded the predicted creep strain by a substantial 14.5% at 10,246 minutes.

A pair of interesting observations can be made based on the two long term creep tests performed. First the predicted long term creep strains were always lower than the actual creep strains. Second, the error in predicting the long term creep strain increases as the temperature increases.

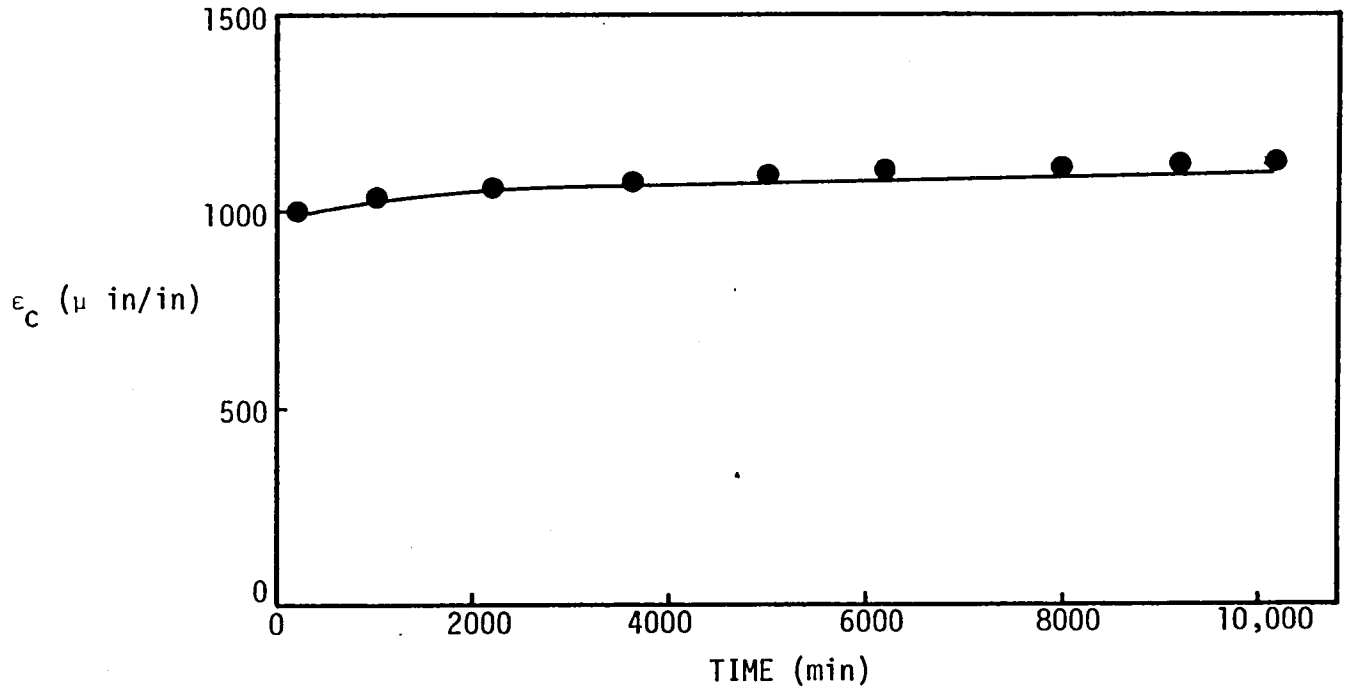

Figure 65. Comparison between the predicted long term creep strain (solid line) and the actual long term creep strain (symbols) for FM-300, σ = 452 psi (3.12 MPa) and T = 79.5°F (26.4°C).

Table 4. Long Term (10^4 min) Experimental Creep Data for FM-300 at σ = 452 psi (3.12 MPa) and T = 79.5°F (26.4°C).

Time (min)	Creep Strain (μin/in)
.25	904
1.0	923
2.0	932
3.0	938
4.0	942
5.0	945
7.0	950
10.0	956
15.0	961
20.0	965
25.0	968
30.0	971
40.0	975
50.0	979
60.0	981
80.0	986
100.0	989
150.0	995
200.0	1002
300.0	1009
400.0	1016
500.0	1020
600.0	1024
700.0	1028
800.0	1031
904.0	1034
1021.0	1039
1426.0	1047
1800.0	1055
2180.0	1061
2250.0	1062
3140.0	1075
3576.0	1078
4535.0	1087
5067.0	1091
5885.0	1097
6150.0	1098
7272.0	1104
7957.0	1111
9780.0	1117
9185.0	1120
9553.0	1122
10200.0	1125

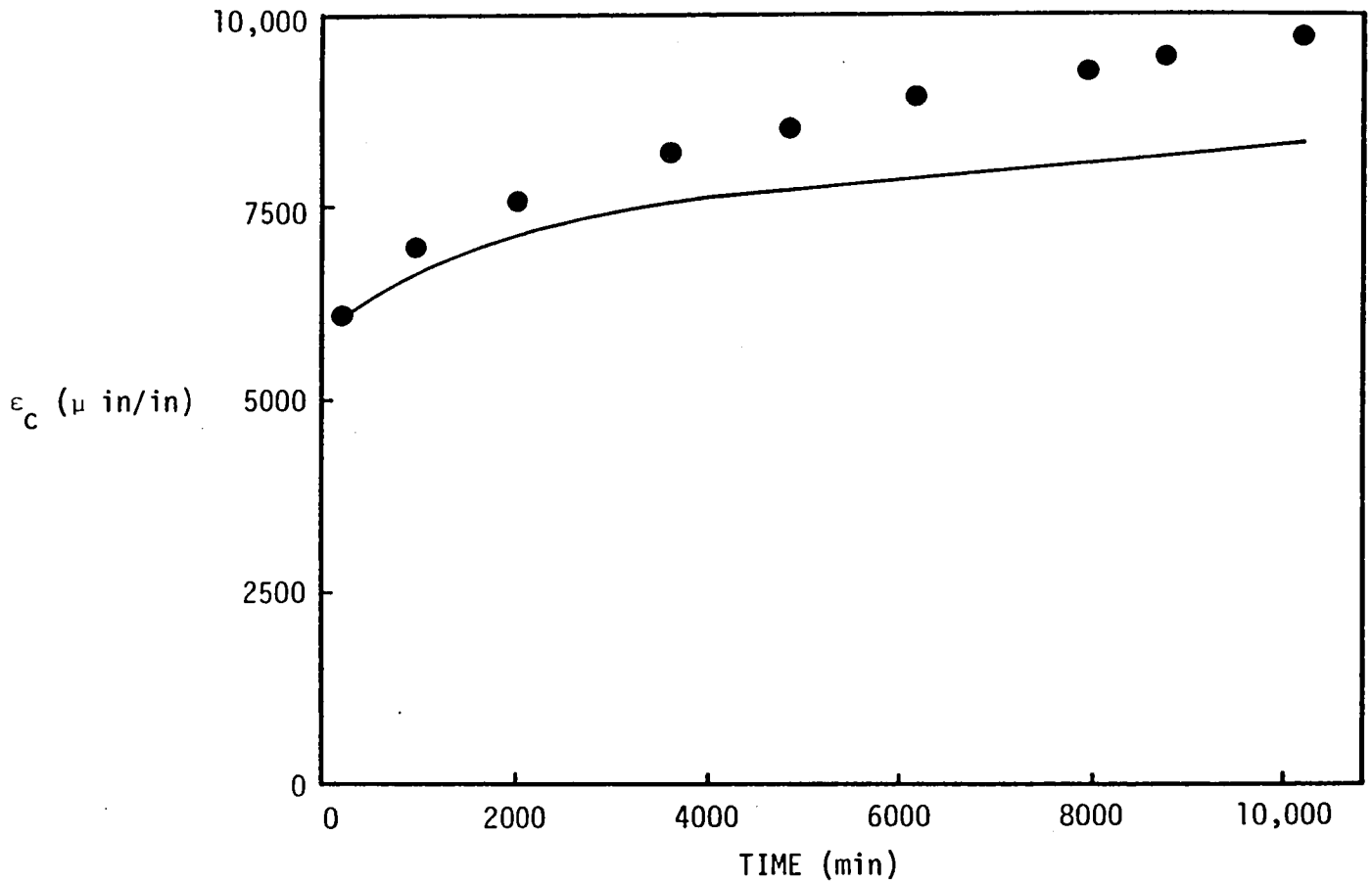

Figure 66. Comparison between the predicted long term creep strain (solid line) and the actual long term creep strain (symbols) for FM-300, σ = 1356 psi (9.35 MPa) and T = 212°F (100°C).

Table 5. Long Term (10^4 min) Experimental Creep Data for FM-300 at σ = 1356 psi (9.35 MPa) and T = 212°F (100°C).

Time (min)	Creep Strain (μin/in)
.25	4544
1.0	4736
2.0	4853
3.0	4925
4.0	4981
5.0	5023
7.0	5098
10.0	5182
15.0	5271
20.0	5343
25.0	5402
30.0	5448
40.0	5531
50.0	5597
60.0	5659
80.0	5744
100.0	5819
150.0	5980
185.0	6065
211.0	6118
255.0	6202
311.0	6305
363.0	6380
460.0	6504
509.0	6560
706.0	6766
810.0	6850
876.0	6916
940.0	6968
1545.0	7366
1708.0	7445
1805.0	7500
2000.0	7590
2930.0	7978
3332.0	8120
3600.0	8210
4516.0	8480
4865.0	8577
6141.0	8907
7535.0	9212
7947.0	9300
8768.0	9462
8915.0	9496
10190.0	9722
10246.0	9734

Chapter 6

SUMMARY AND CONCLUSIONS

The present investigation has been concerned with the nonlinear viscoelastic characterization of two commonly used structural adhesives, FM-73 and FM-300, in bulk form. The goal of the current research was to develop a procedure by which the creep and creep recovery response under arbitrary conditions of temperature and stress could be predicted with reasonable accuracy.

A computerized Schapery procedure was employed to characterize FM-73 at room temperature. Several factors were cited which may have been responsible for the inability to characterize this material at elevated temperature.

The characterization of FM-300 via the computerized Schapery procedure utilized for FM-73, was found to yield inconsistent results for the linear parameters, n and C. Therefore, a "modified" computer procedure consisting of elements of both the Schapery and Findley methods was utilized. The characterization of FM-300 via this "modified" approach was successfully performed for six temperature levels, ranging from room temperature to 100°C (212°F).

It was subsequently shown that the creep and creep recovery response of FM-300 under arbitrary conditions of temperature and stress could be predicted with reasonable accuracy based on the material parameters evaluated at each of the six experimental temperature levels.

Material parameters evaluated from 30 minutes of creep data were then used to predict creep response over 10^4 minutes. It was shown that the predicted strain was always lower than the actual strain, and that this deviation between the predicted strain and the actual strain increased as the temperature increased. This under-prediction of long term creep strain indicates that the value of the power law exponent, n, was too low. With the method used to determine n from creep data approximately 10^3 minutes of linear data are required to determine its value accurately. It might be noted that Peretz and Weitsman using a similar method have indicated that only fifteen minutes of creep data is required. At this time it is not possible to reconcile this apparent contradiction. However, regardless of the method of evaluation or the duration of the test, it is essential that the n-value be known accurately if long term creep response is to be predicted accurately.

Although the results of the current research are encouraging, a word of caution is in order at this point. The FM-300 analyzed in the current work was prepared according to the cure cycle given in Chapter 4. It has been shown [67] that the cure cycle as well as many other factors can have a significant effect on the bulk tensile properties of a structural adhesive. Therefore, results by others on FM-73 or FM-300 processed differently and tested under different conditions might be at variance with those of this study. However, it is appropriate to note that the isochronous stress-strain curves for t = 1 min. obtained for FM-73 and shown in Fig. 4 compare favorably

with the results obtained by Romanko and Knauss [68] and Peretz and Weitsman [33] as was shown by Botha, et al. [69].

REFERENCES

1. Hart-Smith, L. J., "Adhesively-Bonded Joints for Composites-Phenomenological Considerations," Douglas Paper 6707, March 1978.

2. Hart-Smith, L. J., "Further Developments in the Design and Analysis of Adhesive-Bonded Structural Joints," Douglas Paper 6922, April 1980.

3. Hart-Smith, L. J., "Adhesive Bonding of Aircraft Primary Structures," Douglas Paper 6979, October 1980.

4. Hart-Smith, L. J., "Differences Between Adhesive Behavior in Test Coupons and Structural Joints," Douglas Paper 7066, March 1981.

5. Hart-Smith, L. J., "Design and Analysis of Bonded Repairs for Metal Aircraft Structures," Douglas Paper 7089, July 1981.

6. Hart-Smith, L. J., "Design and Analysis of Bonded Repairs for Fibrous Composite Aircraft Structures," Douglas Paper 7133, July 1981.

7. Renton, W. J., "Structural Properties of Adhesives," Vought Corp. ATC, Quarterly Progress Report No. 1, Report No. B-94400/6CR-34, August 1976.

8. Renton, W. J., "Structural Properties of Adhesives," Vought Corp. ATC, Quarterly Progress Report No. 2, Enclosure (1) to Report B-94400/6CRL-59, November 1976.

9. Renton, W. J., "Structural Properties of Adhesives," Vought Corp. ATC, Quarterly Progress Report No. 3, Enclosure (1) to Report B-94400/7CRL-36, February 1977.

10. Renton, W. J., "Structural Properties of Adhesives," Vought Corp. ATC, Quarterly Progress Report No. 4, Enclosure (1) to Report B-94400/7CRL-36, May 1977.

11. Renton, W. J., "Structural Properties of Adhesives," Vought Corp. ATC, Quarterly Progress Report No. 5, Enclosure (1) to Report B-94400/7CRL-36, August 1977.

12. Renton, W. J., "Structural Properties of Adhesives," Vought Corp. ATC, Quarterly Progress Report No. 6, Enclosure (1) to Report B-94400/7CRL-36, November 1977.

13. Renton, W. J., "Structural Properties of Adhesives," Vought Corp. ATC, Quarterly Progress Report No. 7, Enclosure (1) to Report B-94400/8CRL-26, February 1977.

14. _____, "Basis for Accelerated Testing of Adhesively Bonded Joints," Texas Research Institute, Quarterly Progress Report No. 1, October 1980.

15. _____, "Basis for Accelerated Testing of Adhesively Bonded Joints," Texas Research Institute, Quarterly Progress Report No. 2, March 1981.

16. _____, "Basis for Accelerated Testing of Adhesively Bonded Joints," Texas Research Institute, Quarterly Progress Report No. 3, May 1981.

17. _____, "Basis for Accelerated Testing of Adhesively Bonded Joints," Texas Research Institute, Quarterly Progress Report No. 4, July 1981.

18. Francis, E. C., Hufferd, W. L., Lemini, D. G., Thompson, R. G., and Briggs, W. E., "Time Dependent Fracture in Adhesively Bonded Joints," Chemical Systems Division, Report No. CSD 2769-IR-01, May 1982.

19. Francis, E. C., Hufferd, W. L., Lemini, D. G., Thompson, R. G., Briggs, W. E., and Parmerter, R. R., "Time Dependent Fracture in Adhesively Bonded Joints," Chemical Systems Division, Report No. CSD 2769-IR-02, November 1982.

20. Krieger, R. B., "Stiffness Characteristics of Structural Adhesives for Stress Analysis in Hostile Environment," American Cyanamid Company, Report No. BPT 620.

21. Krieger, R. B., "Stress Analysis of Metal-to-Metal Bonds in Hostile Environment," American Cyanamid Company, Report No. BPT 621.

22. Krieger, R. B., "Shear Stress-Strain Properties of Structural Adhesives in Hostile Environments," American Cyanamid Company, Report No. BPT 622.

23. Krieger, R. B., "Fatigue Testing of Structural Adhesives," American Cyanamid Company, Report No. BPT 623.

24. Renton, W. J., "The Symmetric Lap-Shear Test--What Good Is It?," Experimental Mechanics, 23, 2, pp. 409-415, Nov. 1976.

25. Cartner, J. S. and H. F. Brinson, "The Non-Linear Viscoelastic Behavior of Adhesives and Chopped Fiber Composites," VPI-E-78-21, 1978.

26. O'Connor, D. G., "Factors Affecting the Fracture Energy of a Structural Adhesive," M.S. Thesis, VPI & SU, September 1979.

27. Cordon, W. A., Properties, Evaluation, and Control of Engineering Materials, McGraw-Hill, 1979.

28. Plecnik, J. M., Bresler, B., Cunningham, J. D., and Iding, R., "Temperature Effects on Epoxy Adhesives," Journal of the Structural Division (ASCE), Vol. 106, January 1980.

29. Schapery, R. A., "A Theory of Nonlinear Thermoviscoelasticity Based on Irreversible Thermodynamics," Proceedings of the 5th U.S. National Congress of Applied Mechanics, ASME, 1966, pp. 511-530.

30. Schapery, R. A., "Further Development of a Thermodynamic Constitutive Theory: Stress Formulation," Rept. No. 69-2, February 1969, Purdue University.

31. Schapery, R. A., "On the Characterization of Nonlinear Viscoelastic Materials," Poly. Eng. and Science, Vol. 9, No. 4, July 1969, pp. 295-310.

32. Lou, Y. C., and Schapery, R. A., "Viscoelastic Characterization of a Nonlinear Fiber-Reinforced Plastic," Journal of Composite Materials, April 1971.

33. Weitsman, Y., "Residual Stresses in Adhesive Joints. Air Force Wright Aeronautical Laboratory Report AFWAL-TR-81-4121, October 1981.

34. Goland, M. and Reissner, E., "The Stresses in Cemented Joints," J. of Applied Mechanics, pp. 12-27, March 1944.

35. Humphreys, E. A., and Herakovich, C. T., "Nonlinear Analysis of Bonded Joints with Thermal Effects," VPI & SU Report, VPI-E-77-19, June 1977.

36. Sen, J. K., and Jones, R. M., "Stresses in Double-Lap Joints Bonded with a Viscoelastic Adhesive: Part I. Theory and Experimental Corroboration," AIAA Journal, Vol. 18, No. 10, October 1980.

37. Sen, J. K., and Jones, R. M., "Stresses in Double-Lap Joints Bonded with a Viscoelastic Adhesive: Part II. Parametric Study and Joint Design," AIAA Journal, Vol. 18, No. 11, November 1980.

38. Sancaktar, E., "The Viscoelastic Shear Behavior of a Structural Adhesive," Ph.D. Thesis, VPI & SU, 1979.

39. Brinson, H. F., Renieri, M. P., and Herakovich, C. T., "Rate and Time Dependent Failure of Structural Adhesives," Fracture Mechanics of Composites, ASTM STP 593, 1975, pp. 177-199.

40. Renieri, M. P., "Rate and Time Dependent Behavior of Structural Adhesives," Dissertation, VPI & SU, 1976.

41. Chmura, M. and McAbee, E., "Correlation of Mechanical Properties of Resins Obtained in an Adhesive Joint and Bulk Form," TR 3330 Picatinny Arsenal, April 1966.

42. Brinson, H. F. and Dillard, D. A., "The Prediction of Long Term Viscoelastic Properties of Fiber Reinforced Plastics," Progress in Science and Engineering of Composites, T. Hayashi, K. Kawata and S. Umekawa, eds., ICCM-IV, Tokyo, Japan, 1982.

43. Crochet, M. J., "Symmetric Deformations of Viscoelastic-Plastic Cylinders," Journal of Applied Mechanics, Vol. 33, Series E, No. 2, 1966, pp. 327-334.

44. Leaderman, H., "Elastic and Creep Properties of Filamentous Materials and Other High Polymers," The Textile Foundation, Washington, D.C., 1943.

45. Griffith, W. I., "The Accelerated Characterization of Viscoelastic Composite Materials," Ph.D. Dissertation, VPI & SU, Blacksburg, VA, 1979.

46. Kenner, J. H., Knauss, W. G., and Chai, H., "A Simple Creep Torsiometer and Its Use in the Thermorheological Characterization of a Structural Adhesive," Experimental Mechanics, Feb. 1982, p. 75.

47. Green, A. E. and Rivlin, R. S., "The Mechanics of Nonlinear Materials with Memory, Part I," Arch. Rat. Mech. Anal., Vol. 1, 1957, pp. 1-21.

48. Green, A. E., Rivlin, R. S., and Spencer, A. J. M., "The Mechanics of Nonlinear Materials with Memory, Part II," Arch. Rat. Mech. Anal., Vol. 3, 1959, pp. 82-90.

49. Green, A. E. and Naghdi, P. M., "On Continuum Thermodynamics," Archives of Rational Mechanics Analysis, Vol. 48, pp. 353-378, 1972.

50. Walker, K. P., "Representation of Hastelloy-X Behavior at Elevated Temperature with a Functional Theory of Viscoplasticity," presented at the ASME Pressure Vessels Conference, San Francisco, Aug. 12, 1980 (also to appear in ASME Journal of Engineering Materials and Technology).

51. Cernocky, E. P. and Krempl, E., "A Theory of Viscoplasticity Based on Infinitesimal Total Strain," Acta Mechanica, Vol. 36, pp. 263-289, 1980.

52. Krempl, E., "On the Interaction of Rate and History Dependence in Structural Metals," Acta Mechanica, Vol. 22, pp. 53-90, 1975.

53. Cernocky, E. P. and Krempl, E., "A Theory of Thermovisco-Plasticity Based on Infinitesimal Total Strain," Int. J. of Solids Structures, Vol. 16, pp. 723-741, 1980.

54. Liu, M. C., Krempl, E., and Nairn, D. C., Trans. ASME Ser. H, J. Eng. Matls. Technology, Vol. 98, pp. 322-329, 1976.

55. Cernocky, E. P. and Krempl, E., "A Nonlinear Uniaxial Integral Constitutive Equation Incorporating Rate Effects, Creep, and Relaxation, Int. J. Nonlinear Mechanics, Vol. 14, pp. 183-203, 1979.

56. Liu, M. C. M. and Krempl, E., "A Uniaxial Viscoplastic Model Based on Total Strain and Overstress," J. Mech. Phys. Solids, Vol. 27, pp. 377-391, 1979.

57. Findley, W. N., Adams, C. H., and Worley, W. J., "The Effect of Temperature on the Creep of Two Laminated Plastics as Interpreted by the Hyperbolic Sine Law and Activation Energy Theory," ASTM Proc., Vol. 48, 1948.

58. Findley, W. N. and Khosla, G., "Application of the Superposition Principle and Theories of Mechanical Equations of State, Strain, and Time Hardening to Creep of Plastics Under Changing Loads," J. Applied Physics, Vol. 26, No. 7, 1955, pp. 821-831.

59. Findley, W. N., and Peterson, D. B., "Prediction of Long-Time Creep with Ten-Year Creep Data on Four Plastic Laminates," ASTM Proc., Vol. 58, 1958.

60. Findley, W. N. and Lai, J. S. Y., "A Modified Superposition Principle Applied to Creep of Nonlinear Viscoelastic Material Under Abrupt Changes in State of Combined Stress," Transactions of the Society of Rheology, Vol. 11, No. 3, 1967, pp. 361-380.

61. Hiel, Clement, "The Nonlinear Viscoelastic Response of Resin Matrix Composites," Doctoral Thesis, Vrije Universiteit, Brussels, Jan. 1983. (Also, VPI-E-83-6 with A. H. Cardon and H. F. Brinson.)

62. Bertollotti, A., "A Computer-Based Solution for Evaluating the Parameters in Schapery's Nonlinear Viscoelastic Model," Senior Project, VPI & SU, 1982.

63. Yen, S. C., "Creep Characterization of SMC-R50 Under Various Thermomechanical Conditions," Ph.D. Thesis, VPI & SU, 1983.

64. Caplin, E. S., "Nonlinear Viscoelastic Characterization of Polycarbonate," M.S. Thesis, VPI & SU, March 1982. (Also, Report VPI-E-82-7, March 1982 with H. F. Brinson.)

65. Halpin, J. C., "Introduction to Viscoelasticity," Composite Materials Workshop, Tsai, Halpin, Pagano (eds.), Technomic, Stamford, 1968.

66. Dillard, D. A., "Creep and Creep Rupture of Laminated Graphite/Epoxy Composites," Ph.D. Thesis, VPI & SU, March 1981. (Also, VPI-E-81-3, March 1981.)

67. Klein, R. M., Jozavi, H., and Sancaktar, E., "The Effects of Cure Temperature and Time on the Bulk Tensile Properties of a Structural Adhesive," Clarkson College, Report No. M/E-081, May 1982.

68. Romanko, J. and Knauss, W. G., "On the Time Dependence of the Poisson's Ratio of a Commercial Adhesive Material," Journal of Adhesion, Vol. 10, pp. 269-272, October 1980.

69. Botha, L. R., Jones, R. M., and Brinson, H. F., "Viscoelastic Analysis of Adhesive Stresses in Bonded Joints," VPI & SU Report No. VPI-E-83-17, May 1983.

1. Report No.	2. Government Accession No.	3. Recipient's Catalog No.
NASA CR-172279		

4. Title and Subtitle	5. Report Date
NONLINEAR VISCOELASTIC CHARACTERIZATION OF STRUCTURAL ADHESIVES	December 1983
	6. Performing Organization Code

7. Author(s)	8. Performing Organization Report No.
*M. A. Rochefort and Hal F. Brinson	
	10. Work Unit No.

9. Performing Organization Name and Address	11. Contract or Grant No.
Virginia Polytechnic Institute and State University The Center for Adhesion Science and The Dept. of Engrg. Science and Mechanics, Blacksburg, VA 24061	NAG-1-227
	13. Type of Report and Period Covered
12. Sponsoring Agency Name and Address	Contractor Report
National Aeronautics and Space Administration Washington, DC 20546	14. Sponsoring Agency Code

15. Supplementary Notes Langley technical monitor: Dr. W. S. Johnson

The research effort which led to the results in this report was financially supported by Structures Laboratory, U.S. Army Research and Technology Laboratories (AVRADCOM), NASA Langley Research Center, Hampton, VA.

*Now associated with Applied Research Associates, Inc., Alexandria, Virginia.

16. Abstract

Measurements of the nonlinear viscoelastic behavior of two adhesives, FM-73 and FM-300, are presented and discussed. Analytical methods to quantify the measurements are given and fitted into a framework of an accelerated testing and analysis procedure. The single integral model used is shown to function well and is analogous to a time-temperature stress-superposition procedure (TTSSP). Advantages and disadvantages of the creep power law method used in this study are given.

17. Key Words (Suggested by Author(s))	18. Distribution Statement
Adhesives Nonlinear viscoelasticity FM-73 and FM-300 neat resin properties	Unclassified - Unlimited Subject Category 27

19. Security Classif. (of this report)	20. Security Classif. (of this page)	21. No. of Pages	22. Price
Unclassified	Unclassified	130	A07

For sale by the National Technical Information Service, Springfield, Virginia 22161